

UNIVERSITY OF SOUTHAMPTON

**Derivative Expansions  
of the  
Exact Renormalisation Group  
and  
 $SU(N|N)$  Gauge Theory**

by

John Francis Tighe

A thesis submitted for the degree of

Doctor of Philosophy

Department of Physics and Astronomy

July 2001

UNIVERSITY OF SOUTHAMPTON

ABSTRACT

FACULTY OF SCIENCE

PHYSICS

Doctor of Philosophy

Derivative Expansions  
of the Exact Renormalization Group  
and  $SU(N|N)$  Gauge Theory

John Francis Tighe

We investigate the convergence of the derivative expansion of the exact renormalisation group, by using it to compute the  $\beta$  function of scalar  $\lambda\varphi^4$  theory. We show that the derivative expansion of the Polchinski flow equation converges at one loop for certain fast falling smooth cutoffs. The derivative expansion of the Legendre flow equation trivially converges at one loop, but also at two loops: slowly with sharp cutoff (as a momentum-scale expansion), and rapidly in the case of a smooth exponential cutoff. Finally, we show that the two loop contributions to certain higher derivative operators (not involved in  $\beta$ ) have divergent momentum-scale expansions for sharp cutoff, but the smooth exponential cutoff gives convergent derivative expansions for all such operators with any number of derivatives.

In the latter part of the thesis, we address the problems of applying the exact renormalisation group to gauge theories. A regularisation scheme utilising higher covariant derivatives and the spontaneous symmetry breaking of the gauge supergroup  $SU(N|N)$  is introduced and it is demonstrated to be finite to all orders of perturbation theory.

---

*Dedicated to my family*

# Contents

Preface	viii
Acknowledgements	ix
1 Introduction	1
2 Exact renormalisation group	4
2.1 Wilson's renormalisation group . . . . .	4
2.2 Wilson/Polchinski flow equation . . . . .	5
2.3 Legendre flow equation . . . . .	9
2.4 Renormalisability . . . . .	12
2.5 $\beta$ function . . . . .	16
2.6 Approximations . . . . .	18
2.6.1 Truncation . . . . .	18
2.6.2 Derivative/momenta scale expansion . . . . .	19

<b>3</b>	<b>Convergence of derivative expansion</b>	<b>21</b>
3.1	Wilson/Polchinski flow equation . . . . .	22
3.2	Legendre flow equation at one loop . . . . .	26
3.3	Legendre flow equation at two loops . . . . .	27
3.4	Cancellation of self energy diagrams . . . . .	30
3.5	Sharp cutoff . . . . .	32
3.6	Exponential cutoff . . . . .	37
3.7	Power law cutoff . . . . .	42
3.8	Operators of higher powers . . . . .	43
3.9	Summary and conclusions . . . . .	44
<b>4</b>	<b>Towards a gauge invariant exact RG</b>	<b>46</b>
4.1	Consequences of gauge invariance . . . . .	46
4.2	Regularisation techniques . . . . .	47
4.2.1	Dimensional regularisation . . . . .	48
4.2.2	Pauli-Villars regularisation . . . . .	49
4.2.3	Higher covariant derivatives . . . . .	49
4.2.4	Hybrid regularisation . . . . .	50
4.3	Supersymmetric groups . . . . .	52
4.3.1	Grading . . . . .	52

4.3.2	$SU(N M)$	53
4.3.3	$SU(N N)$	60
<b>5 Regularisation via <math>SU(N N)</math></b>		<b>63</b>
5.1	The action of the regulating scheme	63
5.1.1	The gauge field sector	64
5.1.2	Spontaneous symmetry breaking sector	67
5.1.3	Gauge fixing sector	69
5.1.4	Total action	72
5.2	Power counting	73
5.2.1	Multiloop diagrams	75
5.2.2	One-loop diagrams	77
5.2.3	Final list of constraints	80
5.3	Supertrace mechanism	82
5.3.1	One-loop Remainder Diagrams with $\mathcal{A}$ propagators	83
5.3.2	One-loop Remainder Diagrams with $\mathcal{C}$ propagators	85
5.3.3	One-loop Remainder Diagrams with $\eta$ propagators	85
5.3.4	Example of explicit calculation of supergroup factors	86
5.4	Ward identities	88
5.4.1	BRST	88

5.4.2	Finiteness of diagrams with BRST source insertions . . . . .	91
5.4.3	Finiteness of one-loop diagrams using Ward Identities . . . . .	92
5.5	Unitarity . . . . .	93
5.5.1	$U(1 1)$ quantum mechanics . . . . .	94
5.5.2	Recovery of unitarity in $A^1$ sector . . . . .	97
5.6	Summary and conclusions . . . . .	98
<b>A</b>	<b>Proof of eq. (4.29)</b>	<b>100</b>
<b>B</b>	<b>Completeness relations</b>	<b>103</b>
B.1	$SU(N M)$ . . . . .	103
B.2	$SU(N N)$ . . . . .	104
<b>C</b>	<b>Wine notation</b>	<b>106</b>
<b>D</b>	<b>Some Feynman rules for <math>SU(N N)</math> gauge theory</b>	<b>109</b>
<b>Bibliography</b>		<b>113</b>

# List of Figures

2.1	Sketch of the properties of the cutoff functions . . . . .	6
2.2	Graphical representation of the momentum expanded Wilson/Polchinski flow equation. Crosses denote differentiation with respect to $\Lambda$ . . . . .	9
2.3	Procedure for tuning to the massive continuum limit . . . . .	15
3.1	Feynman diagram contributing to the four-point function at one loop, constructed from the tree-level six-point function with two legs joined . . . . .	23
3.2	Graph of partial sum contribution to $\beta_0$ coefficient against number of terms in expansion for the series (3.13) . . . . .	25
3.3	Graph of partial sum contribution to $\beta_0$ coefficient against number of terms in expansion for the series (3.14) . . . . .	26
3.4	Feynman diagrams contributing to four-point function at two loops. .	28
3.5	Diagrams used in forming two loop four-point functions . . . . .	29
3.6	Feynman diagram contributing to wave function renormalization at two loops. . . . .	29

3.7	Partial sum contribution to $\beta$ function against number of terms in expansion for the series (3.39) . . . . .	34
3.8	Average of successive partial sum contributions to $\beta$ function against number of terms in expansion for series (3.39) . . . . .	35
3.9	Partial sum contributions to the $\beta$ function against number of terms in the expansion of the series of (3.40), (3.41) and (3.42) . . . . .	36
3.10	Value of $\beta_1$ coefficient against number of terms in expansion . . . . .	37
3.11	Partial sum contributions to the $\beta$ function against number of terms in the expansion of the series of (3.49), (3.50), (3.53) and (3.54) . . .	41
3.12	Value of $\beta_1$ coefficient against number of terms in expansion . . . . .	41
5.1	1PI diagrams which by power counting alone require conditions (5.45) – (5.47) to be finite. (Curly lines represent $\mathcal{A}$ fields and straight lines $\mathcal{C}$ fields.) . . . . .	77
5.2	1PI diagrams from which the necessity of conditions (5.61)–(5.64) are demonstrated. . . . .	81
5.3	One-loop contributions to the $\mathcal{A}$ propagator . . . . .	86
C.1	Wine expansion, where the thick lines represent the full series. . . . .	107
C.2	Convention for wine labelling . . . . .	107

# List of Tables

4.1	Table of generators of $SU(N M)$	58
-----	----------------------------------	----

# Preface

Original work appears in chapters three (in collaboration with T.R. Morris) and five (in collaboration with S. Arnone, Yu.A. Kubyshin and T.R. Morris) and has appeared in:

- (i) T.R. Morris and J.F. Tighe, JHEP **08** (1999) 007.
- (ii) T.R. Morris and J.F. Tighe, Int. J. Mod. Phys. **A16** (2001) 2905.
- (iii) S. Arnone, Yu.A. Kubyshin, T.R. Morris and J.F. Tighe, [hep-th/0102011](#).
- (iv) S. Arnone, Yu.A. Kubyshin, T.R. Morris and J.F. Tighe, Int. J. Mod. Phys. **A16** (2001) 1989.
- (v) S. Arnone, Yu.A. Kubyshin, T.R. Morris and J.F. Tighe, [hep-th/0106258](#).

No claim to originality is made for the content of chapters one, two and four which were compiled using a variety of other sources.

---

# Acknowledgements

Firstly I wish to thank my supervisor Tim Morris, without whose cheerful enthusiasm, encouragement and guidance, this thesis would not exist. It is also a pleasure to thank my other collaborators Stefano Arnone and Yuri Kubyshin for all their assistance.

Next, I would like to express my gratitude to all the students, postdocs and staff who have made the SHEP group such a friendly and pleasant environment in which to work. A special mention should go to Alex Dougall and Luke Weston who always provided help, encouragement and good company.

Above all, I would like to thank my parents and my sister for their patience and ever present support.

# Chapter 1

## Introduction

Central to the acceptance of quantum field theories (QFTs) as the best description of physics on sub-nuclear scales, has been the deepening in understanding of the process of renormalisation. Through this development, the attitude towards the infinities that pervade QFT calculations has shifted from the opinion that they are a disease that has to be removed by a seemingly *ad hoc* mathematical trick, to the view that they are, in some sense, natural consequences of the underlying physics. This latter view has arisen from the insights gleaned from the formulation of the Wilsonian approach to the Renormalisation Group (RG) [1].

At the heart of this approach lies the concept of effective field theories. The viewpoint of the existence of a fundamental QFT (in the sense that it is valid for all particles at all energy scales) is abandoned, to be replaced by an effective theory that attempts only to describe physics up to a specified high energy cutoff. The Lagrangian that is suitable for this energy range is kept general in the sense that all possible interactions consistent with the symmetries of the system are included. There is no longer a problem with divergences (we have regularised). The issue now is that of predictive power; is the theory now capable of making predictions given that it contains an

infinite number of coupling constants? Remarkably, the answer can often be given in the affirmative. If it can be demonstrated that this is the case, this is equivalent to proving the renormalisability of the theory.

From such ideas, flow equations (that are non-perturbative in the coupling constants) for the QFT can be derived. However, to make progress with calculations it is often necessary to make approximations. One very powerful method is that of using the derivative expansion; a Taylor expansion in the momenta of the vertices of the QFT. An obvious issue which must be considered and which is addressed in this thesis, is under which conditions such an expansion converges.

The extension of the Wilsonian RG from scalar field theory where it has proved very powerful, to the more physically relevant topic, as far as particle physics is concerned, of gauge theories (specifically Yang-Mills theories) has been fraught with difficulty. The main problem lies with the incompatibility of restricting the momentum domain over which the theory is applied with the fact that observables are invariant under internal gauge symmetries.

Until recently, this obstacle has been tackled by initially breaking the gauge invariance with the aim of re-imposing it at the end of the calculation [2]. Obviously such a method is far from ideal. However, a fresh approach [3, 4, 5] enables gauge invariance to be maintained at all stages. This is achieved by first regularising via higher covariant derivatives, the gauge theory equivalent of a momentum space cutoff. It is well established though, that this cannot remove all divergences. However, by adding extra gauge invariant particles known as Pauli-Villars fields, complete regularisation can be achieved. It has been postulated that a similar but more elegant mechanism can be obtained by embedding the gauge group within a larger supersymmetric gauge group which is then spontaneously broken to regain the low energy physics of the original theory. We prove that this is the case in this thesis.

This thesis falls into two main parts and is structured as follows. Chapter 2 is an introductory chapter and presents some of the formalism and background necessary for dealing with the Wilsonian RG. Two versions of the flow equation are constructed followed by a discussion of how renormalisability is expressed within this framework. We conclude with a review of some approximation methods in current use. Chapter 3 then considers some of the conditions necessary for one such approximation method, the derivative expansion, to converge. The Wilson/Polchinski and Legendre flow equations are considered at one and two loops for the  $\beta$  function of scalar  $\lambda\varphi^4$  field theory for a variety of cutoffs. Chapter 4 is another introductory chapter, this time concentrating on the problems concerned with constructing a gauge invariant regularisation scheme compatible with Wilsonian ideas, and some of the group theoretical background for the scheme introduced in chapter 5. The final chapter sets up the regularisation scheme utilising higher covariant derivatives and supersymmetric gauge groups and demonstrates that it does indeed render the desired theory finite.

# Chapter 2

## Exact renormalisation group

### 2.1 Wilson's renormalisation group

The concepts that provide the basis of the exact renormalisation group were first formulated within the context of statistical field theory by Wilson and co-workers [1]. The problem of performing calculations concerning *e.g.* a lattice of spins is exacerbated when the system is undergoing a continuous phase transition since the (already large) number of degrees of freedom which are effectively interacting with one another, diverges in this regime. A procedure for systematically reducing the degrees of freedom yet retaining the basic physics of the model is the concept of blocking, first introduced by Kadanoff [6].

This is the idea that in *e.g.* an array of spins such as a ferromagnet, spins could be grouped together into blocks and treated as if they were single spins with local interactions.<sup>1</sup> Of course these ‘new’ interactions would not be exactly the same as in the original and on short scales the new system would differ markedly from the

---

<sup>1</sup>But not necessarily just nearest neighbour interactions.

old one. However they exhibit the same *long* distance behaviour and it is only this behaviour that we are interested in describing. Since the number of degrees of freedom falls with this procedure, iteration reduces them to a manageable level. The payment for this is that the new system will in general be much more complicated than the original, containing as it does many new interactions. However, as we shall see in the context of quantum field theory, we can obtain flow equations for the changes in coupling constants of the new interactions with the iteration of the procedure and thus extract much useful information from this.

This thesis is concerned with the exact RG<sup>2</sup> which takes these ideas and applies them to quantum field theories directly in the continuum and as such, we will no longer refer to statistical mechanics examples. As we shall see there are a number of different (but equivalent) flow equations that can be derived using the exact RG approach. The work in this chapter is based upon that of [7]–[12] unless otherwise specified.

## 2.2 Wilson/Polchinski flow equation

The partition function for a single scalar field  $\varphi$  in  $D$  Euclidean spacetime dimensions is given by<sup>3</sup>

$$Z[J] = \int \mathcal{D}\varphi \exp\left\{-\frac{1}{2}\varphi \cdot \Delta^{-1} \cdot \varphi - S_{\Lambda_0}^{\text{int}}[\varphi] + J \cdot \varphi\right\}, \quad (2.1)$$

with the propagator denoted by  $\Delta$ , the (bare) interactions contained within  $S_{\Lambda_0}^{\text{int}}$  and we have included a source  $J$  for the field. An effective ultra-violet cutoff is introduced via a modification of the propagator

$$\Delta = \frac{1}{q^2} \quad \rightarrow \quad \Delta_{UV} = \frac{C_{UV}(q^2/\Lambda^2)}{q^2}. \quad (2.2)$$

---

<sup>2</sup>Also referred to as the continuum RG.

<sup>3</sup>The following shorthand is employed  $a \cdot b \cdot c = \int d^D x \int d^D y a(x) b(x, y) c(y)$ ,  
 $d \cdot e = \int d^D x d(x) e(x)$

$C_{UV}(q^2/\Lambda^2)$  is an as yet unspecified function of its argument (the argument has to be  $q^2/\Lambda^2$  from Lorentz invariance and dimensions) with the properties  $C_{UV}(0) = 1$  and  $C_{UV} \rightarrow 0$  sufficiently fast as  $q \rightarrow \infty$ . In a similar fashion, we define an IR modified propagator  $\Delta_{IR} = C_{IR}(q^2/\Lambda^2)/q^2$  (with  $C_{UV}(p^2/\Lambda^2) + C_{IR}(p^2/\Lambda^2) = 1$ ). Figure 2.1 shows the properties of these cutoff functions.

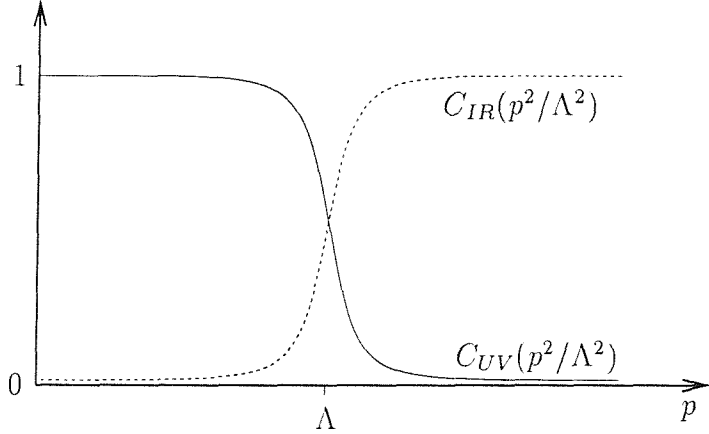


Figure 2.1: Sketch of the properties of the cutoff functions

Although it is not immediately obvious, we are able to rewrite (2.1) (up to an uninteresting constant of proportionality which we drop) as

$$Z[J] = \int \mathcal{D}\varphi_> \mathcal{D}\varphi_< \exp\left\{-\frac{1}{2}\varphi_> \cdot \Delta_{IR}^{-1} \cdot \varphi_> - \frac{1}{2}\varphi_< \cdot \Delta_{UV}^{-1} \cdot \varphi_< - S_{\Lambda_0}^{\text{int}}[\varphi_> + \varphi_<] + J \cdot (\varphi_> + \varphi_<)\right\}, \quad (2.3)$$

The equivalence of (2.3) to (2.1) is evident once the substitutions

$$\varphi_> = \varphi - \varphi_<, \quad \text{followed by} \quad \varphi_< = \varphi' + C_{UV} \cdot \varphi \quad (2.4)$$

are made in (2.3). This leaves (2.3) in the form

$$Z[J] = \int \mathcal{D}\varphi \mathcal{D}\varphi' \exp\left\{-\frac{1}{2}\varphi \cdot \Delta^{-1} \cdot \varphi - \frac{1}{2}\varphi' \cdot (\Delta_{UV}^{-1} + \Delta_{IR}^{-1}) \cdot \varphi' - S_{\Lambda_0}^{\text{int}}[\varphi] + J \cdot \varphi\right\}, \quad (2.5)$$

at which point the Gaussian integral over  $\varphi'$  can be performed, resulting in (2.1) (up

to the aforementioned constant of proportionality).

From the manner in which it propagates, the  $\varphi_>$  ( $\varphi_<$ ) can be interpreted as the momentum modes higher (lower) than  $\Lambda$ , with the modes lower (higher) than  $\Lambda$  damped. If the integral over the higher modes is isolated in (2.3), it can be expressed as

$$Z[J] = \int \mathcal{D}\varphi_< \exp\left\{-\frac{1}{2}\varphi_< \cdot \Delta_{UV}^{-1} \cdot \varphi_<\right\} Z_\Lambda[\varphi_<, J], \quad (2.6)$$

where  $Z_\Lambda[\varphi_<, J]$  is defined as

$$Z_\Lambda[\varphi_<, J] = \int \mathcal{D}\varphi_> \exp\left\{-\frac{1}{2}\varphi_> \cdot \Delta_{IR}^{-1} \cdot \varphi_> - S_{\Lambda_0}^{\text{int}}[\varphi_> + \varphi_<] + J \cdot (\varphi_> + \varphi_<)\right\}. \quad (2.7)$$

However,  $Z_\Lambda[\varphi_<, J]$  does not depend upon  $\varphi_<$  and  $J$  separately but rather on the sum  $\Delta_{IR} \cdot J + \varphi_<$ . Upon the substitution  $\varphi_> = \varphi - \varphi_<$ , (2.7) becomes

$$Z_\Lambda[\varphi_<, J] = \exp\left\{-\frac{1}{2}\varphi_< \cdot \Delta_{IR}^{-1} \cdot \varphi_<\right\} \int \mathcal{D}\varphi \exp\left\{-\frac{1}{2}\varphi \cdot \Delta_{IR}^{-1} \cdot \varphi - S_{\Lambda_0}^{\text{int}}[\varphi] + \varphi \cdot (J + \Delta_{IR}^{-1} \cdot \varphi_<)\right\} \quad (2.8)$$

We proceed by integrating over the  $\varphi$  variable to obtain

$$\begin{aligned} Z_\Lambda[\varphi_<, J] &= \exp\left\{-\frac{1}{2}\varphi_< \cdot \Delta_{IR}^{-1} \cdot \varphi_<\right\} \times \\ &\quad \times \exp\left\{-S_{\Lambda_0}^{\text{int}}\left[\frac{\delta}{\delta J}\right]\right\} \exp\left\{\frac{1}{2}(J + \Delta_{IR}^{-1} \cdot \varphi_<) \cdot \Delta_{IR} \cdot (J + \Delta_{IR}^{-1} \cdot \varphi_<)\right\} \\ &= \exp\left\{\frac{1}{2}J \cdot \Delta_{IR} \cdot J + J \cdot \varphi_<\right\} \exp\left\{-\frac{1}{2}(J + \Delta_{IR}^{-1} \cdot \varphi_<) \cdot \Delta_{IR} \cdot (J + \Delta_{IR}^{-1} \cdot \varphi_<)\right\} \times \\ &\quad \times \exp\left\{-S_{\Lambda_0}^{\text{int}}\left[\frac{\delta}{\delta J}\right]\right\} \exp\left\{\frac{1}{2}(J + \Delta_{IR}^{-1} \cdot \varphi_<) \cdot \Delta_{IR} \cdot (J + \Delta_{IR}^{-1} \cdot \varphi_<)\right\}. \end{aligned} \quad (2.9)$$

When the derivatives in  $S_{\Lambda_0}^{\text{int}}\left[\frac{\delta}{\delta J}\right]$  are performed, they are replaced by either  $\Delta_{IR} \cdot J + \varphi_<$  or by  $\Delta_{IR}$ , a fact which can be expressed as

$$Z_\Lambda[\varphi_<, J] = \exp\left\{\frac{1}{2}J \cdot \Delta_{IR} \cdot J + J \cdot \varphi_< - S_\Lambda[\Delta_{IR} \cdot J + \varphi_<]\right\}, \quad (2.10)$$

for some functional  $S_\Lambda$ , confirming the statement given below (2.7). We refer to  $S_\Lambda$

as the Wilsonian effective action.

The exact RG flow equations follow from the observation that (2.7) carries its dependence upon  $\Lambda$  entirely in the  $\varphi_> \cdot \Delta_{IR}^{-1} \cdot \varphi_>$  term. Consequently, when  $Z_\Lambda$  is differentiated with respect to  $\Lambda$ , the flow equation for  $Z_\Lambda$  is found to be

$$\frac{\partial}{\partial \Lambda} Z_\Lambda[\varphi_<, J] = -\frac{1}{2} \left( \frac{\delta}{\delta J} - \varphi_< \right) \cdot \left( \frac{\partial}{\partial \Lambda} \Delta_{IR}^{-1} \right) \cdot \left( \frac{\delta}{\delta J} - \varphi_< \right) Z_\Lambda[\varphi_<, J]. \quad (2.11)$$

By explicitly performing these functional derivatives using (2.10), Polchinski's version of the Wilson flow equation<sup>4</sup> is obtained<sup>5</sup> (we shall refer to it as the Wilson/Polchinski flow equation):

$$\frac{\partial}{\partial \Lambda} S_\Lambda[\varphi] = \frac{1}{2} \frac{\delta S_\Lambda}{\delta \Lambda} \cdot \frac{\partial \Delta_{UV}}{\partial \Lambda} \cdot \frac{\delta S_\Lambda}{\delta \Lambda} - \frac{1}{2} \text{Tr} \frac{\partial \Delta_{UV}}{\partial \Lambda} \cdot \frac{\delta^2 S_\Lambda}{\delta \varphi \delta \varphi}. \quad (2.12)$$

Furthermore, with the momentum expanded action given by

$$S(\mathbf{p}_1, \dots, \mathbf{p}_n; \Lambda) \equiv \frac{\delta^n S_\Lambda[\varphi]}{\delta \varphi(\mathbf{p}_1) \cdots \delta \varphi(\mathbf{p}_n)}, \quad (2.13)$$

we can obtain the momentum expanded Wilson/Polchinski flow equation which will be extensively used in chapter 3:

$$\begin{aligned} \frac{\partial}{\partial \Lambda} S(\mathbf{p}_1, \dots, \mathbf{p}_n; \Lambda) &= \sum_{\{I_1, I_2\}} S(-\mathbf{P}_1, I_1; \Lambda) K_\Lambda(P_1) S(\mathbf{P}_1, I_2; \Lambda) \\ &\quad - \frac{1}{2} \int \frac{d^4 q}{(2\pi)^4} K_\Lambda(q) S(\mathbf{q}, -\mathbf{q}, \mathbf{p}_1, \dots, \mathbf{p}_n; \Lambda), \end{aligned} \quad (2.14)$$

where  $I_1$  and  $I_2$  are disjoint subsets of external momenta such that  $I_1 \cap I_2 = \emptyset$  and  $I_1 \cup I_2 = \{\mathbf{p}_1, \dots, \mathbf{p}_n\}$ , and we define  $K_\Lambda(p) \equiv \frac{\partial}{\partial \Lambda} \Delta_{UV}(p^2/\Lambda^2)$ . The sum over  $\{I_1, I_2\}$  utilises the Bose symmetry so pairs are counted only once *i.e.*  $\{I_1, I_2\} = \{I_2, I_1\}$ .

---

<sup>4</sup>Wilson's version is recovered from that of Polchinski via the substitution  $\mathcal{H} = -S$  and the change of variables  $\varphi \rightarrow \varphi \sqrt{C_{UV}}$ .

<sup>5</sup> $\text{Tr}$  stands for a spacetime trace *i.e.*  $\text{Tr}(a \cdot b) = \int d^D x \int d^D y a(x, y) b(y, x)$ .

The momentum  $\mathbf{P}_1$  is defined to be  $\mathbf{P}_1 = \sum_{\mathbf{p}_i \in I_1} \mathbf{p}_i$ . The equation can be represented graphically as in figure 2.2, which manifestly displays how the Wilson/Polchinski flow equation is composed of a tree structure contribution and a one-particle irreducible (1PI) part.

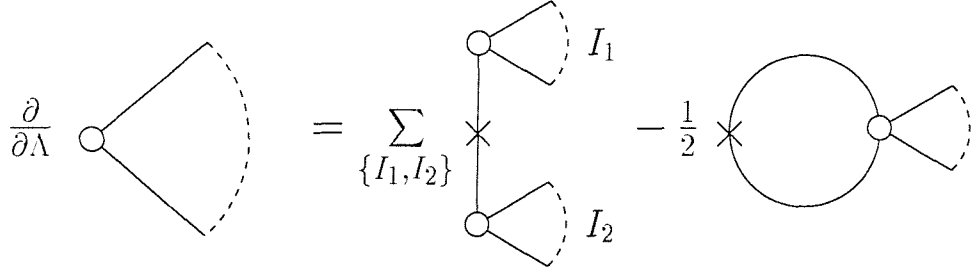


Figure 2.2: Graphical representation of the momentum expanded Wilson/Polchinski flow equation. Crosses denote differentiation with respect to  $\Lambda$ .

## 2.3 Legendre flow equation

We need not consider a Wilson inspired RG flow equation only for the action. A flow equation for the Legendre effective action may also be constructed which has many additional beneficial properties. We start by observing that the cutoff  $\Lambda$  can also be regarded as an infrared cutoff for the modes that have already been integrated out. This can most easily be seen in (2.7) which we can reinterpret as the partition function of an infrared cutoff theory with  $\varphi_<$  regarded as an external field.

We start by introducing the Wilsonian generating functional for connected Green's functions  $W_\Lambda[\varphi_<, J] \equiv \ln Z_\Lambda[\varphi_<, J]$ . Furthermore, with the classical field  $\phi^{cl}$  defined via  $\phi^{cl} \equiv \delta W_\Lambda / \delta J$ , we can construct  $\Gamma_\Lambda[\phi^{cl}]$ , the interaction part of the Legendre effective action:

$$\frac{1}{2}(\phi^{cl} - \varphi_<) \cdot \Delta_{IR}^{-1} \cdot (\phi^{cl} - \varphi_<) + \Gamma_\Lambda[\phi^{cl}] = -W_\Lambda[\varphi_<, J] + J \cdot \phi^{cl}. \quad (2.15)$$

Using (2.11) we obtain the flow equation for  $W_\Lambda$

$$\frac{\partial}{\partial \Lambda} W_\Lambda = -\frac{1}{2} \left\{ \left( \frac{\delta W_\Lambda}{\delta J} - \varphi_{<} \right) \cdot \left( \frac{\partial}{\partial \Lambda} \Delta_{IR}^{-1} \right) \cdot \left( \frac{\delta W_\Lambda}{\delta J} - \varphi_{<} \right) + \text{Tr} \left( \frac{\delta^2 W_\Lambda}{\delta J \delta J} \cdot \frac{\partial}{\partial \Lambda} \Delta_{IR}^{-1} \right) \right\}, \quad (2.16)$$

where **Tr** again denotes a spacetime trace. From (2.15) we can derive the relation

$$\frac{\delta^2 W_\Lambda}{\delta J \delta J} = \left( \Delta_{IR}^{-1} + \frac{\delta^2 \Gamma_\Lambda}{\delta \phi^{cl} \delta \phi^{cl}} \right)^{-1}, \quad (2.17)$$

which, after exploiting (2.15) once more, results in the following flow equation for the effective action:

$$\frac{\partial}{\partial \Lambda} \Gamma_\Lambda[\phi^{cl}] = \frac{1}{2} \text{Tr} \left\{ \frac{\partial \Delta_{IR}^{-1}}{\partial \Lambda} \cdot \left( \Delta_{IR}^{-1} + \frac{\delta^2 \Gamma_\Lambda}{\delta \phi^{cl} \delta \phi^{cl}} \right)^{-1} \right\}. \quad (2.18)$$

This equation is most usefully expressed when we separate off the uninteresting vacuum energy by splitting the two-point function into its field dependent and field independent (effective self energy) parts:

$$\frac{\delta^2 \Gamma_\Lambda}{\delta \phi_x^{cl} \delta \phi_y^{cl}} = \hat{\Gamma}_{xy}[\phi^{cl}] + \Sigma_{xy}. \quad (2.19)$$

This leads to the equation we shall refer to as the Legendre flow equation:

$$\frac{\partial}{\partial \Lambda} \Gamma[\varphi^c] = -\frac{1}{2} \text{Tr} \left\{ \frac{K_\Lambda}{(1 + \Delta_{IR} \Sigma)^2} \cdot \hat{\Gamma} \cdot (1 + [\Delta_{IR}^{-1} + \Sigma]^{-1} \cdot \hat{\Gamma})^{-1} \right\}. \quad (2.20)$$

In the work contained in chapter 3, the most useful form of this expression is in terms of a flow equation for the 1PI vertices

$$\frac{\partial}{\partial \Lambda} \Gamma(p_1, \dots, p_n; \Lambda) = \int \frac{d^4 q}{(2\pi)^4} \frac{q^2 \frac{\partial}{\partial \Lambda} C_{UV}(q^2/\Lambda^2)}{[q^2 + C_{IR}(q^2/\Lambda^2) \Sigma(q; \Lambda)]^2} E(q, p_1, \dots, p_n; \Lambda), \quad (2.21)$$

where

$$\begin{aligned}
E(\mathbf{q}, \mathbf{p}_1, \dots, \mathbf{p}_n; \Lambda) = & -\frac{1}{2} \Gamma(\mathbf{q}, -\mathbf{q}, \mathbf{p}_1, \dots, \mathbf{p}_n; \Lambda) \\
& + \sum_{\{I_1, I_2\}} \Gamma(\mathbf{q}, -\mathbf{q} - \mathbf{P}_1, I_1; \Lambda) G(|\mathbf{q} + \mathbf{P}_1|; \Lambda) \Gamma(\mathbf{q} - \mathbf{P}_2, -\mathbf{q}, I_2; \Lambda) \\
& - \sum_{\{I_1, I_2\}, I_3} \Gamma(\mathbf{q}, -\mathbf{q} - \mathbf{P}_1, I_1; \Lambda) G(|\mathbf{q} + \mathbf{P}_1|; \Lambda) \times \\
& \quad \Gamma(\mathbf{q} + \mathbf{P}_1, -\mathbf{q} + \mathbf{P}_2, I_3; \Lambda) G(|\mathbf{q} - \mathbf{P}_2|; \Lambda) \Gamma(\mathbf{q} - \mathbf{P}_2, -\mathbf{q}, I_2; \Lambda) \\
& + \dots . \quad (2.22)
\end{aligned}$$

Similarly to before,  $\mathbf{P}_i = \sum_{\mathbf{p}_j \in I_i} \mathbf{p}_j$  and  $\sum_{\{I_1, I_2\}, I_3, \dots, I_m}$  is a sum over disjoint subsets  $I_i \cap I_j = \emptyset$  ( $\forall i, j$ ) with  $\bigcup_{i=1}^m I_i = \{\mathbf{p}_1, \dots, \mathbf{p}_n\}$ . Again, the symmetrization  $\{I_1, I_2\}$  means this pair is counted only once.  $G(p; \Lambda)$  is defined by

$$G(p; \Lambda) \equiv \frac{C_{IR}(p^2/\Lambda^2)}{p^2 + C_{IR}(p^2/\Lambda^2)\Sigma(p; \Lambda)} \quad (2.23)$$

where  $\Sigma$  is again the (field independent) self energy.

All the equations following (2.20) apply to smooth cutoff profiles only, as care needs to be taken with regard to sharp cutoffs. If we denote the width over which the cutoff effectively varies as  $2\epsilon$ , *i.e.*  $C_{UV}(q^2/\Lambda^2) \approx 1$  for  $q < \Lambda - \epsilon$  and  $C_{UV}(q^2/\Lambda^2) \approx 0$  for  $q > \Lambda + \epsilon$ , we can investigate the effect of letting  $\epsilon \rightarrow 0$ . First we need to establish the following lemma:

$$-\left(\frac{\partial}{\partial \Lambda} C_{IR}(p^2/\Lambda^2)\right) f(C_{IR}(p^2/\Lambda^2), \Lambda) \rightarrow \delta(\Lambda - p) \int_0^1 dt f(t, p) \quad \text{as } \epsilon \rightarrow 0, \quad (2.24)$$

in which we require  $f(C_{IR}, \Lambda)$  to be a function whose dependence upon  $\Lambda$  is continuous at  $\Lambda = p$  as  $\epsilon \rightarrow 0$ . The proof of (2.24) lies with the identity

$$\left[ \frac{\partial}{\partial \Lambda} \int_{C_{IR}(p^2/\Lambda^2)}^1 dt f(t, \Lambda_1) \right] \Big|_{\Lambda_1=\Lambda} = -\left(\frac{\partial}{\partial \Lambda} C_{IR}(p^2/\Lambda^2)\right) f(C_{IR}(p^2/\Lambda^2), \Lambda). \quad (2.25)$$

We now note that the integral on the left hand side (LHS) is a representation of a (smoothed) step function of height  $\int_0^1 dt f(t, \Lambda_1)$ . On taking the limit  $\epsilon \rightarrow 0$ , the LHS of (2.25) becomes the right hand side (RHS) of (2.24). Thus we find, for example

$$\begin{aligned} -\left(\frac{\partial}{\partial \Lambda} C_{IR}(p^2/\Lambda^2)\right) C_{IR}(p^2/\Lambda^2) &\rightarrow \frac{1}{2}\delta(\Lambda - p), \\ -\left(\frac{\partial}{\partial \Lambda} C_{IR}(p^2/\Lambda^2)\right) C_{IR}^2(p^2/\Lambda^2) &\rightarrow \frac{1}{3}\delta(\Lambda - p), \quad \text{etc.}, \end{aligned} \quad (2.26)$$

in the sharp cutoff limit.

Thus returning to (2.20) we now have the mathematical tools to allow the cutoff to become sharp. We find

$$\frac{\partial}{\partial \Lambda} \Gamma(p_1, \dots, p_n; \Lambda) = \int \frac{d^4 q}{(2\pi)^4} \frac{\delta(q - \Lambda)}{q^2 + \Sigma(q; \Lambda)} E(q, p_1, \dots, p_n; \Lambda), \quad (2.27)$$

where  $E(q, p_1, \dots, p_n; \Lambda)$  is as given in (2.22) except now  $G(p; \Lambda)$  is defined by

$$G(p; \Lambda) \equiv \frac{\theta(p - \Lambda)}{p^2 + \Sigma(p; \Lambda)}. \quad (2.28)$$

## 2.4 Renormalisability

Perhaps the greatest success to date of the Wilsonian approach has been the elegance with which the issue of renormalisability is addressed. The standard cumbersome and complicated method involving skeleton expansions is replaced by a much more physically intuitive argument. As mentioned in chapter 1, it is now a question of whether the theory retains any predictive power with an infinite number of couplings. One manner in which this could be demonstrated is via the introduction of an overall cutoff  $\Lambda_0$ , and to check the  $\Lambda_0 \rightarrow \infty$  limit exists. However, the exact RG does not require such artificial constructions and allows us to deal directly in the continuum using renormalised quantities, an approach which we will follow here. In this section

we will use only dimensionless quantities constructed from the dimensionful ones using appropriate powers of  $\Lambda$ .

A fixed point of the flow of the action<sup>6</sup> in the space of all possible (*i.e.* an infinite number of) interactions,  $S^*$ , is defined by

$$\Lambda \frac{\partial}{\partial \Lambda} S^*[\varphi] = 0. \quad (2.29)$$

Since the flow equation is written in terms of dimensionless quantities, the independence of  $\Lambda$  exhibited by  $S^*$  means that the action at the fixed point must have no scale dependence at all. Since a massive theory has a mass to set a scale and a non-continuum theory has an upper cutoff to perform the same rôle, we conclude that the physics of massless continuum theories must be described entirely by fixed points.

Near a fixed point, we introduce new couplings

$$\eta_i = g_i - g_i^*, \quad (2.30)$$

where  $g_i^*$  is the value of the coupling at the fixed point. We can then approximate the flow of these couplings as

$$\Lambda \frac{\partial \eta_i}{\partial \Lambda} = \sum_j Y_{ij} \eta_j, \quad (2.31)$$

where we have neglected contributions of  $O(\eta^2)$  and higher, and  $Y_{ij}$  is a matrix of constants. The eigenvalues and eigenvectors of  $Y$  are defined by

$$\sum_j Y_{ij} \xi_j^{(k)} = -\lambda_k \xi_i^{(k)} \quad (\text{no sum on } k). \quad (2.32)$$

---

<sup>6</sup>These arguments also be extended to the case of the Legendre flow equation.

The couplings can be expanded in terms of these eigenvectors

$$\eta_i = \sum_k \alpha_k \xi_i^{(k)}, \quad (2.33)$$

and (2.31) requires that the  $\Lambda$ -dependent coefficients  $\alpha_k$  satisfy

$$\Lambda \frac{\partial \alpha_i(\Lambda)}{\partial \Lambda} = -\lambda_i \alpha_i(\Lambda) \quad (\text{no sum on } i), \quad (2.34)$$

where again we have neglected terms of  $O(\alpha^2)$ . This implies that to linear order, we have

$$\eta_i(\Lambda) = \sum_j \left(\frac{\mu}{\Lambda}\right)^{\lambda_j} \alpha_j(\mu) \xi_i^{(j)}, \quad (2.35)$$

for some arbitrary mass scale  $\mu$ . Thus near a fixed point a coupling can flow away from the fixed point value or towards it depending on whether  $\lambda_i$  is positive or negative.<sup>7</sup> The  $\eta_i$  (or  $g_i$ ) for which  $\lambda_i > 0$  are referred to as *relevant* couplings and those where  $\lambda_i < 0$  are known as *irrelevant*. In the vicinity of the fixed point we can also write (to linear order)

$$S_\Lambda[\varphi] = S^* + \sum_i \alpha^i(\mu) \left(\frac{\mu}{\Lambda}\right)^{\lambda_i} \mathcal{O}_i[\varphi], \quad (2.36)$$

which defines the scaling operators  $\mathcal{O}_i$ .

This formalism allows us to tackle the slightly less straight forward situation of massive theories. In the (infinite dimensional) space of actions through which RG trajectories flow, we are able to define the critical manifold. This manifold contains all the actions that will yield a massless continuum limit. The critical manifold is spanned by the infinite number of irrelevant operators with other directions spanned by (typically only one) relevant operators.

After parameterising the bare action, we are able to move slightly off the critical

---

<sup>7</sup>If  $\lambda_i = 0$  the behaviour has to be followed to second order where the power law dependency is replaced by logarithmic evolution. In the following discussion these so-called marginal couplings will not be explicitly considered.

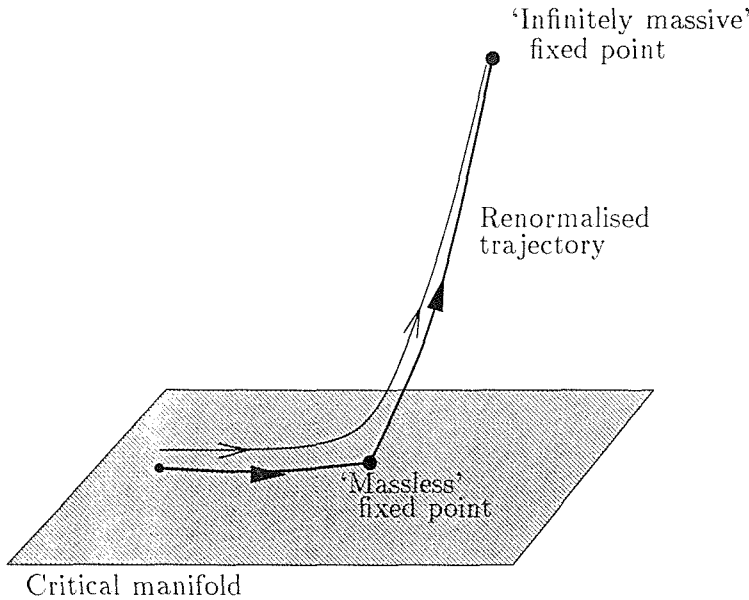


Figure 2.3: Procedure for tuning to the massive continuum limit

manifold (see figure 2.3). Initially the RG flow will still move towards the fixed point. However as the fixed point is approached, the flow will shoot off along one of the relevant directions to reach a fixed point that describes an infinitely massive theory. The continuum limit of a (finite) massive theory can be extracted by the following procedure. With the bare action being tuned back towards the critical manifold, physical quantities are re-expressed in terms of renormalised ones accounting for the diverging correlation length. When it reaches the critical manifold, the RG trajectory splits into a part going into the fixed point and a part that leaves the fixed point in the relevant directions. This is known as a renormalised trajectory and the actions that lie upon it are referred to as ‘perfect actions’. The end of this path has a finite limit when expressed in renormalised quantities. This trajectory is determined by

$$S_\Lambda[\varphi] = S^*[\varphi] + \sum_{\substack{j=1 \\ \{\text{relevant}\}}}^n \alpha^j \left(\frac{\mu}{\Lambda}\right)^{\lambda_j} \mathcal{O}_j[\varphi], \quad (2.37)$$

(the sum over  $j$  is restricted to the  $n$  relevant directions).

Thus given the boundary condition (2.37) and the RG flow equation, the continuum

limit is fully specified

$$S_\Lambda[\varphi] \equiv S_\Lambda[\varphi](\alpha^1, \dots, \alpha^n). \quad (2.38)$$

The next step is to define the renormalised couplings  $g^i(\Lambda)$ . We choose the renormalisation conditions such that

$$g^j \sim \alpha^j (\mu/\Lambda)^{\lambda_j} \quad (2.39)$$

as  $\Lambda \rightarrow \infty$  to be consistent with the form of  $\mathcal{O}_j[\varphi]$ . But these relations can also be inverted *i.e.*

$$\alpha^j = \lim_{\Lambda \rightarrow \infty} \left( \frac{\Lambda}{\mu} \right)^{\lambda_j} g^j(\Lambda), \quad (2.40)$$

and substituting into (2.38) returns the continuum action in terms of the renormalised field ( $\varphi$ ) the relevant renormalised couplings ( $g^1$  to  $g^n$ ) and the anomalous dimension<sup>8</sup> ( $\gamma$ ):

$$S_\Lambda[\varphi] \equiv S_\Lambda[\varphi](g^1(\Lambda), \dots, g^n(\Lambda), \gamma(\Lambda)), \quad (2.41)$$

and  $n$  is finite. This is an equivalent statement to renormalisability since only a finite number of finite quantities need be considered in describing the theory.

## 2.5 $\beta$ function

An important concept in the field of QFTs is that of  $\beta$  functions. This contains information on how the renormalised couplings<sup>9</sup> ( $g_i$ ) vary according to scale and is defined as:

$$\beta_i := \Lambda \frac{\partial}{\partial \Lambda} g_i(\Lambda) \quad (2.42)$$

---

<sup>8</sup>The anomalous dimension ( $\gamma$ ) is obtained from the wavefunction renormalisation ( $Z$ ) via  $\gamma = \Lambda \frac{\partial}{\partial \Lambda} Z$ . The wavefunction renormalisation factor is introduced to ensure the coefficient of the kinetic term is  $\frac{1}{2}$ .

<sup>9</sup>i.e. we restrict ourselves to the relevant directions.

In the next chapter we will make extensive use of the  $\beta$  function for  $\lambda\varphi^4$  scalar field theory. It will prove useful to include wavefunction renormalisation separately within these calculations so there we choose to redefine it as

$$\beta(\lambda) = \Lambda \frac{\partial}{\partial \Lambda} \frac{\lambda}{Z^2(\Lambda)}, \quad (2.43)$$

where  $Z$  is the wavefunction renormalisation. An important property displayed by the  $\beta$  function is that the first two orders in the perturbative expansion are universal, *i.e.* they are independent of renormalisation scheme. We write the perturbative expansion as

$$\beta(\lambda) = \beta_0 \lambda^2 + \beta_1 \lambda^3 + \dots \quad (2.44)$$

If we have another renormalisation scheme with different coupling  $\lambda'$ , we can define a  $\beta$  function for this scheme as well:

$$\beta(\lambda') = \beta'_0 \lambda'^2 + \beta'_1 \lambda'^3 + \dots \quad (2.45)$$

The couplings in the two schemes must be related

$$\lambda' = \lambda + a_1 \lambda^2 + \dots, \quad (2.46)$$

which can be re-written as

$$\lambda = \lambda' - a_1 \lambda'^2 + \dots \quad (2.47)$$

If we operate with  $\Lambda \frac{\partial}{\partial \Lambda}$  upon (2.47) and use the definition of (2.42) we find

$$\beta_0 \lambda^2 + \beta_1 \lambda^3 + \dots = \beta'_0 \lambda'^2 + \beta'_1 \lambda'^3 - 2a_1 \lambda' (\beta'_0 \lambda'^2 + \beta'_1 \lambda'^3) + \dots, \quad (2.48)$$

and expressing  $\lambda'$  as a function of  $\lambda$  on the RHS of (2.48) shows that

$$\beta_0 \lambda^2 + \beta_1 \lambda^3 + \dots = \beta'_0 \lambda^2 + \beta'_1 \lambda^3 + \dots, \quad (2.49)$$

from which we can see that, as promised,  $\beta'_0 = \beta_0$  and  $\beta'_1 = \beta_1$ . The  $\beta$  function for massless  $\lambda\varphi^4$  theory in four dimensions can be calculated using standard perturbation theory [14] to be

$$\beta(\lambda) = 3\frac{\lambda^2}{(4\pi)^2} - \frac{17}{3}\frac{\lambda^3}{(4\pi)^4} + O(\lambda^4). \quad (2.50)$$

## 2.6 Approximations

The complexity of the flow equations has prevented the formulation of general solutions. This has resulted in a number of approximation techniques being developed and investigated. In this section two of the most widely used methods are discussed.

### 2.6.1 Truncation

The most obvious method of approximation that can be employed is to truncate the number of operators that appear in the effective action  $S_\Lambda$ . We can then construct a number of flow equations for the coefficients of these operators by equating the terms on the two sides of the original flow equation (2.12) [or (2.20)]. The approximation lies in neglecting terms from the RHS of the equation which are not members of the chosen set of operators.

The main problem with using such an approximation scheme is its restricted area of applicability. Since this approach corresponds to a truncation in the powers of the field about a selected point, sensible answers can only be obtained if the field  $\varphi$  does not fluctuate much. This amounts to stating that  $\varphi$  is always close to the mean field, a regime in which weak coupling theory is valid anyhow. In non-perturbative settings it is found that the expansion fails to converge and spurious fixed points are also generated [10].

## 2.6.2 Derivative/momentum scale expansion

Within statistical mechanics a successfully applied approximation has been truncations in real space spin systems. The analogue in QFT is to perform a short distance expansion of the effective action. If the cutoff utilised has a smooth profile, this corresponds to a derivative expansion

$$S_\Lambda \sim \int d^D x \left\{ V(\varphi, \Lambda) + \frac{1}{2} (\partial_\mu \varphi)^2 K(\varphi, \Lambda) + O(\partial^4) \right\}, \quad (2.51)$$

Such an expansion seems a particularly natural one, amounting to an expansion in external momenta around  $\mathbf{p} = \mathbf{0}$ . If the higher derivative terms are not ‘small’ the expansion will fail, but this is probably also an indication that the description of the theory in terms of the field content is not appropriate and that other degrees of freedom need to be considered.

When a sharp cutoff is imposed, care needs to be taken when taking a short distance expansion. Due to the non-analyticity that is introduced, we are no longer able to expand in powers of momentum. The solutions to the flow equation (2.27) depend upon the angles between the  $\mathbf{p}_i$  even when any  $\mathbf{p}_i \rightarrow 0$ ; *i.e.* the solutions are not analytic in this regime. This behaviour is displayed by terms such as  $\theta(|\mathbf{p} + \mathbf{q}| - \Lambda) \sim \theta(\mathbf{q} \cdot \mathbf{p})$  for  $p \ll \Lambda$  since  $|\mathbf{q}| = \Lambda$ , which could appear in the second term of (2.22). As a consequence, expansions have to be made in momentum scale  $|\mathbf{p}|$ .

It is evident that if a sharp cutoff (*i.e.*  $C_{UV}(p^2/\Lambda^2) = \theta(\Lambda - p)$ ) is employed then the momentum scale expansion of the Wilson/Polchinski equation runs into additional problems. The expansion corresponds to expanding  $S_\Lambda$  in the scale of external momenta, regarding this as small compared to  $\Lambda$ . The differentiation of the internal propagator of the tree term of (2.14) (*c.f.* figure 2.2) results in a delta function restricting momentum flow to be  $\Lambda$ . However momentum conservation requires the flow should be of order the external momenta which is typically much lower. Conse-

quently, the tree term of the Wilson/Polchinski equation gets discarded along with loop diagrams with more than one vertex (since these arise from the substitution of the tree parts of  $S_\Lambda$  into the second term of the equation). Since this is such a great mutilation of the theory we apply the such an expansion only to the 1PI parts of the action, *i.e.* only to the Legendre flow equation.

The momentum scale expansion can be incorporated via the introduction of a parameter,  $\rho$ , which can be set equal to one at a later time. The 1PI vertices of (2.22) are expanded in terms of homogeneous functions of non-negative integer degree

$$\Gamma(\mathbf{p}_1, \dots, \mathbf{p}_n; \Lambda) = \sum_{m=0}^{\infty} \Gamma^{(m)}(\mathbf{p}_1, \dots, \mathbf{p}_n; \Lambda) \quad (2.52)$$

where we define  $\Gamma^{(m)}(\mathbf{p}_1, \dots, \mathbf{p}_n; \Lambda)$  via

$$\Gamma^{(m)}(\rho \mathbf{p}_1, \dots, \rho \mathbf{p}_n; \Lambda) = \rho^m \Gamma^{(m)}(\mathbf{p}_1, \dots, \mathbf{p}_n; \Lambda) \quad (2.53)$$

Other external momentum dependence in the flow equation can also be expanded in integer degree homogeneous functions.

The approximation lies in restricting these sums over an infinite number of terms to some designated order. If the derivative/momentum scale expansion is truncated at  $O(p^0)$ , we obtain the well established local potential approximation which has proved to be both reliable and accurate [15].

Of the approximation methods mentioned the most promising appears the derivative/momentum scale expansion and this is the one which we will investigate in the following chapter.

# Chapter 3

## Convergence of derivative expansion

As discussed in section 2.6, the difficulty in dealing with the functional differential equation that expresses the exact RG flow usually results in one of a variety of analytic non-perturbative approximation methods being employed. Of the methods available, the derivative expansion (or momentum scale expansion if a sharp cutoff is utilised) appears the most promising. However, the question that must be addressed when using this approximation scheme is whether the expansion converges and, if so, whether it converges to the correct answer.

Obviously it is an extremely challenging task to settle this issue non-perturbatively and in all generality. It must be stressed that this is not a controlled expansion in some small parameter. Rather, the approximation we make in using the derivative expansion lies in neglecting powers of  $(p^2/\Lambda^2)$  where  $p$  is some typical momentum of the system and  $\Lambda$  the effective cutoff. Consideration of the flow equations (2.12) and (2.20) leads to the conclusion that the typical momentum that contribute are of order the effective cutoff, *i.e.*  $p \sim \Lambda$ . Hence the issue is a numerical one.

In this chapter we investigate some aspects of the applicability of the derivative expansion in the weak coupling regime of massless scalar  $\lambda\varphi^4$  theory<sup>1</sup> in four Euclidean spacetime dimensions. The derivative expanded  $\beta$  function at one- and two-loop order is calculated and convergence (or otherwise) is shown for a variety of different cutoff functions and flow equations [16, 17].

### 3.1 Wilson/Polchinski flow equation

We start from the expanded Wilson/Polchinski flow equation (2.14)

$$\begin{aligned} \frac{\partial}{\partial \Lambda} S(p_1, \dots, p_n; \Lambda) = & \sum_{\{I_1, I_2\}} S(-\mathbf{P}_1, I_1; \Lambda) K_\Lambda(P_1) S(\mathbf{P}_1, I_2; \Lambda) \\ & - \frac{1}{2} \int \frac{d^4 q}{(2\pi)^4} K_\Lambda(q) S(\mathbf{q}, -\mathbf{q}, p_1, \dots, p_n; \Lambda), \end{aligned} \quad (3.1)$$

utilising the same notation as before. We impose the renormalisation condition

$$S(0, 0, 0, 0; \Lambda) \equiv \lambda. \quad (3.2)$$

If the four-point vertex is considered exactly (*i.e.* without a derivative expansion or similar approximation), the exact one-loop  $\beta$  function can be obtained. The sole contribution to the flow equation at this order comes from the tree-level six-point function that has two of its legs joined together to give figure 3.1.

The tree-level six-point function is found by setting  $n = 6$  in (3.1) and substituting  $S(p_1, p_2, p_3, p_4) = \lambda$  (*i.e.* to lowest order) in the tree-level part of the RHS:

$$S(p_1, p_2, p_3, p_4, p_5, p_6; \Lambda) = -\lambda^2 \int_\Lambda^\infty d\Lambda_1 \left[ \sum_{i=3}^6 K_{\Lambda_1}(p_1 + p_2 + p_i) \right]$$

---

<sup>1</sup>with  $\varphi \leftrightarrow -\varphi$  symmetry

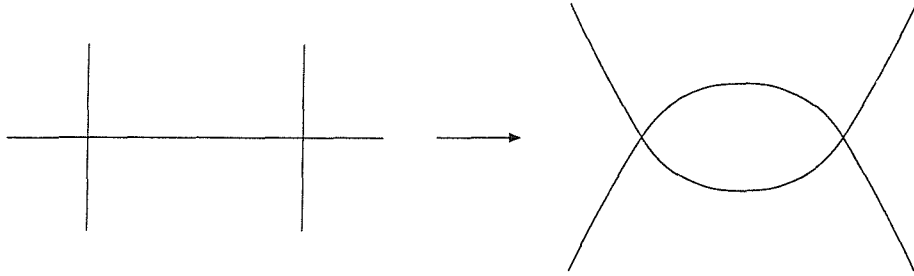


Figure 3.1: Feynman diagram contributing to the four-point function at one loop, constructed from the tree-level six-point function with two legs joined

$$+ \sum_{j=4}^6 K_{\Lambda_1}(p_1 + p_3 + p_j) + \sum_{k=5}^6 K_{\Lambda_1}(p_1 + p_4 + p_k) + K_{\Lambda_1}(p_1 + p_5 + p_6) \Big]. \quad (3.3)$$

Note that because the integral over  $\Lambda_1$  is UV convergent we can proceed directly to the continuum without introducing an overall cutoff. This is a reflection of the ability of the exact RG to deal directly in the continuum using renormalised quantities as we will see later. Substituting (3.3) into the quantum correction part of (3.1) for the flow of the four-point vertex (*i.e.* fix  $n = 4$ ), we set all external momenta to zero and obtain

$$\frac{\partial}{\partial \Lambda} \lambda = -\frac{1}{2} \int \frac{d^4 q}{(2\pi)^4} K_{\Lambda}(q) \left[ -6\lambda^2 \int_{\Lambda}^{\infty} d\Lambda_1 K_{\Lambda_1}(q) \right] \quad (3.4)$$

$$= 3\lambda^2 \int \frac{d^4 q}{(2\pi)^4} K_{\Lambda}(q) \Delta_{IR}(q^2/\Lambda^2) \quad (3.5)$$

$$= \frac{6\lambda^2}{(4\pi)^2} \frac{1}{\Lambda} \int_0^{\infty} dx C'_{IR}(x) C_{IR}(x) \quad (3.6)$$

$$= \frac{3\lambda^2}{(4\pi)^2} \frac{1}{\Lambda} [C_{IR}^2(\infty) - C_{IR}^2(0)], \quad (3.7)$$

where the term in the square bracket of (3.4) is the six-point contribution of (3.3), and the prime in (3.6) means differentiation with respect to the argument of the function. Using the definition for the  $\beta$  function (2.43), we find that

$$\beta(\lambda) = \frac{3}{(4\pi)^2} \lambda^2, \quad (3.8)$$

the expected result at this order [*c.f.* (2.50)].

Although we have seen that no approximation is required at this stage, we are investigating the consequences of using a derivative expansion. As such, we expand the six-point function in terms of its external momentum. In effect,  $\Delta_{IR}(q^2/\Lambda^2)$  of (3.5) is expanded in  $q^2$ , and so, recalling that  $C_{IR} = 1 - C_{UV}$ , we find that (3.6) is replaced by

$$\beta = \frac{6\lambda^2}{(4\pi)^2} \sum_{n=1}^{\infty} \frac{C_{UV}^{(n)}(0)}{n!} \int_0^{\infty} dx x^n C'_{UV}(x), \quad (3.9)$$

with the  $n$ -th derivative with respect to  $x$  denoted by  $C_{UV}^{(n)}(x)$ . If one naïvely allows the cutoff to be sharp, *i.e.*  $C_{UV} = \theta(1-x)$ , we see immediately that this converges to the wrong answer. Since,  $C_{UV}^{(n)}(0) = 0$  for all  $n \geq 1$ , (3.9) will yield a zero  $\beta$  function at this order. However, as discussed earlier, the sharp cutoff should not be applied to the Wilson/Polchinski flow equation, so for the remainder of this section, we shall only consider smooth cutoffs.

If we impose a power law cutoff, then there is a finite value of  $n$  larger than which the integrals in (3.9) diverge. Choosing a cutoff which falls faster than a power is also not sufficient to obtain a convergent series. Consider a cutoff of the form  $C_{UV}(q^2/\Lambda^2) = \exp(-q^2/\Lambda^2)$ . The  $\beta$  function is found to be

$$\beta = \frac{6\lambda^2}{(4\pi)^2} \sum_{n=1}^{\infty} (-1)^{n+1}. \quad (3.10)$$

Clearly this is an oscillating series that fails to converge.

However convergence can be found with certain UV cutoff profiles if the chosen function falls fast enough as  $x \rightarrow \infty$ . Two such examples are

$$C_{UV}(x) = \exp(1 - e^x), \quad (3.11)$$

$$C_{UV}(x) = \exp[e - \exp(e^x)]. \quad (3.12)$$

We can (numerically) calculate the one-loop  $\beta$  function for these cutoffs using (3.9). From the first choice of cutoff (3.11) we find

$$\beta = \frac{3\lambda^2}{(4\pi)^2} (1.193 + 0 - 0.194 - 0.060 + 0.032 + \dots). \quad (3.13)$$

(The second term in this series vanishes since  $\frac{d^2}{dx^2} \exp(1 - e^x) \Big|_{x=0} = 0$ .)

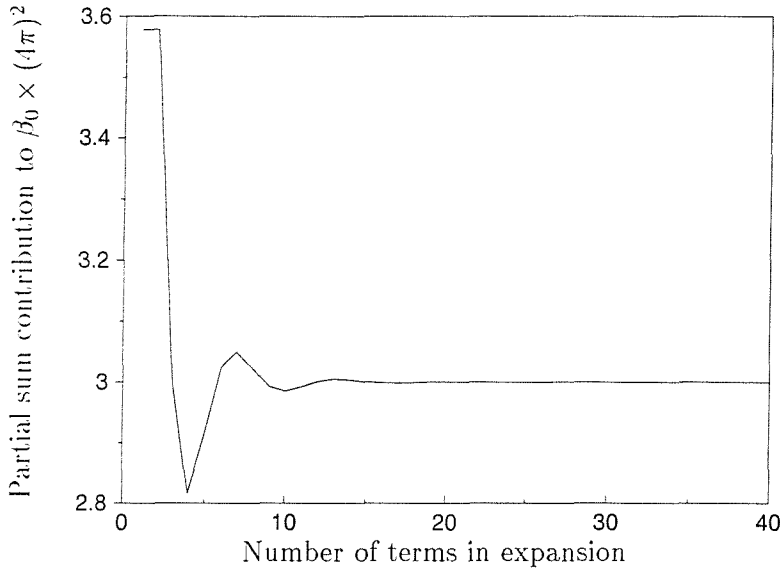


Figure 3.2: Graph of partial sum contribution to  $\beta_0$  coefficient against number of terms in expansion for the series (3.13)

If we calculate the partial sum contribution to the  $\beta_0$  coefficient [*c.f.* (2.44)] at each order of the expansion in (3.13), we obtain the graph contained in figure 3.2. With the second choice of cutoff function (3.12), the following expansion is obtained for the one-loop  $\beta$  function, with the graph of the partial sums of the series displayed in figure 3.3:

$$\beta = \frac{3\lambda^2}{(4\pi)^2} (1.278 - 0.164 - 0.130 - 0.014 + 0.019 + \dots). \quad (3.14)$$

In both these cases convergence towards the correct value of the one-loop  $\beta$  function is manifest. Although such convergence is encouraging, we now leave the Wil-

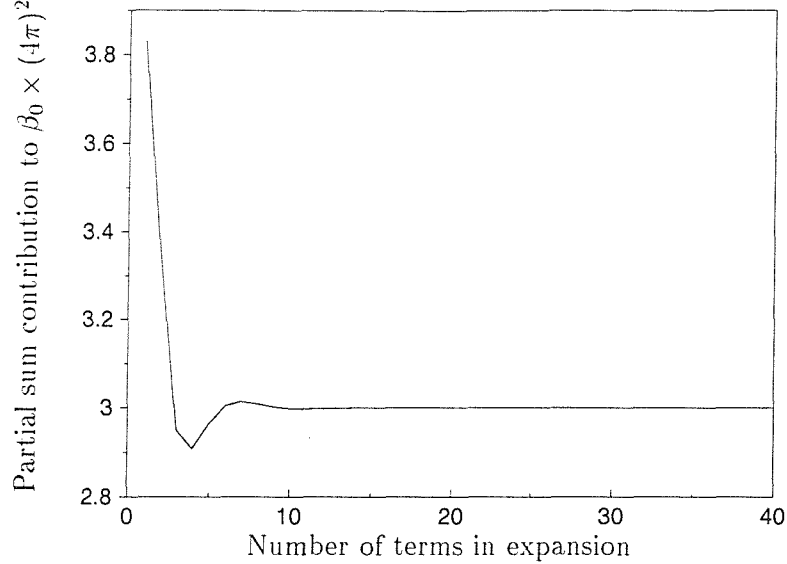


Figure 3.3: Graph of partial sum contribution to  $\beta_0$  coefficient against number of terms in expansion for the series (3.14)

son/Polchinski flow equation to concentrate on the rather more promising Legendre flow equation. This has inherently better convergence properties, not least because as we are dealing with 1PI functions, hence there are no tree-level corrections and so a numerical series arising from a derivative expansion cannot arise until at least two-loop order.

### 3.2 Legendre flow equation at one loop

The momentum expanded Legendre flow equation was given in (2.27), (2.22) and (2.28) for sharp cutoff or (2.21), (2.22) and (2.23) if the cutoff profile is smooth. Irrespective of whether the cutoff is sharp or smooth, the flow of the four-point function at one-loop is given by

$$\frac{\partial}{\partial \Lambda} \Gamma(p_1, p_2, p_3, p_4; \Lambda) = \int \frac{d^4 q}{(2\pi)^4} K_\Lambda(q) \times$$

$$\times \sum_{\{I_1, I_2\}} \Gamma(\mathbf{q}, -\mathbf{q} - \mathbf{P}_1, I_1; \Lambda) \Delta_{IR}(|\mathbf{q} + \mathbf{P}_1|) \Gamma(\mathbf{q} - \mathbf{P}_2, -\mathbf{q}, I_2; \Lambda), \quad (3.15)$$

Imposing the renormalisation condition (*c.f.* condition (3.2))

$$\Gamma(0, 0, 0, 0; \Lambda) = \lambda, \quad (3.16)$$

and substituting the tree-level value of the four-point 1PI vertex ( $\Gamma(\mathbf{p}_1, \mathbf{p}_2, \mathbf{p}_4, \mathbf{p}_4; \Lambda) = \lambda$ ) in the RHS of (3.15), the  $\beta$  function is found to be

$$\begin{aligned} \beta(\lambda) &= -3\lambda^2 \Lambda \int \frac{d^4 q}{(2\pi)^4} \frac{1}{q^4} \left( \frac{d}{d\Lambda} C_{IR}(q^2/\Lambda^2) \right) C_{IR}(q^2/\Lambda^2) \\ &= \frac{6\lambda^2}{(4\pi)^2} \int_0^\infty dx C'_{IR}(x) C_{IR}(x) \\ &= \frac{3\lambda^2}{(4\pi)^2}. \end{aligned} \quad (3.17)$$

Note that no derivative expansion has been (or indeed can be) performed. Unlike the previous situation with the Wilson/Polchinski equation, there is nothing to expand in. At one-loop, the Wilson/Polchinski equation had the external momentum of the tree-level six-point function in which to expand; in the case of the Legendre flow equation the property of being 1PI means that the only object is that of figure 3.1 which (within the calculation of the  $\beta$  function) has no external momentum. Hence the exact one-loop  $\beta$  function is obtained irrespective of the exact form of cutoff function.

### 3.3 Legendre flow equation at two loops

To iterate the flow equation to two-loop order, care must be taken in using renormalised quantities. The four-point function is split into two parts, momentum free

$[\lambda(\Lambda)]$  and momentum dependent  $[\gamma(\mathbf{p}_1, \mathbf{p}_2, \mathbf{p}_3, \mathbf{p}_4; \Lambda)]$  [18]:

$$\Gamma(\mathbf{p}_1, \mathbf{p}_2, \mathbf{p}_3, \mathbf{p}_4; \Lambda) = \lambda(\Lambda) + \gamma(\mathbf{p}_1, \mathbf{p}_2, \mathbf{p}_3, \mathbf{p}_4; \Lambda), \quad (3.18)$$

$$\text{where } \gamma(0, 0, 0, 0; \Lambda) = 0. \quad (3.19)$$

It is  $\gamma(\mathbf{p}_1, \mathbf{p}_2, \mathbf{p}_3, \mathbf{p}_4; \Lambda)$  which must be iterated as the momentum dependent four-point function.

The three topological variants allowed for two-loop diagrams with four external legs are shown in figure 3.4. Actually only topologies (b) and (c) contribute to the  $\beta$  function. Upon setting external momenta to zero, (3.19) ensures that the iterand of diagram (a) vanishes. In fact diagram (a) is already incorporated in the one-loop running  $\lambda(\Lambda)$  since renormalised quantities are being calculated directly. If this calculation was to be performed in the more traditional manner using bare parameters, topology (a) would only contribute a divergent part which would be removed upon renormalisation.

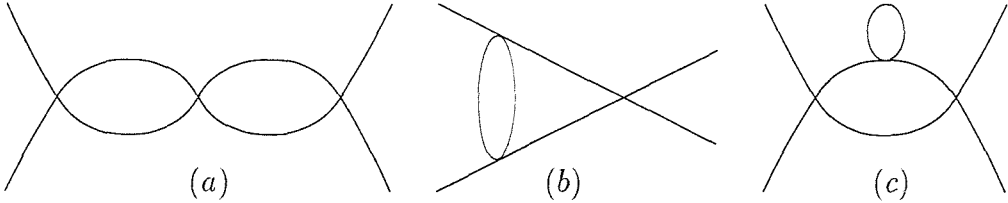


Figure 3.4: Feynman diagrams contributing to four-point function at two loops.

Topology (b) of figure 3.4 can be formed in the flow equation in one of two ways: by joining two legs from different vertices of the one-loop six-point 1PI function (shown in figure 3.5 (a)), or by attaching two legs from different vertices of the one-loop four-point function to the tree-level vertex. Topology (c) can also be formed two ways: from the one-loop six-point 1PI function by joining two legs from the same vertex, or by inserting the one-loop correction to the propagator (shown in figure 3.5 (b))

into the one-loop four-point function. As we shall see in the next section, the two contributions to the  $\beta$  function of the form of topology 3.4 (c) cancel one another, irrespective of the exact form of the cutoff profile employed.

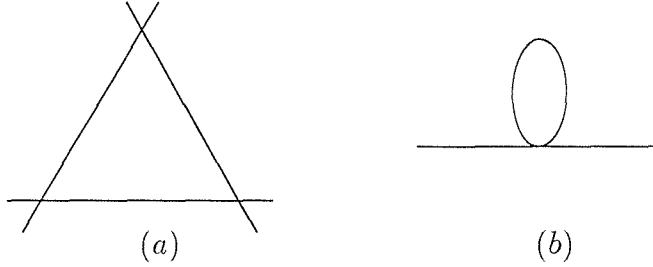


Figure 3.5: Diagrams used in forming two loop four-point functions

At this order of the  $\beta$  function, wavefunction renormalisation also needs to be taken into account:

$$\begin{aligned}\beta(\lambda) &= \Lambda \frac{\partial}{\partial \Lambda} \frac{\lambda}{Z^2} \\ &= \frac{\Lambda}{Z^2} \frac{\partial}{\partial \Lambda} \lambda - 2\Lambda \lambda \frac{\partial}{\partial \Lambda} Z,\end{aligned}\tag{3.20}$$

where  $Z$  is the wavefunction renormalisation and up until now use has been made of the fact that  $Z(\Lambda) = 1 + O(\lambda^2)$ . At two-loop order its contribution to the  $\beta$  function arises from the diagram of figure 3.6.

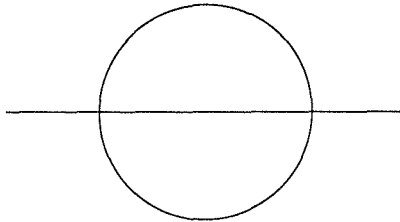


Figure 3.6: Feynman diagram contributing to wave function renormalization at two loops.

### 3.4 Cancellation of self energy diagrams

We shall now demonstrate that the diagrams of the form of figure 3.4 (c) do not contribute to the  $\beta$  function irrespective of the specific shape of the cutoff. We will start by looking at a general smooth cutoff and then consider the special case of the sharp cutoff.

The self energy correction to the propagator is obtained directly from the flow equation. To  $O(\lambda)$  it is:

$$\frac{\partial}{\partial \Lambda} \Sigma(p; \Lambda) = -\frac{\lambda}{2} \int \frac{d^4 q}{(2\pi)^4} \frac{\partial}{\partial \Lambda} \Delta_{UV}(q^2/\Lambda^2) \quad (3.21)$$

Integrating up (3.21) we must not introduce a mass scale as we are dealing with a massless theory. Consequently, the uniquely determined self energy has to be

$$\Sigma(p; \Lambda) = -\frac{\lambda}{2} \int \frac{d^4 q}{(2\pi)^4} \Delta_{UV}(q^2/\Lambda^2). \quad (3.22)$$

For example if an exponential cutoff,  $C_{UV}(q^2/\Lambda^2) = e^{-q^2/\Lambda^2}$ , is utilised, the self energy is  $-\frac{\lambda}{(4\pi)^2} \frac{\Lambda^2}{2}$ , while a power law cutoff such as  $C_{UV}(q^2/\Lambda^2) = (1 + (q^2/\Lambda^2)^3)^{-1}$  gives rise to a self energy of  $-\frac{\lambda}{(4\pi)} \frac{\Lambda^2}{16\sqrt{2}}$ . The general contribution to the flow of  $\lambda$  by the insertion of the self energy correction into the one-loop four-point function is found to be

$$-9\Lambda\lambda^2 \int \frac{d^4 q}{(2\pi)^4} \Delta_{IR}^2(q^2/\Lambda^2) \left( \frac{\partial}{\partial \Lambda} \Delta_{UV}(q^2/\Lambda^2) \right) \Sigma(q; \Lambda) \Big|_{O(\lambda)} \quad (3.23)$$

$$= -\frac{3}{2}\Lambda\lambda^3 \int \frac{d^4 q}{(2\pi)^4} \frac{\partial}{\partial \Lambda} \Delta_{IR}^3(q^2/\Lambda^2) \int \frac{d^4 p}{(2\pi)^4} \Delta_{UV}(p^2/\Lambda^2) \quad (3.24)$$

with the numerical factor 9 in (3.23) arising from various combinatorics. Since there are disjoint integrals over  $\mathbf{p}$  and  $\mathbf{q}$ , it is evident that no derivative expansion is possible.

The flow of the one-loop six-point 1PI function is

$$\begin{aligned} \frac{\partial}{\partial \Lambda} \Gamma(p_1, p_2, p_3, p_4, p_5, p_6; \Lambda) &= \int \frac{d^4 q}{(2\pi)^4} \left( \frac{\partial}{\partial \Lambda} \Delta_{UV}(q^2/\Lambda^2) \right) \times \\ &\times \sum_{i=1}^3 \sum_{j=i+1}^6 \Delta_{IR}(\mathbf{q} + \mathbf{p}_i + \mathbf{p}_j) \sum_{\substack{k=i+1 \\ k \neq j}}^6 \sum_{\substack{l=j+1 \\ l \neq j}}^6 \Delta_{IR}(\mathbf{q} - \mathbf{p}_k - \mathbf{p}_l). \end{aligned} \quad (3.25)$$

This provides contributions to the  $\beta$  function of both topology (b) and (c) of figure 3.4. Extracting just the part relating to topology (c) we find that its contribution to the  $\beta$  function is:

$$-\frac{9}{2} \Lambda \lambda^3 \int \frac{d^4 q}{(2\pi)^4} \frac{\partial}{\partial \Lambda} \Delta_{UV}(q^2/\Lambda^2) \int_{\Lambda}^{\infty} d\Lambda_1 \int \frac{d^4 p}{(2\pi)^4} \Delta_{IR}^2(p^2/\Lambda^2) \frac{\partial}{\partial \Lambda_1} \Delta_{UV}(p^2/\Lambda_1^2) \quad (3.26)$$

$$= -\frac{3}{2} \Lambda \lambda^3 \int \frac{d^4 q}{(2\pi)^4} \frac{\partial}{\partial \Lambda} \Delta_{UV}(q^2/\Lambda^2) \int \frac{d^4 p}{(2\pi)^4} \Delta_{IR}^3(p^2/\Lambda^2) \quad (3.27)$$

Combining (3.24) and (3.27), the total input to the  $\beta$  function from figure 3.4 (c) is

$$-\frac{3}{2} \Lambda \lambda^3 \frac{\partial}{\partial \Lambda} \int \frac{d^4 q}{(2\pi)^4} \Delta_{UV}(q^2/\Lambda^2) \int \frac{d^4 p}{(2\pi)^4} \Delta_{IR}^3(p^2/\Lambda^2) \quad (3.28)$$

$$= -\frac{6}{(4\pi)^2} \Lambda \lambda^3 \frac{\partial}{\partial \Lambda} \int_0^{\infty} dx C_{UV}(x) \int_0^{\infty} dy \frac{C_{IR}^3(y)}{y^2} \quad (3.29)$$

$$= 0 \quad (3.30)$$

The situation with regard to the sharp cutoff is very similar, with the self energy (3.22) replaced by

$$\Sigma(p; \Lambda) = -\frac{\lambda}{2} \int \frac{d^4 q}{(2\pi)^4} \frac{\theta(\Lambda - q)}{q^2} = -\frac{1}{(4\pi^2)} \frac{\Lambda^2}{2}. \quad (3.31)$$

The different form of the flow equation for sharp cutoffs means that the part of the  $\beta$  function arising from self energy insertion is

$$3\Lambda \lambda^3 \int \frac{d^4 q}{(2\pi)^4} \frac{\delta(q - \Lambda) \theta(q - \Lambda)}{q^6} \int \frac{d^4 p}{(2\pi)^4} \frac{\theta(p - \Lambda)}{p^2} = \frac{3}{(4\pi)^2} \lambda^3. \quad (3.32)$$

The  $\beta$  function contribution of the topology of figure 3.4 coming from the six-point function is

$$-\frac{9}{2}\Lambda\lambda^3 \int \frac{d^4q}{(2\pi)^4} \frac{\delta(q-\Lambda)}{q^2} \int_{\Lambda}^{\infty} d\Lambda_1 \int \frac{d^4p}{(2\pi)^4} \frac{\delta(p-\Lambda_1)}{p^2} \frac{\theta^2(p-\Lambda_1)}{p^4} = -\frac{3}{(4\pi)^2}\lambda^3, \quad (3.33)$$

where we use the fact that here<sup>2</sup>  $\theta^2(0) = 1/3$ . Obviously (3.32) and (3.33) combine to provide the desired cancellation.

### 3.5 Sharp cutoff

We use the momentum expanded Legendre flow equation for a sharp cutoff contained in (2.27), (2.22) and (2.28). The momentum dependent part of the four-point function at one loop is calculated to be

$$\gamma(p_1, p_2, p_3, p_4; \Lambda) = -\lambda^2 \int_{\Lambda}^{\infty} d\Lambda_1 \int \frac{d^4q}{(2\pi)^4} \frac{\delta(q-\Lambda_1)}{q^2} \sum_{i=2}^4 \left\{ \frac{\theta(|\mathbf{q} + \mathcal{P}_i| - \Lambda_1)}{(\mathbf{q} + \mathcal{P}_i)^2} - \frac{\theta(q - \Lambda_1)}{q^2} \right\} \quad (3.34)$$

$$= -\lambda^2 \sum_{i=2}^4 \int_{\Lambda}^{\infty} \frac{d^4q}{(2\pi)^4} \left( \frac{\theta(\frac{\mathcal{P}_i}{2q} + x)}{q^4} \left\{ 1 + 2x \frac{\mathcal{P}_i}{q} + \left( \frac{\mathcal{P}_i}{q} \right)^2 \right\}^{-1} - \frac{1}{2} \right) \quad (3.35)$$

$$= + \frac{\lambda^2}{4\pi^3} \sum_{i=2}^4 \left\{ \frac{1}{6} \frac{\mathcal{P}_i}{\Lambda} + \frac{1}{720} \left( \frac{\mathcal{P}_i}{\Lambda} \right)^3 + \frac{3}{44800} \left( \frac{\mathcal{P}_i}{\Lambda} \right)^5 + \dots \right\}, \quad (3.36)$$

where  $\mathcal{P}_i = p_1 + p_i$  and  $x = \mathcal{P}_i \cdot \mathbf{q} / \mathcal{P}_i q$ . Note that it is the subtraction in (3.34) of the part independent of external momentum that allows the upper limit of the  $\Lambda_1$  integral to be set as  $\infty$  as the integral is now convergent. In (3.34) the integral over  $\Lambda_1$  is performed by noting that  $\theta(0)$  can be treated as being equal to  $\frac{1}{2}$  [c.f. (2.26)]. After changing variables, the step function in (3.35) can be accounted for in the limits the integral over  $x$  allowing the term in braces to be expanded in momentum-scale

---

<sup>2</sup>See section 2.3.

$\mathcal{P}_i = |\mathcal{P}_i|$  [7, 12]. Alternatively the step function may be expanded directly [7]

$$\theta\left(\frac{\mathcal{P}_i}{2q} + x\right) = \theta(x) + \sum_{n=1}^{\infty} \frac{1}{n!} \left(\frac{\mathcal{P}_i}{2q}\right)^n \delta^{(n-1)}(x), \quad (3.37)$$

where  $\delta^{(n-1)}(x)$  is the  $(n-1)$ th derivative of  $\delta(x)$  with respect to  $x$ . The same result as (3.36) was calculated in ref. [7] but using bare parameters instead of renormalised ones as here.

Dropping the terms related to the self energy diagram of figure 3.4 (c), we find the flow equation for  $\lambda$  to  $\mathcal{O}(\lambda^3)$  is

$$\begin{aligned} \frac{\partial}{\partial \Lambda} \lambda(\Lambda) = & \frac{1}{\Lambda} \frac{3\lambda^2}{(4\pi)^2} \\ & - \frac{3\lambda^3}{2} \int \frac{d^4 q}{(2\pi)^4} \frac{\delta(q - \Lambda)}{q^2} \int_{\Lambda}^{\infty} d\Lambda_1 \int \frac{d^4 p}{(2\pi)^4} \frac{\delta(p - \Lambda_1)}{p^2} \\ & \left\{ \frac{4\theta^2(|\mathbf{p} + \mathbf{q}| - \Lambda_1)}{|\mathbf{p} + \mathbf{q}|^4} + \frac{8\theta(|\mathbf{p} + \mathbf{q}| - \Lambda_1)\theta(p - \Lambda_1)}{p^2|\mathbf{p} + \mathbf{q}|^2} \right. \\ & \left. + \frac{8\theta(q - \Lambda)}{q^2} \left( \frac{\theta(|\mathbf{p} + \mathbf{q}| - \Lambda_1)}{|\mathbf{p} + \mathbf{q}|^2} - \frac{\theta(p - \Lambda_1)}{p^2} \right) \right\}. \end{aligned} \quad (3.38)$$

The first two terms arise from the one-loop six-point 1PI function (3.25) with legs joined so as to be of the form of figure 3.4 (b). The final line of (3.38) arises from iterating the one-loop four-point function of (3.36) through the flow equation. These contributions can be calculated using the momentum expansion; in this case the embedded one-loop terms are expanded in  $q/p$ . For the first one we find:

$$\begin{aligned} & -6\lambda^3 \int \frac{d^4 q}{(2\pi)^4} \frac{\delta(q - \Lambda)}{q^2} \int_{\Lambda}^{\infty} d\Lambda_1 \int \frac{d^4 p}{(2\pi)^4} \frac{\delta(p - \Lambda_1)}{p^2} \frac{\theta^2(|\mathbf{p} + \mathbf{q}| - \Lambda_1)}{|\mathbf{p} + \mathbf{q}|^4} \\ & = -\frac{6\lambda^3}{4\pi^3} \int \frac{d^4 q}{(2\pi)^4} \frac{\delta(q - \Lambda)}{q^2} \int_{\Lambda}^{\infty} \frac{dp}{p^3} \left\{ \frac{\pi}{4} - \frac{5}{6} \left( \frac{q}{p} \right) + \frac{\pi}{4} \left( \frac{q}{p} \right)^2 + \right. \\ & \quad \left. - \frac{63}{80} \left( \frac{q}{p} \right)^3 + \frac{\pi}{4} \left( \frac{q}{p} \right)^4 + \dots \right\} \end{aligned}$$

$$= -12 \frac{\lambda^3}{(4\pi)^4} \frac{1}{\Lambda} \frac{1}{\pi} \left( \frac{\pi}{2} - \frac{10}{9} + \frac{\pi}{4} - \frac{63}{100} + \frac{\pi}{6} - \frac{7035}{15680} + \dots \right) \quad (3.39)$$

This oscillating series converges, but only does so very slowly. The partial sum contributions to the  $\beta$  function from the series of (3.39) are displayed in figure 3.7. The average of successive partial sums is shown in figure 3.8 allowing an estimate of

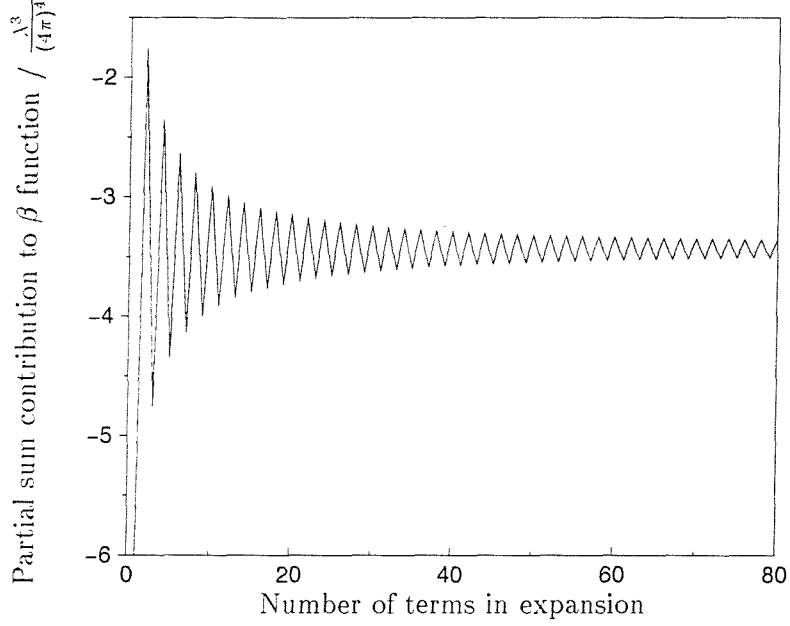


Figure 3.7: Partial sum contribution to  $\beta$  function against number of terms in expansion for the series (3.39)

$-3.430 \frac{\lambda^3}{(4\pi)^4 \Lambda}$  to be made for the convergence of (3.39).

The next contribution in (3.38) provides a series which converges rapidly to a value of  $-5.13764 \frac{\lambda^3}{(4\pi)^4 \Lambda}$ :

$$\begin{aligned} & -12\lambda^3 \int \frac{d^4 q}{(2\pi)^4} \frac{\delta(q - \Lambda)}{q^2} \int_{\Lambda}^{\infty} d\Lambda_1 \int \frac{d^4 p}{(2\pi)^4} \frac{\delta(p - \Lambda_1)}{p^2} \frac{\theta(|\mathbf{p} + \mathbf{q}| - \Lambda_1) \theta(p - \Lambda_1)}{p^2 |\mathbf{p} + \mathbf{q}|^2} \\ &= -\frac{6\lambda^3}{4\pi^3} \int \frac{d^4 q}{(2\pi)^4} \frac{\delta(q - \Lambda)}{q^2} \int_{\Lambda}^{\infty} \frac{dp}{p^3} \left\{ \frac{\pi}{4} - \frac{1}{6} \left( \frac{q}{p} \right) - \frac{1}{240} \left( \frac{q}{p} \right)^3 - \frac{3}{8960} \left( \frac{q}{p} \right)^5 + \dots \right\} \\ &= -12 \frac{\lambda^3}{(4\pi)^4} \frac{1}{\Lambda} \frac{1}{\pi} \left( \frac{\pi}{2} - \frac{2}{9} - \frac{1}{300} - \frac{3}{15680} + \dots \right). \end{aligned} \quad (3.40)$$

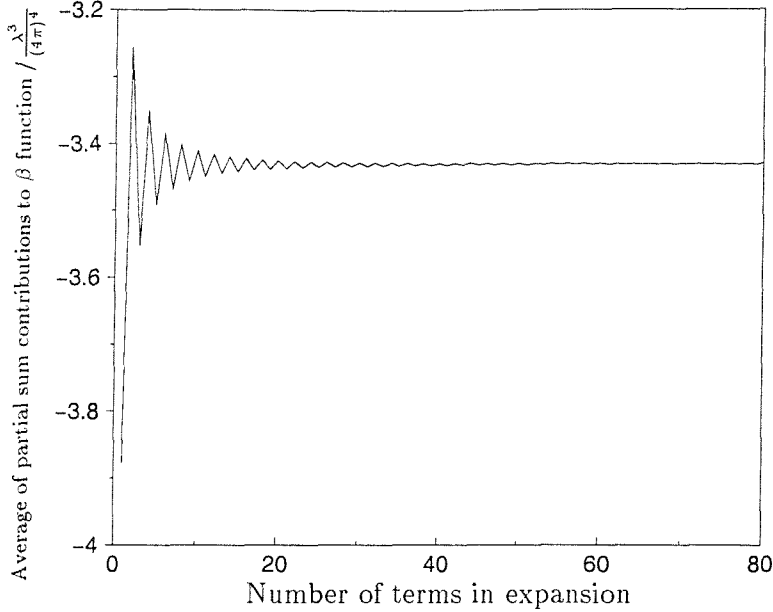


Figure 3.8: Average of successive partial sum contributions to  $\beta$  function against number of terms in expansion for series (3.39)

Iterating the one-loop result of (3.36), the final part of (3.38) returns the previously published value<sup>3</sup>

$$\begin{aligned}
& -6\lambda^3 \int \frac{d^4 q}{(2\pi)^4} \frac{\delta(q - \Lambda)}{q^2} \int_{\Lambda}^{\infty} d\Lambda_1 \int \frac{d^4 p}{(2\pi)^4} \frac{\delta(p - \Lambda_1)}{p^2} \frac{\theta(q - \Lambda)}{q^2} \times \\
& \quad \times \left( \frac{\theta(|\mathbf{p} + \mathbf{q}| - \Lambda_1)}{|\mathbf{p} + \mathbf{q}|^2} - \frac{\theta(p - \Lambda_1)}{p^2} \right) \\
& = -\frac{6\lambda^3}{4\pi^3} \int \frac{d^4 q}{(2\pi)^4} \frac{\delta(q - \Lambda)}{q^4} \int_{\Lambda}^{\infty} \frac{dp}{p} \left\{ \frac{1}{6} \left( \frac{q}{p} \right) + \frac{1}{240} \left( \frac{q}{p} \right)^3 + \frac{3}{8960} \left( \frac{q}{p} \right)^5 + \dots \right\} \\
& = \frac{\lambda^3}{(4\pi)^4} \frac{1}{\Lambda} \frac{1}{\pi} \left( 8 + \frac{1}{15} + \frac{9}{2800} + \dots \right), \tag{3.41}
\end{aligned}$$

which converges to  $2.56882 \frac{\lambda^3}{(4\pi)^4 \Lambda}$ . As previously discussed, wavefunction renormalisation must be accounted for through  $\Sigma(k; \Lambda)|_{\mathcal{O}(k^2)} = [Z(\Lambda) - 1]k^2$  arising from figure 3.6.

$$k^2 \frac{\partial}{\partial \Lambda} Z(\Lambda)$$

---

<sup>3</sup>Calculated using bare parameters [7].

$$\begin{aligned}
&= \lambda^2 \int \frac{d^4 q}{(2\pi)^4} \frac{\delta(q - \Lambda)}{q^2} \int_{\Lambda}^{\infty} d\Lambda_1 \int \frac{d^4 p}{(2\pi)^4} \frac{\delta(p - \Lambda_1)}{p^2} \frac{\theta(|\mathbf{p} + \mathbf{q} + \mathbf{k}| - \Lambda_1)}{|\mathbf{p} + \mathbf{q} + \mathbf{k}|^2} \Big|_{O(k^2)} \\
&= -\frac{\lambda^2}{24\pi^3} \int \frac{d^4 q}{(2\pi)^4} \frac{\delta(q - \Lambda)}{q^2} \left\{ \frac{|\mathbf{q} + \mathbf{k}|}{\Lambda} + \frac{1}{120} \frac{|\mathbf{q} + \mathbf{k}|^3}{\Lambda^3} + \frac{1}{22400} \frac{|\mathbf{q} + \mathbf{k}|^5}{\Lambda^5} + \dots \right\} \Big|_{O(k^2)} \\
&= -\frac{\lambda^2 k^2}{(4\pi)^4} \frac{1}{\Lambda} \frac{1}{\pi} \left( \frac{1}{2} + \frac{1}{48} + \frac{3}{1280} + \dots \right). \tag{3.42}
\end{aligned}$$

The second line of (3.42) is obtained using the expanded one-loop four-vertex of (3.36). The final line then follows upon the realisation that the net effect of expanding to second order in  $k$  and then averaging over the angles is to convert  $|\mathbf{q} + \mathbf{k}|^n$  into  $\frac{1}{8}n(n+2)q^{n-2}k^2$ . We find that (3.42) converges to  $-0.16667 \frac{\lambda^3}{(4\pi)^4 \Lambda}$ . In figure 3.9 we display the partial sum contributions to the  $\beta$  function from each of the series in (3.40), (3.41) and (3.42).

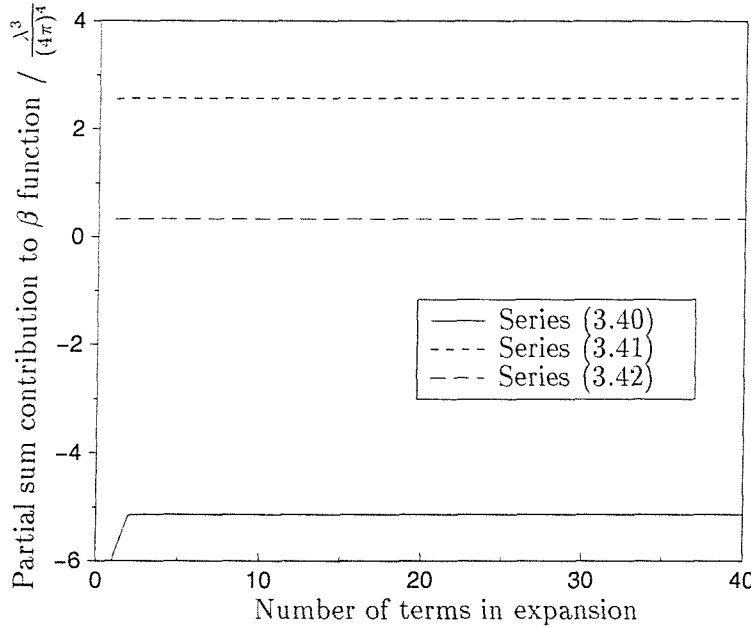


Figure 3.9: Partial sum contributions to the  $\beta$  function against number of terms in the expansion of the series of (3.40), (3.41) and (3.42)

Thus the momentum expanded  $\beta$  function at two loops using a sharp cutoff is

$$\beta(\lambda) = 3 \frac{\lambda^2}{(4\pi)^2} - \frac{\lambda^3}{(4\pi)^4} \frac{1}{\pi} \left\{ 12 \left( \frac{\pi}{2} - \frac{10}{9} + \frac{\pi}{4} - \frac{63}{100} + \frac{\pi}{6} - \frac{7035}{15680} + \dots \right) \right\}$$

$$\begin{aligned}
& + 12 \left( \frac{\pi}{2} - \frac{2}{9} - \frac{1}{300} - \frac{3}{15680} + \dots \right) - \left( 8 + \frac{1}{15} + \frac{9}{2800} + \dots \right) \\
& - \left( 1 + \frac{1}{24} + \frac{3}{640} + \dots \right) \} ,
\end{aligned} \tag{3.43}$$

which converges (albeit slowly) towards the exact expression (2.50). In figure 3.10 we show the value of the  $\beta_1$  coefficient [*c.f.* (2.44)] if we just consider the specified number of terms from each of the series.

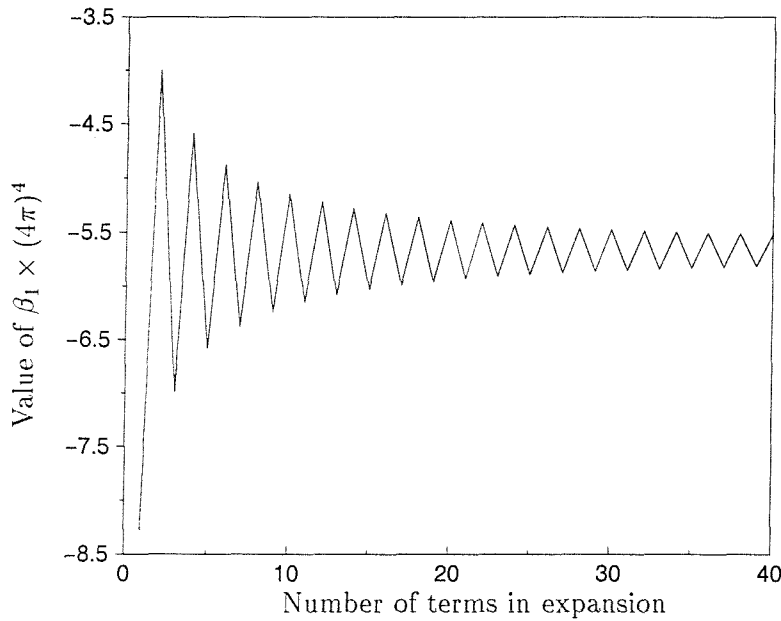


Figure 3.10: Value of  $\beta_1$  coefficient against number of terms in expansion

### 3.6 Exponential cutoff

The momentum expanded Legendre flow equation for smooth cutoffs is given in (2.21) and (2.23). Using an exponential cutoff  $C_{UV} = e^{-q^2/\Lambda^2}$ , the renormalised four-point

function is given by<sup>4</sup>

$$\begin{aligned} \gamma(\mathbf{p}_1, \mathbf{p}_2, \mathbf{p}_3, \mathbf{p}_4; \Lambda) \\ = -\lambda^2 \sum_{i=2}^4 \int_{\Lambda}^{\infty} d\Lambda_1 \int \frac{d^4 q}{(2\pi)^4} \left( \frac{\partial}{\partial \Lambda_1} \frac{e^{-q^2/\Lambda_1^2}}{q^2} \right) \left\{ \frac{\left(1 - e^{-|\mathbf{q} + \mathcal{P}_i|^2/\Lambda_1^2}\right)}{|\mathbf{q} + \mathcal{P}_i|^2} \right. \\ \left. - \frac{\left(1 - e^{-q^2/\Lambda_1^2}\right)}{q^2} \right\} \end{aligned} \quad (3.44)$$

$$= -2 \frac{\lambda^2}{(4\pi)^2} \sum_{i=2}^4 \int_{\Lambda}^{\infty} \frac{d\Lambda_1}{\Lambda_1} \left\{ \left( \frac{\Lambda_1}{\mathcal{P}_i} \right)^2 \left( 1 - e^{-\mathcal{P}_i^2/2\Lambda_1^2} \right) - \frac{1}{2} \right\} \quad (3.45)$$

$$= -\frac{\lambda^2}{2(4\pi)^2} \sum_{i=2}^4 \sum_{n=1}^{\infty} \frac{(-1)^n}{(n+1)! n} \left( \frac{\mathcal{P}_i^2}{2\Lambda_1^2} \right)^n. \quad (3.46)$$

The expression in (3.45) can be obtained from (3.44) either by expanding the exponential of  $-|\mathbf{q} + \mathcal{P}_i|^2/\Lambda_1^2$ , performing the integration over momentum space and then resumming, or by using

$$\frac{\left(1 - e^{-q^2/\Lambda^2}\right)}{q^2} = \frac{1}{\Lambda^2} \int_0^1 da e^{-aq^2/\Lambda^2} \quad (3.47)$$

and interchanging the order of integration.

Using the results of section 3.4 and dropping the self energy diagrams, the flow of the coupling to  $\mathcal{O}(\lambda^3)$  is

$$\begin{aligned} \frac{\partial}{\partial \Lambda} \lambda(\Lambda) = \frac{1}{\Lambda} \frac{3\lambda^2}{(4\pi)^2} \\ - \frac{3\lambda^3}{2} \int \frac{d^4 q}{(2\pi)^4} \frac{\frac{\partial}{\partial \Lambda} \left( e^{-q^2/\Lambda^2} \right)}{q^2} \int_{\Lambda}^{\infty} d\Lambda_1 \int \frac{d^4 p}{(2\pi)^4} \frac{\frac{\partial}{\partial \Lambda_1} \left( e^{-p^2/\Lambda_1^2} \right)}{p^2} \\ \left\{ \frac{4 \left( 1 - e^{-|\mathbf{p} + \mathbf{q}|^2/\Lambda_1^2} \right)^2}{|\mathbf{p} + \mathbf{q}|^4} + \frac{8 \left( 1 - e^{-|\mathbf{p} + \mathbf{q}|^2/\Lambda_1^2} \right) \left( 1 - e^{-p^2/\Lambda_1^2} \right)}{p^2 |\mathbf{p} + \mathbf{q}|^2} \right. \\ \left. + \frac{8 \left( 1 - e^{-q^2/\Lambda^2} \right)}{q^2} \left( \frac{\left( 1 - e^{-|\mathbf{p} + \mathbf{q}|^2/\Lambda_1^2} \right)}{|\mathbf{p} + \mathbf{q}|^2} - \frac{\left( 1 - e^{-p^2/\Lambda_1^2} \right)}{p^2} \right) \right\}. \end{aligned} \quad (3.48)$$

---

<sup>4</sup>In agreement with previous calculations using bare parameters [12].

To perform these integrals, the inner ( $p$ ) integral must be expanded in terms of the momentum external to it (*i.e.*  $q$  momentum).

The first two contributions come from the 1PI one-loop six-point diagram with two of its legs joined to give figure 3.4 (b). The first of these gives the convergent series

$$12 \frac{\lambda^3}{(4\pi)^4} \frac{1}{\Lambda} \left( \ln \frac{3}{4} + \sum_{n=2}^{\infty} (-1)^n \left[ \ln \frac{4}{3} - \frac{1}{n} \sum_{s=2}^n \binom{n}{s} \frac{(-1)^s}{s-1} \left\{ 1 - \frac{1}{2^{s-2}} + \frac{1}{3^{s-1}} \right\} \right] \right), \quad (3.49)$$

(when expanded) which numerically sums to  $\frac{\lambda^3}{(4\pi)^4} \frac{1}{\Lambda} (-2.45411725)$ . The second is

$$-24 \frac{\lambda^3}{(4\pi)^4} \frac{1}{\Lambda} \left( \ln \frac{4}{3} + \sum_{n=1}^{\infty} \frac{(-1)^n}{n(n+1)} \left\{ \left(\frac{2}{3}\right)^n - \left(\frac{1}{2}\right)^n \right\} \right). \quad (3.50)$$

Using the fact that

$$\ln(1+x) = \sum_{n=1}^{\infty} \frac{(-1)^{n+1}}{n} x^n \quad (-1 < x \leq 1), \quad (3.51)$$

we integrate to find

$$\sum_{n=1}^{\infty} \frac{(-1)^n}{n(n+1)} x^n = 1 - \frac{(x+1)}{x} \ln(x+1), \quad (3.52)$$

which is of the same form of the sums of (3.50). Hence (3.50) sums exactly to  $12 \frac{\lambda^3}{(4\pi)^4} \frac{1}{\Lambda} [9 \ln 3 - 2 \ln 2 - 5 \ln 5]$ . The final line of (3.48) comes from the iterated value of  $\gamma(p_1, p_2, p_3, p_4; \Lambda)$  of (3.46) and gives [12]

$$-12 \frac{\lambda^3}{(4\pi)^4} \frac{1}{\Lambda} \sum_{n=1}^{\infty} \frac{(-1)^n}{n(n+1)} \frac{1}{2^n} \left( 1 - \frac{1}{2^{n+1}} \right). \quad (3.53)$$

Using (3.52), this sums to  $6 \frac{\lambda^3}{(4\pi)^4} \frac{1}{\Lambda} [6 \ln 3 + 4 \ln 2 - 5 \ln 5 - 1]$ .

As for the case of the sharp cutoff we need figure 3.6 at second order in external

momentum to calculate wavefunction renormalisation. We have

$$\begin{aligned}
k^2 \frac{\partial}{\partial \Lambda} Z(\Lambda) &= -\lambda^2 \int \frac{d^4 q}{(2\pi)^4} \left( \frac{\partial}{\partial \Lambda} \frac{e^{-q^2/\Lambda^2}}{q^2} \right) \\
&\quad \times \int_{\Lambda}^{\infty} d\Lambda_1 \int \frac{d^4 p}{(2\pi)^4} \left( \frac{\partial}{\partial \Lambda_1} \frac{e^{-p^2/\Lambda_1^2}}{p^2} \right) \left( \frac{1 - e^{-|p+q+k|^2/\Lambda_1^2}}{|p+q+k|^2} \right) \Big|_{O(k^2)} \\
&= \frac{\lambda^2 k^2}{(4\pi)^4} \frac{1}{\Lambda} \sum_{n=2}^{\infty} \frac{(-1)^{n+1}}{2^n}.
\end{aligned} \tag{3.54}$$

Using the binomial expansion

$$\frac{1}{1+x} = \sum_{n=0}^{\infty} (-1)^n x^n, \tag{3.55}$$

and setting  $x = \frac{1}{2}$  enables the sum of (3.54) to be computed, and so

$$\frac{\partial}{\partial \Lambda} Z(\Lambda) = -\frac{1}{6} \frac{\lambda^2}{(4\pi)^4} \frac{1}{\Lambda}. \tag{3.56}$$

In figure 3.11 we display the partial sum contributions to the  $\beta$  function against the number of terms in the expansion for the series coming from (3.49), (3.50), (3.53) and (3.54). The  $\beta$  function to two loops using an exponential cutoff is found by adding together these series (each of which are separately convergent):

$$\begin{aligned}
\beta(\lambda) &= 3 \frac{\lambda^2}{(4\pi)^2} - \frac{12\lambda^3}{(4\pi)^4} \left\{ \ln \frac{4}{3} + \right. \\
&\quad + \sum_{n=1}^{\infty} (-1)^n \left[ \ln \frac{4}{3} + \frac{1}{12} \left( \frac{1}{2} \right)^n + \frac{1}{n(n+1)} \left( 2 \left( \frac{2}{3} \right)^n - \frac{1}{2^n} - \frac{1}{2^{2n+1}} \right) \right. \\
&\quad \left. \left. - \frac{1}{n+1} \sum_{s=2}^{n+1} \binom{n+1}{s} \frac{(-1)^s}{s-1} \left\{ 1 - \frac{1}{2^{s-2}} + \frac{1}{3^{s-1}} \right\} \right] \right\} \\
&= 3 \frac{\lambda^2}{(4\pi)^2} - \frac{\lambda^3}{(4\pi)^4} \left[ 72 \ln 3 - 48 \ln 2 - 30 \ln 5 + 2.45411725 + 6 - \frac{1}{3} \right], \tag{3.57}
\end{aligned}$$

which gives the expected form of (2.50). The quick convergence to the correct value of the  $\beta_1$  coefficient is displayed in figure 3.12.

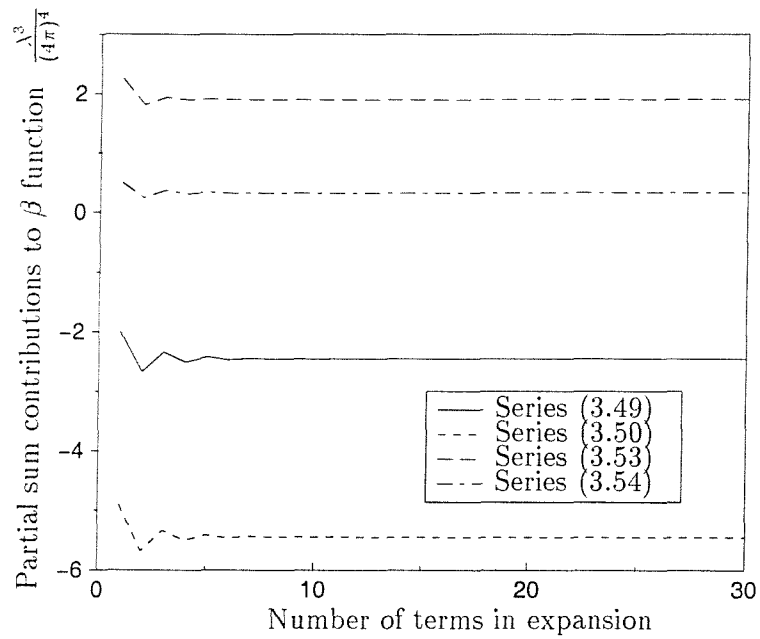


Figure 3.11: Partial sum contributions to the  $\beta$  function against number of terms in the expansion of the series of (3.49), (3.50), (3.53) and (3.54)

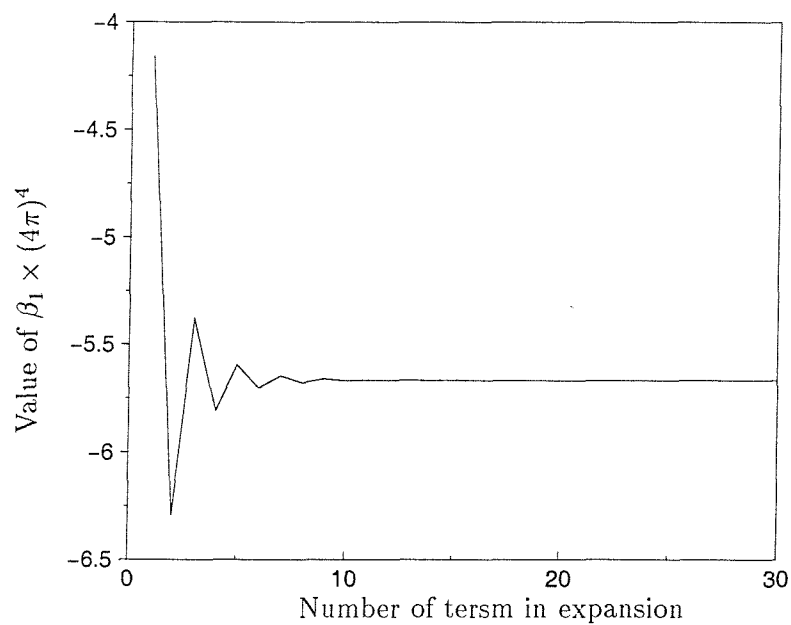


Figure 3.12: Value of  $\beta_1$  coefficient against number of terms in expansion

### 3.7 Power law cutoff

The final form of cutoff under consideration is that of a power law, *i.e.*  $C_{UV} = 1/(1 + (q^2/\Lambda^2)^{\kappa+1})$  where  $\kappa$  is a non-negative integer. For a derivative expansion of the (non-perturbative) flow equation (2.20), it would appear that if  $\kappa$  is chosen such that  $\kappa > D/2 - 1$  (with  $D$  the spacetime dimension) all momentum integrals will converge. However within the method we have utilised in this chapter, major problems arise. If we consider the integral pertaining to figure 3.4 (b) obtained by iterating the one-loop four-point function, we have

$$\begin{aligned} &\sim \frac{\lambda^3}{\Lambda^{2\kappa+3}} \int d^4 q \frac{q^{4\kappa}}{[1 + (q/\Lambda)^{2\kappa+2}]^3} \int_{\Lambda}^{\infty} \frac{d\Lambda_1}{\Lambda_1^{2\kappa+3}} \int d^4 p \\ &\quad \times \frac{p^{2\kappa}}{[1 + (p/\Lambda_1)^{2\kappa+2}]^2} \left[ 1 - \frac{1}{1 + (|\mathbf{q} + \mathbf{p}|/\Lambda_1)^{2\kappa+2}} \right] \frac{1}{|\mathbf{q} + \mathbf{p}|^2}. \end{aligned} \quad (3.58)$$

A derivative expansion requires an expansion in the external momentum of the one-loop four-point function which translates as expanding the inner integral in powers of the momentum  $q$ . This expansion can be performed to all orders. However, once the power  $q^{2m}$  is such that  $m \geq \kappa + 1$ , the outer integral over  $q$  will cease to converge. Hence with a power law cutoff even the coefficients of the derivative expansion are infinite and hence such an expansion ceases to make sense.

This problem arises purely because we are also working within a perturbation expansion. As stated earlier, non-perturbatively all integrals will converge if  $\kappa > D/2 - 1$ . The improved behaviour here can be traced to the  $(q^2 + C_{IR}\Sigma)^{-3}$  factor contained in (2.21) and (2.23). For small  $\lambda$ ,  $\Sigma \sim \lambda^2 q^{2m}$  at  $O(\partial^{2m})$ , from figure 3.6. The extra powers of  $q$  in the denominator always stabilise the integral providing  $\kappa > D/2 - 1$ , but clearly the integral will then diverge as  $\lambda \rightarrow 0$ .

## 3.8 Operators of higher powers

The results presented in this chapter can, to a certain extent, also address the issue of convergence for operators of higher momentum powers than the (zeroth order)  $\beta$  function. Let us first consider the sharp cutoff of section 3.5.

The  $n$ th term in the momentum scale expansion of an  $O(\partial^{2r})$  operator is given by that of the derivative-free operator (with the same number of fields) but with the  $q^n$  in the expanded terms of (3.38) replaced by  $\sim \binom{n/2}{2r} q^{n-2r} k^{2r}$ , with  $k$  some external momentum. For large  $n$  this will yield a multiplier  $\sim n^{2r}$ . Thus, if convergence is to occur for all operators, the coefficients of the expansion must fall faster than a power of  $n$ . We saw that the series (3.39) barely managed to converge and the coefficients certainly did not fall faster than any power of  $n$ . Without the need for further calculation, it is evident that the contribution of figure 3.4 (b) will have a momentum scale expansion that ceases to converge at second or higher order in its external momenta. In particular, the  $O(k^{2r})$   $r \geq 1$  coefficients of

$$-6\lambda^3 \int \frac{d^4 q}{(2\pi)^4} \frac{\delta(q - \Lambda)}{q^2} \int_{\Lambda}^{\infty} d\Lambda_1 \int \frac{d^4 p}{(2\pi)^4} \frac{\delta(p - \Lambda_1)}{p^2} \frac{\theta^2(|\mathbf{p} + \mathbf{q}| - \Lambda_1)}{|\mathbf{p} + \mathbf{q}|^4} \quad (3.59)$$

will not provide a convergent momentum scale expansion.

The situation is much more promising with the smooth exponential cutoff of section 3.6. The series (3.50), (3.53) and (3.54) all fall faster than  $1/R^n$ , with  $R > 1$  (*i.e.* faster than a power of  $n$ ). The equivalent of the troublesome diagram for the sharp cutoff is series (3.49) which can best be analysed by recasting the original integral

$$\begin{aligned} & -6\lambda^3 \int \frac{d^4 q}{(2\pi)^4} \frac{\frac{\partial}{\partial \Lambda} (e^{-q^2/\Lambda^2})}{q^2} \int_{\Lambda}^{\infty} d\Lambda_1 \int \frac{d^4 p}{(2\pi)^4} \frac{\frac{\partial}{\partial \Lambda_1} (e^{-p^2/\Lambda_1^2})}{p^2} \frac{(1 - e^{-|\mathbf{p} + \mathbf{q}|^2/\Lambda_1^2})^2}{|\mathbf{p} + \mathbf{q}|^4} \\ &= \frac{6\lambda^3}{\Lambda^3 (4\pi)^2} \sum_{n=0}^{\infty} \int \frac{d^4 q}{(2\pi)^4} \frac{e^{-q^2/\Lambda^2}}{q^2} \int_{\Lambda}^{\infty} d\Lambda_1 \frac{(-1)^n}{\Lambda_1 n!} \left(\frac{q}{\Lambda_1}\right)^{2n} \end{aligned}$$

$$\times \int_0^1 da \left\{ \left( \frac{1+a}{2+a} \right)^n - \left( \frac{a}{1+a} \right)^n \right\} \quad (3.60)$$

It is evident that the integral over  $a$  is bounded from above by  $(2/3)^n$  and from below by zero. Together with the  $1/n!$  factor, this provides a sufficiently fast rate of convergence.

We can take this analysis further by repeating that used with the sharp cutoff. For an  $O(\partial^2)$  operator, the power of  $q^{2n}$  of the expanded terms of (3.48), is replaced by  $\sim n^{2r} k^{2r} q^{2n-2r}$  (with  $k$  again being some external momentum). With the coefficients going like  $\sim 1/n!$  or better, the  $q$  integral will not completely cancel, leaving a remainder  $\sim 1/n^{2r}$  for large  $n$ . Hence we see that the derivative expansions of higher derivative operators will converge.

### 3.9 Summary and conclusions

In summary, the derivative expansion for the  $\beta$  function was calculated at one-loop order for the Wilson/Polchinski flow equation and was found to converge for certain fast falling profiles. The equivalent for the Legendre flow equation trivially converged as no expansion was possible. With a sharp cutoff used within the Legendre flow equation, slow convergence was found for the two-loop  $\beta$  function and it was demonstrated that higher momentum operators have divergent momentum scale expansions. While a power law cutoff proved not to provide meaningful results, the most promising profile was an exponential which, when used in the Legendre flow equation, has rapid convergence of the derivative expansion of the  $\beta$  function and higher momentum operators. The properties exhibited by the exponential cutoff has resulted in it being favoured by many authors [9, 19].

The technique of approximation using derivative expansions within exact RG flow equations has been shown to be applicable in the calculation of perturbative quanti-

ties. However, it has been demonstrated that scalar field theory is largely perturbative in nature both in  $D = 4$  [20] and  $D = 3$  [14], so the successes recorded here also go some way to explaining the accurate results found using derivative expansions in a non-perturbative setting (see *e.g.* [11, 12, 15, 21]).

# Chapter 4

## Towards a gauge invariant exact RG

In this chapter we identify the manner of regularisation as one of the stumbling blocks in the establishment of a gauge invariant RG. One approach suggests a regularisation scheme using the ideas of supersymmetry might exist and we introduce some of the necessary concepts before formulating the regularisation scheme in the next chapter. Unless otherwise stated, this chapter is based upon material from sources<sup>1</sup> [3, 14, 23, 24, 25].

### 4.1 Consequences of gauge invariance

Problems arise when we attempt to carry over the concepts of the Wilsonian RG to QFTs which have local internal symmetry groups. To see this we need only consider a theory consisting of just a gauge field  $A_\mu(x) \equiv A_\mu^a(x) T_a$ , where the  $T_a$  are generators

---

<sup>1</sup>The mathematics of supergroups is also discussed in [22]

of the gauge group. We define the covariant derivative  $\nabla_\mu$  with coupling  $g$  to be  $\nabla_\mu := \partial_\mu - igA_\mu$  with the gauge field acting by commutation. We can take the bare Lagrangian to be

$$\mathcal{L}_{gauge} = \frac{1}{2}\text{tr}(F_{\mu\nu}F_{\mu\nu}), \quad (4.1)$$

where the field strength is given by  $F_{\mu\nu} := \frac{i}{g}[\nabla_\mu, \nabla_\nu]$  and the trace is over group indices. The Lagrangian is invariant under a gauge transformation of the type

$$A_\mu \rightarrow \partial_\mu\omega - ig[A_\mu, \omega], \quad (4.2)$$

where  $\omega$  is the gauge parameter. When we transform (4.2) to momentum space, the second term leads to a convolution over all momentum. Thus the restrictions placed upon allowed values of momentum that we employed in the scalar field theory, do not respect this invariance.

This restriction upon momentum space is known as a *regularisation scheme*. We therefore have to make a choice: either break gauge invariance and hope to restore at a later stage [2] or find an alternative regularisation scheme. In the next section we consider whether a regularisation scheme can be found that will enable Wilsonian ideas to be applied, yet allow us to retain gauge invariance.

## 4.2 Regularisation techniques

Throughout the subject of QFT, one is confronted with physical calculations that involve divergent integrals. The need to manipulate these integrals and to rigorously define the theory, provide the motivation for regularisation - the process of making the integrals finite at intermediary steps of the calculation. Regularisation is achieved via a modification of the theory at high energies which renders all integrals finite in a manner that is determined by a single parameter. This parameter can also be

tuned to a specified limit in such a way as to regain the original (divergent) theory. It must be stressed that the procedure of regularisation is completely separate from that of renormalisation (in old-fashioned parlance the process by which divergences are removed via redefinitions of the couplings). The final renormalised theory is independent of regularisation technique utilised and the control parameter will not appear in calculated physical quantities.

There are a wide variety of regularisation techniques available in the literature, each with its own advantages and disadvantages and hence its own area of applicability. In this section, some of the most important methods of regularisation are introduced and the reasons for their unsuitability as a regulating scheme for a gauge invariant exact RG are discussed.

#### 4.2.1 Dimensional regularisation

In the case of gauge invariant theories, the most widely utilised regularisation is dimensional regularisation as this has the attractive property of maintaining gauge invariance at all stages. The central idea is to generalise the spacetime dimension from  $D$  to an arbitrary (not necessarily integer) dimension  $d$ . For sufficiently small  $d$ , all the Feynman diagrams are finite. The UV divergences of the theory appear as simple or multiple poles at  $d = D$ . All symmetries, including gauge symmetries (although problems arise with chiral fields), that are independent of the dimension of spacetime are preserved.

While this regularisation scheme is the most widely used and practical technique for gauge theories, it suffers from a number of drawbacks if it is to be incorporated into an exact RG framework. Firstly, it does not sit easily with the Wilsonian approach of suppression of high energy modes since dimensional regularisation has no such physical interpretation. Secondly, it is not clear whether this scheme has any meaning

non-perturbatively since it is applied directly to (perturbative) Feynman diagrams and the non-perturbative capability of the Wilsonian approach is one which we would like to preserve.

### 4.2.2 Pauli-Villars regularisation

This technique [26] (like momentum space cutoffs) modifies the behaviour of the propagator at high momenta. It achieves this by introducing fictitious particles with the same interactions but which have no effect at low energies. However, at high energies the propagator of the new field exactly cancels that of the original one. This is achieved by giving these Pauli-Villars particles large masses,  $M_k$ . Thus we have

$$\Delta_{\mu\nu}^{reg}(p) = \Delta_{\mu\nu}(p) + \sum_k C_k \Delta_{\mu\nu}^k(p, M_k) \quad (4.3)$$

When the limit  $M_k \rightarrow \infty$  is taken, the regularisation is removed.

### 4.2.3 Higher covariant derivatives

This method attempts to extend the idea of a momentum space cutoff to the realm of gauge theories [27]. If we view the scalar theory in Euclidean space, we have cutoff functions appearing as  $C_{UV}(-\partial^2/\Lambda^2)$ . Thus to proceed in a gauge invariant manner we replace all ordinary derivatives by covariant derivatives. In this way we may hope to regularise the action of (4.1) by replacing it with the following.

$$\mathcal{L}_{gauge} = \frac{1}{2} \text{tr}(F_{\mu\nu} C_{UV}(-\nabla^2/\Lambda^2) \cdot F^{\mu\nu}), \quad (4.4)$$

with the dot signifying that the covariant derivatives act via commutation. Unfortunately, this is not enough to completely regularise the theory; the insertion of covari-

ant derivatives introduces fresh interactions. If the cutoff function  $C_{UV}(-\nabla^2/\Lambda^2)$  is a polynomial in its argument of rank  $n$ , then the superficial degree of divergence of a (1PI) Feynman diagram in  $D$  dimensions is (ignoring gauge-fixing terms which do not affect the argument)

$$\mathcal{D}_\Gamma = DL - (2n + 2)I + \sum_{i=3}^{2n+4} (2n + 4 - i)V_{A^i} \quad (4.5)$$

where  $L$  is the number of loops of the diagram,  $I$  the number of internal propagators it possesses and  $V_{A^i}$  the number of vertices at which  $i$   $A$  fields are present. Using the relations

$$L = 1 + I - \sum_i V_{A^i}, \quad (4.6)$$

$$E = -2I + \sum_i i V_{A^i}, \quad (4.7)$$

(with  $E$  the number of external lines of the Feynman graph), (4.5) becomes

$$\mathcal{D}_\Gamma = (D - 4)L - 2n(L - 1) - E + 4. \quad (4.8)$$

In  $D = 4$  (the case of most physical relevance), the rank  $n$  can always be chosen such that  $\mathcal{D}_\Gamma$  is always negative (and hence all diagrams are superficially convergent) *except* when  $L = 1$  and  $E \leq 4$ , where this regularisation fails.

#### 4.2.4 Hybrid regularisation

This takes the methods of Pauli-Villars and higher covariant derivatives and combines them to produce a gauge-invariant regularisation [28, 29]. The higher covariant derivatives takes care of all the divergences appearing in diagrams with more than one loop, and all but a small subset at one loop which are taken care of by the Pauli-Villars regularisation. Unfortunately further one-loop divergences then typically arise when

the Pauli-Villars fields are external. It may be argued that this could be ignored on the grounds that the Pauli-Villars particles cannot be regarded as physical. However, these divergences will reappear in internal subdiagrams embedded at higher loops. This is referred to as the problem of overlapping divergences. It can be cured by adding yet more Pauli-Villars fields and by carefully choosing their actions [29]. The Pauli-Villars fields need to appear bilinearly in the action so that upon integrating out, they provide missing one-loop counterterms. Unfortunately this is not a property that can be preserved by the exact RG framework.

In a series of papers [3, 4, 5] a manner of constructing a  $SU(N)$  gauge invariant exact RG was suggested. Using the insight that the freedom in the construction of exact RG equations amounts to a general field redefinition [30], a flow equation is formulated. The necessary regularisation is provided by a form of the hybrid regularisation. However, for the regularisation scheme to prove effective, many requirements were placed upon the properties of the Pauli-Villars fields including the presence of a wrong-sign gauge field, fermionic gauge partners and scalar fields. The required cancellations forced the flow equation itself to be of a complicated form [5]. Other shortcomings of the scheme were that it could only be applied at  $N = \infty$  and that it suffered from the problem of overlapping divergences. It was realised however that the plethora of particles might be more elegantly described (except for a few minor discrepancies) by embedding the  $SU(N)$  gauge group within the larger  $SU(N|N)$  supergroup and allowing this larger group to be spontaneously broken. Unlike the bilinear Pauli-Villars regularisation, the spontaneously broken  $SU(N|N)$  structure can be preserved under exact RG flows. The aim of chapter 5 is to show that spontaneously broken  $SU(N|N)$  with covariant derivatives provides a regularisation scheme to all loop orders at finite  $N$ .

## 4.3 Supersymmetric groups

An important concept that has attracted wide attention in the field of theoretical physics since the 1970s is that of supersymmetry, a symmetry which mixes bosons and fermions. Usually it is considered as a symmetry of the space-time background [31]. However, work where the supersymmetry exists in the internal symmetry of the QFT in an ordinary background actually predates this [32] (although largely ignored at the time) and is what we shall concern ourselves with here. In this section we shall introduce some of the properties of these supergroups within the context of the supergroups  $SU(N|M)$  and  $SU(N|N)$ .

### 4.3.1 Grading

The set of integers provide the simplest example of a graded structure. They have the property of being either even or odd. With ordinary addition denoted by the symbol ‘ $\cdot$ ’, the additive group of integers has the following behaviour.

$$\begin{aligned} \text{even} \cdot \text{even} &= \text{even}, \\ \text{even} \cdot \text{odd} &= \text{odd}, \\ \text{odd} \cdot \text{odd} &= \text{even}. \end{aligned} \tag{4.9}$$

This structure is the same as that of  $Z_2$ , the cyclic group of order 2:

$$e \cdot e = e, \quad e \cdot a = a \cdot e = a, \quad a \cdot a = e, \tag{4.10}$$

where  $e$  is the identity and  $a$  the other element of the group being identified with even and odd integers respectively. Hence, the grading structure of (4.9) is known as  $Z_2$  grading and appears in the Lie superalgebras which are of interest in this work, with the characteristic of being odd or even replaced by the property of being fermionic or

bosonic.

### 4.3.2 $SU(N|M)$

An even supermatrix  $\mathbf{M}$  is a  $(p+q) \times (r+s)$  matrix partitioned such that

$$\mathbf{M} = \begin{pmatrix} \mathbf{A} & \mathbf{B} \\ \mathbf{C} & \mathbf{D} \end{pmatrix}, \quad (4.11)$$

where  $\mathbf{A}$  ( $\mathbf{D}$ ) is a  $p \times r$  ( $q \times s$ ) submatrix whose elements are even under the grading structure and  $\mathbf{B}$  ( $\mathbf{C}$ ) is a  $q \times r$  ( $p \times s$ ) submatrix constructed from odd elements.

The set of  $(N+M) \times (N+M)$  even supermatrices define the Lie supergroup  $U(N|M)$  (with  $N \neq M$ ) if any element  $\mathbf{G}$  of the set satisfies the condition

$$\mathbf{G}^\dagger \mathbf{G} = 1, \quad (4.12)$$

where  $\mathbf{G}^\dagger$  denotes the adjoint of  $\mathbf{G}$ . The adjoint of a supermatrix is defined such that the adjoint of the matrix  $\mathbf{M}$  of (4.11) is

$$\mathbf{M}^\dagger = \begin{pmatrix} \tilde{\mathbf{A}}^\# & \tilde{\mathbf{C}}^\# \\ \tilde{\mathbf{B}}^\# & \tilde{\mathbf{D}}^\# \end{pmatrix}, \quad (4.13)$$

where the tilde means that we take the transpose of the submatrix. The hash operator represents the Grassmann adjoint of the submatrix and is defined as follows. In the vector space in which the submatrix  $\mathbf{N}$  lies, it can be written as

$$\mathbf{N} = \sum_\mu (u_\mu + i v_\mu) \epsilon_\mu, \quad (4.14)$$

where each  $u_\mu$  and  $v_\mu$  are real numbers and the  $\epsilon_\mu$  form a particular basis. Then we

define

$$\mathbf{N}^\sharp = \sum_\mu (u_\mu - iv_\mu) \epsilon_\mu^\sharp, \quad (4.15)$$

where for this basis

$$\epsilon_\mu^\sharp = \begin{cases} \epsilon_\mu & \text{if } \epsilon_\mu \text{ is bosonic,} \\ -i\epsilon_\mu & \text{if } \epsilon_\mu \text{ is fermionic.} \end{cases} \quad (4.16)$$

This implies for a general bosonic element written as  $X + iY$  ( $X$  and  $Y$  real) that

$$(X + iY)^\sharp = X - iY, \quad (4.17)$$

while for a general fermionic element  $\Theta + i\Psi$  ( $\Theta$  and  $\Psi$  real Grassmann numbers) we find

$$(\Theta + i\Psi)^\sharp = -i\Theta - \Psi. \quad (4.18)$$

In turn,  $SU(N|M)$  is the subgroup of  $U(N|M)$  whose supermatrices have the additional property that

$$\text{sdet } \mathbf{G} = 1, \quad (4.19)$$

with the superdeterminant defined [again with regard to the supermatrix of (4.11)] as

$$\text{sdet } \mathbf{M} = \frac{\det(\mathbf{A} - \mathbf{B} \mathbf{D}^{-1} \mathbf{C})}{\det \mathbf{D}}. \quad (4.20)$$

Let  $\mathcal{H}$  be a member of the Lie superalgebra of  $U(N|M)$ , partitioned as an even supermatrix:

$$\mathcal{H} = \begin{pmatrix} \mathbf{P} & \mathbf{Q} \\ \mathbf{R} & \mathbf{S} \end{pmatrix}. \quad (4.21)$$

Condition (4.12) implies that

$$\mathcal{H} + \mathcal{H}^\sharp = 0, \quad (4.22)$$

which in turn implies that

$$\mathbf{P} = -\tilde{\mathbf{P}}^\sharp, \quad (4.23)$$

$$\mathbf{S} = -\tilde{\mathbf{S}}^\sharp, \quad (4.24)$$

$$\mathbf{Q} = -\tilde{\mathbf{R}}^\sharp, \quad (4.25)$$

where, for example  $(\tilde{\mathbf{P}}^\sharp)_j^i = (P_i^j)^\sharp$ . Using (4.17) and (4.18), we find we are able to write the algebra of  $U(N|M)$  in the  $(N+M)$  dimensional fundamental representation is of the form of  $(N+M) \times (N+M)$  even supermatrices

$$\mathcal{H} = \begin{pmatrix} H_N & \theta \\ \theta^\dagger & H_M \end{pmatrix}. \quad (4.26)$$

$H_N$  ( $H_M$ ) is an  $N \times N$  ( $M \times M$ ) Hermitian matrix.  $\theta$  is a  $N \times M$  matrix composed of complex Grassmann numbers and  $\theta^\dagger$  is its Hermitian conjugate. Together  $\theta$  and  $\theta^\dagger$  contain  $2NM$  real anti-commuting Grassmann numbers.

Using the supermatrix of (4.11) as an example once more, the supertrace is defined to be

$$\text{str } \mathbf{M} = \text{tr} \mathbf{A} - \text{tr} \mathbf{D} \quad (4.27)$$

$$= \text{tr}(\sigma_3 \mathbf{M}), \quad (4.28)$$

where we have taken the opportunity to introduce the  $(N+M) \times (N+M)$  version of the third Pauli matrix.<sup>2</sup> The supertrace of supermatrices is cyclically invariant.

If we require that  $\mathcal{H}$  is a member of the Lie superalgebra of  $SU(N|M)$ , we take account of the condition placed on the elements of the group (4.19), by noting that

---

<sup>2</sup>i.e.  $\sigma_3 = \begin{pmatrix} \mathbb{1}_N & 0 \\ 0 & -\mathbb{1}_M \end{pmatrix}$  with  $\mathbb{1}_{N(M)}$  being the  $N \times N$  ( $M \times M$ ) identity matrix

(see Appendix A)

$$\text{sdet}(\exp(\mathbf{M})) = \exp(\text{str } \mathbf{M}), \quad (4.29)$$

and hence require

$$\text{str } \mathcal{H} = 0. \quad (4.30)$$

Imposing (4.30) has the effect that the traceless part of  $H_N$  ( $H_M$ ) can be identified with an  $SU(N)$  ( $SU(M)$ ) subgroup with the traceful part giving rise to a  $U(1)$ . Hence the bosonic sector of  $SU(N|M)$  forms a  $SU(N) \times SU(M) \times U(1)$  subgroup.

As a concrete example of an  $SU(N|M)$  group we can consider  $SU(2|1)$ ; a supergroup that has been studied within the context of the Standard Model [33]. A general element of the algebra may be written as

$$\mathcal{H} = \frac{1}{2} \left( \begin{array}{c|c} \sum_{i=1}^3 \eta^i \sigma_i + \eta^4 \mathbb{1}_2 & \theta^1 - i\theta^2 \\ \hline \theta^1 + i\theta^2 & \theta^3 - i\theta^4 \\ \theta^3 + i\theta^4 & 2\eta^4 \end{array} \right) \quad (4.31)$$

$$= \sum_{m=1}^4 \eta^m U_m + \sum_{\mu=1}^4 \theta^\mu V_\mu, \quad (4.32)$$

where  $\sigma_i$  are the  $(2 \times 2)$  Pauli matrices,  $\eta^m$  are real bosonic parameters and  $\theta^\mu$  real fermionic variables. The bosonic generators  $U_M$  are

$$U_i = \frac{1}{2} \left( \begin{array}{c|c} \sigma_i & 0 \\ \hline 0 & 0 \\ 0 & 0 \end{array} \right), \quad U_4 = \left( \begin{array}{cc|c} \frac{1}{2} & 0 & 0 \\ 0 & \frac{1}{2} & 0 \\ 0 & 0 & 1 \end{array} \right), \quad (4.33)$$

and the fermionic sector generators  $V_\mu$  are given by

$$\begin{aligned} V_1 &= \frac{1}{2} \begin{pmatrix} 0 & 0 & 1 \\ 0 & 0 & 0 \\ 1 & 0 & 0 \end{pmatrix}, \quad V_2 = \frac{1}{2} \begin{pmatrix} 0 & 0 & -i \\ 0 & 0 & 0 \\ i & 0 & 0 \end{pmatrix}, \\ V_3 &= \frac{1}{2} \begin{pmatrix} 0 & 0 & 0 \\ 0 & 0 & 1 \\ 0 & 1 & 0 \end{pmatrix}, \quad V_4 = \frac{1}{2} \begin{pmatrix} 0 & 0 & 0 \\ 0 & 0 & -i \\ 0 & i & 0 \end{pmatrix}. \end{aligned} \tag{4.34}$$

While these generators bear many similarities to those of  $SU(3)$ , note that the fermionic generators  $V_n$  close onto the bosonic generators by *anticommutation*, *i.e.*  $\{V_\mu, V_\nu\} = C_{\mu\nu}^m T_m$ . However, by including the parameters in these relations, we can retain the usual Lie commutation rule:

$$[\mathcal{H}, \mathcal{H}'] = i \mathcal{H}''. \tag{4.35}$$

For general  $SU(N|M)$  we have (in the adjoint representation)

$$\mathcal{H}^i{}_j = \omega^A (T_A)^i{}_j, \tag{4.36}$$

where  $\omega^A$  is a bosonic or fermionic parameter depending on the index  $A$ . The first  $N^2 + M^2 - 1$  are chosen to be bosonic and the remaining  $2NM$  are fermionic.

The generators thus contain only ordinary numbers. They are chosen to be those of table 4.1, where  $\tau_A^{(N)}$  are the traceless generators of  $SU(N)$  normalised such that

$$\text{tr}(\tau_A^{(N)} \tau_B^{(N)}) = \frac{1}{2} \delta_{AB} \quad \begin{cases} 1 \leq A \leq N^2 - 1 \\ 1 \leq B \leq N^2 - 1 \end{cases} \tag{4.37}$$

and similarly for  $\tau^{(M)}$ .

$A = 0$	$\sqrt{\frac{NM}{2 N-M }} \begin{pmatrix} \frac{1\mathbb{I}_N}{N} & 0 \\ 0 & \frac{1\mathbb{I}_M}{M} \end{pmatrix}$	$U(1)$
$A = 1, \dots, N^2 - 1$	$\begin{pmatrix} \tau_A^{(N)} & 0 \\ 0 & 0 \end{pmatrix}$	$SU(N)$
$A = N^2, \dots, N^2 + M^2 - 2$	$\begin{pmatrix} 0 & 0 \\ 0 & \tau_A^{(M)} \end{pmatrix}$	$SU(M)$
$A = N^2 + M^2 - 1, \dots, (N+M)^2 - 1$	$\begin{pmatrix} 0 & 0 & \dots & 1 & 0 & \dots \\ 0 & 0 & \dots & 0 & 0 & \dots \\ \vdots & \vdots & & \vdots & \vdots & \\ \hline 1 & 0 & \dots & 0 & 0 & \dots \\ 0 & 0 & \dots & 0 & 0 & \dots \\ \vdots & \vdots & & \vdots & \vdots & \end{pmatrix}$ $etc.$ $\begin{pmatrix} 0 & 0 & \dots & -i & 0 & \dots \\ 0 & 0 & \dots & 0 & 0 & \dots \\ \vdots & \vdots & & \vdots & \vdots & \\ \hline i & 0 & \dots & 0 & 0 & \dots \\ 0 & 0 & \dots & 0 & 0 & \dots \\ \vdots & \vdots & & \vdots & \vdots & \end{pmatrix}$	Super

Table 4.1: Table of generators of  $SU(N|M)$

This enables us to define the super Killing metric of the group as

$$g_{AB} = 2 \text{str}(T_A T_B), \quad (4.38)$$

and with the generators normalised as in table 4.1, this results in

$$g_{AB} = \begin{pmatrix} \pm 1 & & & & \\ & 1 & & & \\ & & \ddots & & \\ & & & -1 & \\ & & & & -1 \\ & & & & \ddots \\ & & & & 0 & i \\ & & & & -i & 0 \\ & & & & 0 & i \\ & & & & -i & 0 \\ & & & & & \ddots \end{pmatrix} \quad (4.39)$$

$\underbrace{\phantom{...}}_{U(1)}$     $\underbrace{\phantom{...}}_{SU_1(N)}$     $\underbrace{\phantom{...}}_{SU_2(N)}$     $\underbrace{\phantom{...}}_{\text{Fermionic}}$

with the sign of the  $U(1)$  sector determined as positive for  $N > M$  and negative for  $N < M$ . Note that while the metric is symmetric in the bosonic part, it is antisymmetric in the fermionic sector, a fact that we express as

$$g_{AB} = g_{BA} (-1)^{f(A)f(B)}, \quad (4.40)$$

by introducing  $f(A)$ , the grade of the index  $A$  defined such that

$$f(A) = \begin{cases} 0 & \text{if } A \text{ is a bosonic index} \\ 1 & \text{if } A \text{ is a fermionic index} \end{cases} \quad (4.41)$$

We are also able to define another metric  $g^{AB}$  which is the inverse of that of (4.39)

$$g^{AB} g_{BC} = g_{CB} g^{BA} = \delta^A_C, \quad (4.42)$$

with a sum over  $B$ . This enables us to lower indices on the parameters:

$$X_A := g_{AB} X^B, \quad (4.43)$$

(note that it is the second index of the metric that is summed over; from (4.40) it is clear that the ordering of indices is important), and raise indices on the generators

$$T^A := g^{AB} T_B. \quad (4.44)$$

Since the generators of  $SU(N|M)$  form a complete set of  $(N+M) \times (N+M)$  supertraceless matrices, we can derive (see Appendix B.1) a completeness relation:

$$(T^A)_j^i (T_A)^k_l = \frac{1}{2} (\sigma_3)_l^i \delta_j^k - \frac{1}{2(N-M)} \delta_j^i \delta_l^k. \quad (4.45)$$

### 4.3.3 $SU(N|N)$

It is evident from consideration of the denominator of the  $U(1)$  generator in table 4.1 and that of the last term in the completeness relation (4.45) that a naïve setting of  $N = M$  will not be sufficient to define  $SU(N|N)$ . All of the problems that arise can be traced back to the  $U(1)$  subgroup of the bosonic sector. In the case of  $SU(N|N)$ , this generator becomes proportional to the identity in  $2N$  dimensions,  $\mathbb{1}_{2N}$ , and commutes with every other generator in the Lie algebra. This will give rise to a number of interesting properties when  $SU(N|N)$  is employed as a gauge group, a discussion of which we delay until chapter 5. In fact the  $U(1)$  part has proved to be so unpalatable, that some authors have dropped it completely [25]. We will not take such a drastic step (a deeper discussion of such subtleties is contained in chapter 5). Instead we note that the identity matrix does indeed have a special rôle to play and so separate it from the other generators.

We split the generators  $T_A = \{1\!\!1, S_\alpha\}$ , *i.e.*  $S_\alpha$  are the traceless generators of  $SU(N|N)$ ,  $A \equiv \{0, \alpha\}$  and  $\alpha$  runs from 1 to  $4N^2 - 1$ , with the first  $2(N^2 - 1)$  of these being bosonic indices. Once again we can define a super Killing metric as in (4.38). The normalisation of the generators means that the metric is

$$g_{AB} = \left( \begin{array}{c|c|c|c} 0 & & & \\ \hline & 1 & & \\ & & 1 & \\ & & \ddots & \\ \hline & & & -1 \\ & & & & -1 \\ & & & & \ddots \\ \hline & & & & 0 & i \\ & & & & -i & 0 \\ & & & & 0 & i \\ & & & & -i & 0 \\ & & & & & \ddots \end{array} \right) \quad (4.46)$$

$\underbrace{\phantom{\Bigg(}}_{U(1)}$     $\underbrace{\phantom{\Bigg(}}_{SU_1(N)}$     $\underbrace{\phantom{\Bigg(}}_{SU_2(N)}$     $\underbrace{\phantom{\Bigg(}}_{\text{Fermionic}}$

Obviously we cannot define an inverse to this metric. However if we restrict ourselves to just the traceless  $S_\alpha$  generators, we are able to define

$$h_{\alpha\beta} = h_{\beta\alpha} (-1)^{f(\alpha)f(\beta)} = 2 \text{str} (S_\alpha S_\beta), \quad (4.47)$$

with the inverse  $h^{\alpha\beta}$  determined by

$$h^{\alpha\beta} h_{\beta\gamma} = h_{\gamma\beta} h^{\beta\alpha} = \delta_\gamma^\alpha. \quad (4.48)$$

This then allows us to raise indices as in (4.43) and (4.44). Since the  $S_\alpha$  generators form a complete set of supertraceless and traceless matrices, a completeness relation

can be constructed for them (see Appendix B.2):

$$(S^\alpha)^i{}_j (S_\alpha)^k{}_l = \frac{1}{2} (\sigma_3)^i{}_l \delta^k{}_j - \frac{1}{4N} [(\sigma_3)^i{}_j \delta^k{}_l + \delta^i{}_j (\sigma_3)^k{}_l]. \quad (4.49)$$

This is most usefully cast in the following forms

$$\text{str}(XS_\alpha) \text{str}(S^\alpha Y) = \frac{1}{2} \text{str}(XY) - \frac{1}{4N} [\text{tr}X \text{str}Y + \text{str}X \text{tr}Y], \quad (4.50)$$

$$\text{str}(S_\alpha XS^\alpha Y) = \frac{1}{2} \text{str}X \text{str}Y - \frac{1}{4N} \text{tr}(XY + YX), \quad (4.51)$$

for arbitrary supermatrices  $X$  and  $Y$ . In chapter 5 we will use  $SU(N|N)$  as a gauge group and demonstrate how it can act as a regulator.

# Chapter 5

## Regularisation via $SU(N|N)$

As we saw in subsection 4.2.4 it is possible to construct a gauge invariant regularisation scheme by combining the techniques of regularisation via covariant higher derivatives and Pauli-Villars fields. It could also be noted that such a technique appears cumbersome and unsuited to the exact RG approach. In this chapter we introduce an extension of these ideas in which the combination of these methods appears more natural and also more promising as regards the exact RG [34]–[36].

### 5.1 The action of the regulating scheme

In this section we describe the action for the regulating scheme using covariant derivatives in spontaneously broken  $SU(N|N)$  gauge theory.

### 5.1.1 The gauge field sector

We start by introducing  $\mathcal{A}_\mu$ , the gauge field of  $SU(N|N)$  :

$$\begin{aligned}
\mathcal{A}_\mu &\equiv \mathcal{A}_\mu^A T_A \\
&= \mathcal{A}_\mu^\alpha S_\alpha + \mathcal{A}_\mu^0 \mathbb{1} \\
&= \begin{pmatrix} A_\mu^1 & B_\mu \\ \bar{B}_\mu & A_\mu^2 \end{pmatrix} + \begin{pmatrix} \mathcal{A}_\mu^0 & 0 \\ 0 & \mathcal{A}_\mu^0 \end{pmatrix}, \tag{5.1}
\end{aligned}$$

where  $S_\alpha$  are traceless and supertraceless generators of  $SU(N|N)$ . Note we have also included the unity generator and its associated bosonic field in (5.1). The  $A_1$  field is the usual  $SU(N)$  gauge boson which we wish to regulate, with the  $A_2$  field being a  $SU(N)$  copy which, as we shall see, will enter the Lagrangian with the wrong sign. The  $B$  field is fermionic and will eventually play the rôle of the fermionic Pauli-Villars regulating particles.

The Lagrangian we require will be ultra-violet regulated. The first step in achieving this is to utilise the supergroup variant of higher covariant derivatives. The covariant derivative is chosen to be

$$\nabla_\mu := \partial_\mu - ig\Lambda^{2-D/2}\mathcal{A}_\mu, \tag{5.2}$$

where we have chosen to make the coupling dimensionless by explicitly including the appropriate powers of  $\Lambda$ . The field strength is then given by

$$\mathcal{F}_{\mu\nu} := \Lambda^{D/2-2} \frac{i}{g} [\nabla_\mu, \nabla_\nu]. \tag{5.3}$$

Using the wine notation explained in Appendix C we can then write the pure Yang-Mills part of the action as

$$S_{YM} = \frac{1}{2} \mathcal{F}_{\mu\nu} \{c^{-1}\} \mathcal{F}_{\mu\nu}. \tag{5.4}$$

The function  $c^{-1}$  that appears in the wine is chosen to be a polynomial in its ar-

gument [in this case  $(\nabla^2/\Lambda^2)$ ] of rank  $r$ . The action is invariant under the gauge transformations

$$\delta\mathcal{A}_\mu = \frac{1}{g}\Lambda^{D/2-2}[\nabla_\mu, \omega]. \quad (5.5)$$

There are two features of (5.4) which must be commented upon. Firstly, the  $\mathcal{A}^0$  field plays no part in it. We note that all  $\mathcal{A}$  field interactions occur via commutators and since the  $\mathcal{A}^0$  field (uniquely) commutes with everything, it cannot interact. Furthermore, because  $\text{str}(\mathbb{1} T_A) = 0$ , we see that it cannot propagate and is non-dynamical. The effect of integrating over the  $\mathcal{A}^0$  field in the partition function is therefore just to introduce an (infinite) constant which can be factored out. However, we are not allowed to simply exclude  $\mathcal{A}^0$  as gauge transformations do appear in the  $\mathbb{1}$  direction since the identity is generated by fermionic elements of the superalgebra, *e.g.*

$$\frac{1}{2} \left\{ \left( \begin{array}{cc} 0 & \mathbb{1}_N \\ \mathbb{1}_N & 0 \end{array} \right), \left( \begin{array}{cc} 0 & \mathbb{1}_N \\ \mathbb{1}_N & 0 \end{array} \right) \right\} = \mathbb{1}_{2N}. \quad (5.6)$$

An alternative procedure for tackling the troublesome  $U(1)$  sector is that favoured by ref. [25]. This redefines the Lie bracket to ensure that  $\mathbb{1}_{2N}$  does not appear. Thus the \*bracket is given by

$$[ , ]_\pm^* = [ , ]_\pm - \frac{\mathbb{1}}{2N} \text{tr}[ , ]_\pm \quad (5.7)$$

where  $[ , ]_\pm$  is a graded commutator.<sup>1</sup> The super Jacobi identity is still satisfied since

$$[\mathcal{H}_1, [\mathcal{H}_2, \mathcal{H}_3]]^* = [\mathcal{H}_1, [\mathcal{H}_2, \mathcal{H}_3]]^* \quad (5.8)$$

$$= [\mathcal{H}_1, [\mathcal{H}_2, \mathcal{H}_3]] - \frac{\mathbb{1}}{2N} \text{tr}[\mathcal{H}_1, [\mathcal{H}_2, \mathcal{H}_3]]. \quad (5.9)$$

The equality in (5.8) follows upon the realisation that  $\text{tr}[\mathcal{H}_2, \mathcal{H}_3]$  is always bosonic. Thus we can conclude that the \*bracket is a perfectly acceptable representation of

---

<sup>1</sup>i.e. it is a commutator if at least one of its two arguments is bosonic or an anticommutator otherwise.

the super Lie product. Hence, a member of the Lie algebra may be written as  $\omega^\alpha S_\alpha$  and the gauge field as  $\mathcal{A} \equiv \mathcal{A}^\alpha S_\alpha$ , with the commutators of (5.3) and (5.5) being replaced by the \*bracket.

These two alternatives actually amount to the same thing. The rôle of the \*bracket is to set to zero all the structure constants that generated  $\mathbb{1}\mathbb{l}$ . However, since the Killing supermetric that appears in the ' $\mathcal{A}^0$ -free' representation vanishes in the  $\mathbb{1}\mathbb{l}$  direction [*c.f.* (4.46)], the interactions in the two choices are the same and hence are physically equivalent. We shall concentrate on the ' $\mathcal{A}^0$ -free' representation as it is more elegant.

The second aspect of (5.4) worthy of comment is with regard to the  $A_2$  field. Due to the properties of the supertrace and its position within the  $\mathcal{A}$  supermatrix, the  $A_2$  propagator comes from

$$-\text{tr} \left\{ (\partial_\mu A_\nu^2 - \partial_\nu A_\mu^2) c^{-1} \left( -\partial^2/\Lambda^2 \right) \partial_\mu A_\nu^2, \right\} \quad (5.10)$$

*i.e.* it has the wrong sign. This has been interpreted as a sign of instability and deemed physically unacceptable [37], but we argue on the basis of the consideration of a quantum mechanical analogue described in subsection 5.5.1 that rather it is a loss of unitarity. However, we expect this not to be problematic since such a loss of unitarity is confined to terms that will disappear when the regularisation cutoff ( $\Lambda$ ) is removed.

Of course more has to be added to this scheme if we are to have a satisfactory regularisation technique for  $SU(N)$  gauge theory. The problem is we have also altered the low energy physics of the embedded  $SU(N)$  Yang-Mills theory by the introduction of new fields. To redress this shortcoming, we must ensure that the fermionic and  $A_2$  fields only have an influence on the  $A_1$  sector at high energies, and this can be achieved by giving the fermionic fields large masses. The  $A_2$  field can only interact with the physically important  $A_1$  gauge boson via the  $B$  fields.

It could be asked whether in giving the fermionic fields mass, we really need to maintain the full  $SU(N|N)$  invariance as ultimately the only physically relevant group is one of the  $SU(N)$  subgroups; *i.e.* could the  $B$  fields be given mass by introducing explicit mass terms. Unfortunately if the action was of the form

$$S = \frac{1}{2} \mathcal{F}_{\mu\nu} \{c^{-1}\} \mathcal{F}^{\mu\nu} + \frac{1}{2} m B \bar{B}, \quad (5.11)$$

the  $B$  propagator would not be transverse (as such a property is only guaranteed by gauge invariance) and divergences would appear in the longitudinal direction. These can be regulated by the introduction of a scalar field [3]. Since the appearance of this scalar field seems to be essential, we incorporate it in the most elegant method available, keeping the full  $SU(N|N)$  invariance and introducing spontaneous symmetry breaking.

### 5.1.2 Spontaneous symmetry breaking sector

To this end we introduce a superscalar field

$$\mathcal{C} = \begin{pmatrix} C^1 & D \\ \bar{D} & C^2 \end{pmatrix}. \quad (5.12)$$

We require that the fermionic parts of the  $\mathcal{A}$  field obtain masses so we must spontaneously break in these (and only these) directions. This is achieved by introducing a non-zero vacuum expectation value along a direction

$$\sigma_3 + a \mathbf{l} \quad (5.13)$$

(*a* real) in the Lie superalgebra. Thus  $\mathcal{C}$  must lie in the adjoint of  $U(N|N)$  but transform locally under  $SUN(N|N)$ . Under gauge transformations (5.5),  $\mathcal{C}$  transforms

as

$$\delta\mathcal{C} = -i[\mathcal{C}, \omega]. \quad (5.14)$$

It is *not* possible to replace this commutator by the \*bracket as the result would not be gauge invariant in general. This can be seen by considering an example such as the supertrace of an  $n^{\text{th}}$  order monomial that could arise in a potential term. With the gauge transformation given by  $\delta\mathcal{C} = -i[\mathcal{C}, \omega]^*$ , we find

$$\delta \text{str} \mathcal{C}^n = \frac{in}{2N} \text{str} \mathcal{C}^{n-1} \text{tr}[\mathcal{C}, \omega], \quad (5.15)$$

i.e. non-vanishing in general. Thus the identity cannot be excluded<sup>2</sup> from the  $\mathcal{C}$  field which can be expanded as

$$\mathcal{C} = \mathcal{C}^0 \mathbb{1}_{2N} + \mathcal{C}^\sigma \sigma_3 + \mathcal{C}^\alpha S_\alpha. \quad (5.16)$$

In the unbroken action we introduce a kinetic term for the  $\mathcal{C}$  field and the usual form for the Higgs' potential

$$S_{\mathcal{C}}^{\text{unbroken}} = \frac{1}{2} \nabla_\mu \cdot \mathcal{C} \{\tilde{c}^{-1}\} \nabla_\mu \cdot \mathcal{C} + \frac{\lambda}{4} \Lambda^{4-D} \text{str} \int d^D x (\mathcal{C}^2 - \Lambda^{D-2})^2. \quad (5.17)$$

We have introduced another cutoff function,  $\tilde{c}^{-1}$ , which is chosen to be a polynomial of rank  $\tilde{r}$ . The combined action (5.4) and (5.17), is invariant under the transformations of the fields (5.5) and (5.14). In contrast to the gauge field, the  $\sigma_3$  and  $\mathbb{1}\mathbb{l}$  components of  $\mathcal{C}$  are dynamical. They propagate into one another through the term

$$2N \partial_\mu \mathcal{C}^0 \tilde{c}^{-1} (-\partial^2/\Lambda^2) \partial_\mu \mathcal{C}^\sigma. \quad (5.18)$$

When we shift to the stationary point of the  $\mathcal{C}$  field, the  $SU(N|N)$  gauge group will be

---

<sup>2</sup>We could still dispense with the  $\mathcal{A}^0$  in a consistent manner by using the \*bracket for all pure gauge interactions but using the usual commutator for interactions concerning  $\mathcal{C}$  fields.

spontaneously broken to  $SU(N) \times SU(N)$  (*i.e.* the symmetries of the bosonic sector). Upon expanding about the stationary point (*i.e.*  $\mathcal{C} \rightarrow \Lambda^{D/2-1}\sigma_3 + \mathcal{C}$ ), (5.17) becomes

$$\begin{aligned} S_{\mathcal{C}}^{broken} = & -\frac{1}{2}g^2\Lambda^2[\mathcal{A}_\mu, \sigma_3]\{\tilde{c}^{-1}\}[\mathcal{A}_\mu, \sigma_3] - ig\Lambda[\mathcal{A}_\mu, \sigma_3]\{\tilde{c}^{-1}\}\nabla_\mu \cdot \mathcal{C} \\ & + \frac{1}{2}\nabla_\mu \cdot \mathcal{C}\{\tilde{c}^{-1}\}\nabla_\mu \cdot \mathcal{C} + \frac{\lambda}{4}\Lambda^{4-D} \text{str} \int d^Dx (\Lambda^{D/2-1}\{\sigma_3, \mathcal{C}\} + \mathcal{C}^2)^2. \end{aligned} \quad (5.19)$$

The first term of (5.19) gives a mass of order the effective cutoff,  $\Lambda$  to the fermionic part of  $\mathcal{A}$ . The bosonic part of  $\mathcal{C}$  also gains a mass via the last part of (5.19). The action given by (5.4) and (5.19) is invariant when the fields transform as (5.5) and

$$\delta\mathcal{C} \rightarrow -i[\mathcal{C}, \omega] - i\Lambda^{D/2-1}[\sigma_3, \omega]. \quad (5.20)$$

### 5.1.3 Gauge fixing sector

As with all gauge invariant theories, the gauge must be fixed<sup>3</sup> to extract physically relevant quantities from the theory. Otherwise when Greens' functions are computed, integrating over an infinite number of copies of the same theory occurs, leading to spurious divergences being obtained. Obviously the manner in which the gauge is fixed should not have an influence on the physical predictions extracted from the theory. At this point we also note that the second term in (5.19) gives rise to a term linear in both  $\mathcal{A}$  and  $\mathcal{C}$  which could prove troublesome. As such, we follow the lead of 't Hooft who faced a similar problem [38] and fix the gauge in a manner which enables this contribution to the action to be cancelled.

---

<sup>3</sup>This is true in standard perturbation theory as this procedure is required to properly define propagators; gauge invariant ERG does not require gauge fixing to calculate certain quantities [3, 4, 5].

The following choice of gauge fixing function is made

$$F = \partial_\mu \mathcal{A}_\mu - ig \frac{\Lambda}{2\xi} \frac{\tilde{c}^{-1}}{\hat{c}^{-1}} [\sigma_3, \mathcal{C}], \quad (5.21)$$

where yet another new cutoff function,  $\hat{c}^{-1}$ , has been employed. However, since this term is not required to be gauge invariant,  $\hat{c}^{-1}$  is not covariantised; *i.e.* it is a polynomial of rank  $\hat{r}$  in  $(-\partial^2/\Lambda^2)$  rather than  $(-\nabla^2/\Lambda^2)$ . The process of 't Hooft averaging results in the gauge fixing contribution to the action being

$$\begin{aligned} S_{gauge} &= \xi F \cdot \hat{c}^{-1} \cdot F \\ &= \xi (\partial_\mu \mathcal{A}_\mu) \cdot \hat{c}^{-1} \cdot (\partial_\nu \mathcal{A}_\nu) - ig \Lambda (\partial_\mu \mathcal{A}_\mu) \cdot \hat{c}^{-1} \cdot [\sigma_3, \mathcal{C}] \\ &\quad - g^2 \frac{\Lambda^2}{4\xi} [\sigma_3, \mathcal{C}] \cdot \frac{\tilde{c}^{-2}}{\hat{c}^{-1}} \cdot [\sigma_3, \mathcal{C}], \end{aligned} \quad (5.22)$$

where we have used the notation  $u \cdot W \cdot v \equiv \text{str} \int d^D x u(x) W(-\partial^2/\Lambda^2) v(y)$ . When this is combined with the other parts of the broken action, the second term provides the required cancellation. The final part of (5.22) contains a mass term for the fermionic subfield of the superscalar  $\mathcal{C}$ .

The final contribution to the action comes from the Faddeev-Popov superghosts which are defined to be

$$\eta = \begin{pmatrix} \eta^1 & \phi \\ \psi & \eta^2 \end{pmatrix}. \quad (5.23)$$

In the case of the usual bosonic symmetry groups, the process of gauge fixing leads to the Faddeev-Popov determinant which can be rewritten in terms of fermionic ghosts [39]. Likewise we would naïvely expect the ghosts in our theory to have the opposite grading to that of the gauge and scalar fields. However, it must be stressed that superfields are actually of indeterminate grading and the usual requirement of (anti)commutativity is replaced by (anti)cyclicity of the supertrace. As the grading stands however, we find that, as required,  $\text{str} \eta X = -\text{str} X \eta$  if  $X$  is ghost number

odd, but that  $\text{str} \eta X = \text{str} X \sigma_3 \eta \sigma_3$  if  $X$  has even ghost number.

There is an elegant solution to this problem. Since we are free to choose whether different fermionic flavours commute or anticommute [41], we take the opportunity to introduce multiple grading. As well as the usual supergroup grading  $f$  [*c.f.* (4.41)], we also assign a ghost grading  $g$ . All superfields (including ghosts) have supergroup-odd block off-diagonal elements ( $f = 1$ ) and supergroup-even block diagonal entries ( $f = 0$ ).  $\mathcal{A}$  and  $\mathcal{C}$  are both ghost-even ( $g = 0$ ) while  $\eta$  and  $\bar{\eta}$  are ghost-odd ( $g = 1$ ). We therefore require that elements commute up to a multiplicative extra sign whenever odd elements of the same grading are pushed passed one another, *i.e.* for elements  $a$  and  $b$

$$ab = ba(-1)^{f(a)f(b)+g(a)g(b)}. \quad (5.24)$$

We now find that

$$\text{str} \eta X = (-1)^{g(X)} \text{str} X \eta, \quad (5.25)$$

as required. The ghost action arises from the variation of the gauge fixing function (5.21) with gauge transformations (5.5) and (5.20). We find that

$$S_{ghost} = -\frac{2}{g} \Lambda^{D/2-2} \bar{\eta} \cdot \partial_\mu \nabla_\mu \cdot \eta - g \frac{\Lambda}{\xi} \frac{\tilde{c}^{-1}}{\hat{c}^{-1}} \text{str} \int d^D x [\sigma_3, \bar{\eta}] [\Lambda^{D/2-1} \sigma_3 + \mathcal{C}, \eta]. \quad (5.26)$$

The contribution to the bare action can be tidied up by shifting the antighost variables  $\bar{\eta} \rightarrow g \Lambda^{2-D/2} \hat{c}^{-1} \tilde{c} \bar{\eta}$ . We shall see in section 5.2 that this shift has the added benefit of assigning the correct momentum behaviour to the different legs of the ghost interaction vertices. The ghost sector of the action is then

$$S_{ghost} = -2 \bar{\eta} \cdot \hat{c}^{-1} \tilde{c} \partial_\mu \nabla_\mu \cdot \eta - \frac{g^2}{\xi} \Lambda^{3-D/2} \text{str} \int d^D x [\sigma_3, \bar{\eta}] [\Lambda^{D/2-1} \sigma_3 + \mathcal{C}, \eta]. \quad (5.27)$$

### 5.1.4 Total action

Gathering together all the elements of the action we have

$$\begin{aligned}
S^{broken} = & \frac{1}{2} \mathcal{F}_{\mu\nu} \{c^{-1}\} \mathcal{F}^{\mu\nu} - g^2 \Lambda^2 [\mathcal{A}_\mu, \sigma_3] \{\tilde{c}^{-1}\} [\mathcal{A}_\mu, \sigma_3] - ig\Lambda [\mathcal{A}_\mu, \sigma_3] \{\tilde{c}^{-1}\} \nabla_\mu \cdot \mathcal{C} \\
& + \frac{1}{2} \nabla_\mu \cdot \mathcal{C} \{\tilde{c}^{-1}\} \nabla_\mu \cdot \mathcal{C} + \frac{\lambda}{4} \Lambda^{4-D} \text{str} \int d^D x (\Lambda^{D/2-1} \{\sigma_3, \mathcal{C}\} + \mathcal{C}^2)^2 \\
& + \xi (\partial_\mu \mathcal{A}_\mu) \cdot \hat{c}^{-1} \cdot (\partial_\nu \mathcal{A}_\nu) + ig\Lambda (\partial_\mu \mathcal{A}_\mu) \cdot \tilde{c}^{-1} \cdot [\sigma_3, \mathcal{C}] \\
& - g^2 \frac{\Lambda^2}{4\xi} [\sigma_3, \mathcal{C}] \cdot \frac{\tilde{c}^{-2}}{\hat{c}^{-1}} \cdot [\sigma_3, \mathcal{C}] - 2 \bar{\eta} \cdot \hat{c}^{-1} \tilde{c} \partial_\mu \nabla_\mu \cdot \eta \\
& - \frac{g^2}{\xi} \Lambda^{3-D/2} \text{str} \int d^D x [\sigma_3, \bar{\eta}] [\Lambda^{D/2-1} \sigma_3 + \mathcal{C}, \eta].
\end{aligned} \tag{5.28}$$

Some of the Feynman rules for this action are contained in Appendix D. To ensure that the high momentum behaviour of the  $\mathcal{A}$  propagator is unaffected by the introduction of the scalar field and gauge-fixing we are forced to bound the ranks of the polynomials:

$$\hat{r} \geq r > \tilde{r} - 1. \tag{5.29}$$

If we had not spontaneously broken the symmetry, the action would be (in covariant gauge,  $F = \partial_\mu \mathcal{A}_\mu$ )

$$\begin{aligned}
S^{unbroken} = & \frac{1}{2} \mathcal{F}_{\mu\nu} \{c^{-1}\} \mathcal{F}^{\mu\nu} + \frac{1}{2} \nabla_\mu \cdot \mathcal{C} \{\tilde{c}^{-1}\} \nabla_\mu \cdot \mathcal{C} \\
& + \frac{\lambda}{4} \Lambda^{4-D} \text{str} \int d^D x (\mathcal{C}^2 - \Lambda^{D-2})^2 + \xi (\partial_\mu \mathcal{A}_\mu) \cdot \hat{c}^{-1} \cdot (\partial_\nu \mathcal{A}_\nu) \\
& - 2 \bar{\eta} \cdot \hat{c}^{-1} \tilde{c} \partial_\mu \nabla_\mu \cdot \eta,
\end{aligned} \tag{5.30}$$

a form which will prove to be of use later as many of the important aspects of the physics (especially as regards to issues of finiteness) can be discovered by consideration of just the unbroken sector.

## 5.2 Power counting

Within the theory defined in (5.28) and (5.29), the superficial degree of divergence,  $\mathcal{D}_\Gamma$ , of a 1PI diagram in  $D$  spacetime dimensions is calculated using the standard rules [23] to be

$$\begin{aligned} \mathcal{D}_\Gamma = & DL - (2r + 2) I_{\mathcal{A}} - (2\tilde{r} + 2) I_{\mathcal{C}} - (2\hat{r} - 2\tilde{r} + 2) I_\eta + \sum_{i=3}^{2r+4} (2r + 4 - i) V_{\mathcal{A}^i} \\ & + \sum_{j=2}^{2\tilde{r}+2} (2\tilde{r} + 2 - j) V_{\mathcal{A}^j \mathcal{C}} + \sum_{k=1}^{2\hat{r}+2} (2\tilde{r} + 2 - k) V_{\mathcal{A}^k \mathcal{C}^2} + (2\hat{r} - 2\tilde{r} + 1) V_{\eta^2 \mathcal{A}}, \end{aligned} \quad (5.31)$$

utilising the following nomenclature:  $L$  is the number of loops,  $I_s$  the number of internal propagators of type  $s$ , and  $V_t$  the number of vertices containing the set of fields  $t$ . We aim to show that for all but a small sub-class of 1PI diagrams, the ranks of the polynomials can be chosen so that  $\mathcal{D}_\Gamma$  is negative. This sub-class will then be shown to be finite by other methods developed in sections 5.3 and 5.4. Since the superficial degree of divergence of any given diagram and all its connected subdiagrams is thus shown to be negative, finiteness to all orders of perturbation theory follows from the convergence theorem [23].

Unfortunately, (5.31) does not adequately take account of 1PI diagrams with external antighost legs. The formula treats the whole momentum dependence of the associated  $V_{\eta^2 \mathcal{A}}$  vertex as if it was loop momentum, whereas it depends only upon the (external)  $\bar{\eta}$  line. Thus the superficial degree of divergence calculated via (5.31) is overestimated in these diagrams. To remedy this we include an extra term:  $-(2\hat{r} - 2\tilde{r} + 1) E_{\bar{\eta}}^{\mathcal{A}}$ , where  $E_{\bar{\eta}}^{\mathcal{A}}$  is the number of external antighost lines which enter a  $V_{\eta^2 \mathcal{A}}$  vertex. The improved formula for the superficial degree of divergence is

$$\begin{aligned} \mathcal{D}_\Gamma = & DL - (2r + 2) I_{\mathcal{A}} - (2\tilde{r} + 2) I_{\mathcal{C}} - (2\hat{r} - 2\tilde{r} + 2) I_\eta + \sum_i (2r + 4 - i) V_{\mathcal{A}^i} \\ & + \sum_j (2\tilde{r} + 2 - j) V_{\mathcal{A}^j \mathcal{C}} + \sum_k (2\tilde{r} + 2 - k) V_{\mathcal{A}^k \mathcal{C}^2} + (2\hat{r} - 2\tilde{r} + 1) (V_{\eta^2 \mathcal{A}} - E_{\bar{\eta}}^{\mathcal{A}}). \end{aligned} \quad (5.32)$$

The form of (5.32) is unhelpful as written since diagrams are easier to classify by external, rather than internal, propagators. As such, we use the geometric relations

$$L = I_{\mathcal{A}} + I_{\mathcal{C}} + I_{\eta} + 1 - \sum_i V_{\mathcal{A}^i} - \sum_j V_{\mathcal{A}^j \mathcal{C}} - \sum_k V_{\mathcal{A}^k \mathcal{C}^2} - V_{\eta^2 \mathcal{A}} - V_{\eta^2 \mathcal{C}} - V_{\mathcal{C}^3} - V_{\mathcal{C}^4}, \quad (5.33)$$

$$E_{\mathcal{A}} = -2I_{\mathcal{A}} + \sum_i iV_{\mathcal{A}^i \mathcal{C}} + \sum_j jV_{\mathcal{A}^j \mathcal{C}} + \sum_k kV_{\mathcal{A}^k \mathcal{C}^2} + V_{\eta^2 \mathcal{A}}, \quad (5.34)$$

$$E_{\mathcal{C}} = -2I_{\mathcal{C}} + \sum_j V_{\mathcal{A}^j \mathcal{C}} + 2 \sum_k V_{\mathcal{A}^k \mathcal{C}^2} + V_{\eta^2 \mathcal{C}} + 3V_{\mathcal{C}^3} + 4V_{\mathcal{C}^4}, \quad (5.35)$$

$$E_{\eta}^{\mathcal{A}} + E_{\eta}^{\mathcal{C}} + E_{\bar{\eta}}^{\mathcal{A}} + E_{\bar{\eta}}^{\mathcal{C}} = -2I_{\eta} + 2V_{\eta^2 \mathcal{A}} + 2V_{\eta^2 \mathcal{C}}. \quad (5.36)$$

The Euler relation (5.33) assumes that all diagrams are connected since the first term on the RHS (denoting the number of connected components) has been set to 1. Note that in the relation (5.36), the external ghost and antighost lines have been classified according to the vertex to which they are attached. They satisfy the constraint  $E_{\eta}^{\mathcal{A}} + E_{\eta}^{\mathcal{C}} = E_{\bar{\eta}}^{\mathcal{A}} + E_{\bar{\eta}}^{\mathcal{C}}$ , and so (5.36) can be rewritten as

$$E_{\bar{\eta}}^{\mathcal{A}} + E_{\bar{\eta}}^{\mathcal{C}} = -I_{\eta} + V_{\eta^2 \mathcal{A}} + V_{\eta^2 \mathcal{C}}. \quad (5.37)$$

The four relations (5.33) – (5.36) are used to rewrite  $\mathcal{D}_{\Gamma}$  as

$$\begin{aligned} \mathcal{D}_{\Gamma} = & (D - 2r - 4)(L - 2) - E_{\mathcal{A}} - (r - \tilde{r} - \hat{r})E_{\mathcal{C}} - 2(r + \tilde{r} - \hat{r} + 1)E_{\bar{\eta}}^{\mathcal{C}} \\ & - (2r + 3)E_{\eta}^{\mathcal{A}} - (r - \tilde{r} + 1) \sum_j V_{\mathcal{A}^j \mathcal{C}} + (r - 3\tilde{r} - 1)V_{\mathcal{C}^3} + 2(r - 2\tilde{r})V_{\mathcal{C}^4} \\ & + (r + \tilde{r} - 2\hat{r} - 1)V_{\eta^2 \mathcal{C}} + 2(D - r - 2). \end{aligned} \quad (5.38)$$

While it is straightforward to choose sufficient conditions so that all diagrams (except certain one-loop cases) are superficially convergent, it is trickier to ascertain those that are also necessary. The strategy we adopt is to consider one- and multi-loop diagrams separately and establish the sufficient conditions required to make  $\mathcal{D}_{\Gamma}$  as

negative in as many diagrams as possible. We will introduce a theorem which will demonstrate that some of these conditions are not strictly necessary. We will then show the remaining conditions are necessary by considering examples where they are needed.

We will temporarily relax the condition that  $r$ ,  $\tilde{r}$  and  $\hat{r}$  are integers. Instead we consider them as general real numbers and re-impose the restriction to integers at the end. In this case we then have to impose the additional constraint

$$\tilde{r} > -1, \quad (5.39)$$

which is required to ensure the high momentum behaviour of the  $\mathcal{C}$  propagator is unaffected by the spontaneous symmetry mass term in (5.28).

### 5.2.1 Multiloop diagrams

If we stipulate that  $L > 1$ , all such 1PI diagrams can be made superficially convergent merely by requiring that all the coefficients in (5.38) are negative. Hence the following sufficient conditions are obtained:

$$r > D - 2, \quad (5.40)$$

$$r > -3/2, \quad (5.41)$$

$$r < 2\tilde{r}, \quad (5.42)$$

$$\hat{r} < r + \tilde{r} + 1, \quad (5.43)$$

as well as the assumed conditions (5.29) and (5.39).

Combining the inequalities (5.40)–(5.42), we obtain a lower bound upon  $\tilde{r}$  as well, namely  $\tilde{r} > \frac{1}{2} \max(D - 2, -\frac{3}{2})$ . The lower bounds on  $r$  and  $\tilde{r}$  are to be expected since

the higher the number of spacetime dimensions the more divergent the diagrams. However, there is no obvious physical reason why upper bounds such as (5.43) are found and one is lead to suspect that such conditions are not necessary. We can prove that these restrictions are not necessary by the use of the following proposition:

**Proposition 1** *If we denote by  $\mathcal{S}$  the collection of triples  $(r, \tilde{r}, \hat{r})$  s.t.  $\mathcal{D}_\Gamma < 0$ , then  $\forall (r_0, \tilde{r}_0, \hat{r}_0) \in \mathcal{S}$ , the subset  $\{(r, \tilde{r}, \hat{r}) \text{ s.t. } r \geq r_0, \tilde{r} = \tilde{r}_0, \hat{r} \geq \hat{r}_0, \tilde{r}_0 \leq r \leq \hat{r}\} \subset \mathcal{S}$ .*

*Proof:*

We note that (5.38) depends upon  $\hat{r}$  as  $+2\hat{r}(E_{\bar{\eta}}^C - V_{\eta^2 C})$ . This term is always non-positive since it is not possible to have more external antighost lines entering  $V_{\eta^2 C}$  vertices than  $V_{\eta^2 C}$  vertices themselves. Thus increasing  $\hat{r}$  above  $\hat{r}_0$  cannot increase  $\mathcal{D}_\Gamma$ .

The dependence upon  $r$  is carried by

$$\begin{aligned} r \left( -2L + 2 - E_C - 2E_{\bar{\eta}}^C - 2E_{\bar{\eta}}^A - \sum_j V_{A^j C} + V_{C^3} + 2V_{C^4} + V_{\eta^2 C} \right) \\ = 2r \left( \sum_i V_{A^i} - I_A \right), \quad (5.44) \end{aligned}$$

with the equality following from (5.31). Since every  $V_{A^i}$  must be attached to at least two internal  $A$  lines in a 1PI diagram, this contribution is also non-positive and so increasing  $r$  above  $r_0$  does not increase  $\mathcal{D}_\Gamma$ .  $\square$

Proposition 1 implies that inequalities (5.42) and (5.43) are unnecessary so the sufficient relations for convergence of multiloop diagrams are:

$$r > \max \left( D - 2, -\frac{3}{2} \right), \quad (5.45)$$

$$\tilde{r} > \max \left( \frac{D}{2} - 1, -\frac{3}{4} \right), \quad (5.46)$$

$$\hat{r} \geq r > \tilde{r} - 1. \quad (5.47)$$

At first glance these conditions are apparently necessary to regulate the diagrams of figure 5.1 (in  $D \geq \frac{1}{2}$ ). However the naïve power counting we have employed does not take into account other considerations such as the supergroup factors. It transpires that these two diagrams are already regulated by the supertrace mechanism that will be discussed in section 5.3 and as such, the necessity of the above conditions is actually unproven. We leave a demonstration of why these conditions really are necessary until after the discussion of the one-loop case.

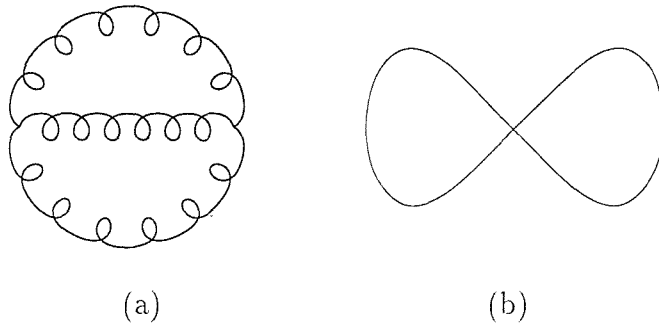


Figure 5.1: 1PI diagrams which by power counting alone require conditions (5.45) – (5.47) to be finite. (Curly lines represent  $\mathcal{A}$  fields and straight lines  $\mathcal{C}$  fields.)

### 5.2.2 One-loop diagrams

While the covariant derivatives are not able to regularise all one-loop diagrams, they are able to ensure finiteness in a number of sub-classes. At one-loop the superficial degree of divergence is

$$\begin{aligned}
 \mathcal{D}_\Gamma^{1-loop} &= D - E_{\mathcal{A}} - (r - \tilde{r} + 1)E_{\mathcal{C}} - 2(r + \tilde{r} - \hat{r} + 1)E_{\bar{\eta}}^{\mathcal{C}} - (2r + 3)E_{\bar{\eta}}^{\mathcal{A}} \\
 &\quad - (r - \tilde{r} + 1) \sum_j V_{\mathcal{A}^j \mathcal{C}} + (r - 3\tilde{r} - 1)V_{\mathcal{C}^3} + 2(r - 2\tilde{r})V_{\mathcal{C}^4} \\
 &\quad + (r + \tilde{r} - 2\hat{r} - 1)V_{\eta^2 \mathcal{C}}
 \end{aligned} \tag{5.48}$$

$$= \alpha \cdot \mathbf{v}, \tag{5.49}$$

where we define the elements of  $\alpha$  and  $\mathbf{v}$  to be

$$\begin{aligned}
\alpha_1 &= D & v_1 &= 1, \\
\alpha_2 &= -1 & v_2 &= E_{\mathcal{A}}, \\
\alpha_3 &= -(r - \tilde{r} + 1) & v_3 &= E_{\mathcal{C}}, \\
\alpha_4 &= -2(r + \tilde{r} - \hat{r} + 1) & v_4 &= E_{\bar{\eta}}^C, \\
\alpha_5 &= -(2r + 3) & v_5 &= E_{\bar{\eta}}^{\mathcal{A}}, \\
\alpha_6 &= -(r - \tilde{r} + 1) & v_6 &= \sum_j V_{\mathcal{A}^j \mathcal{C}}, \\
\alpha_7 &= (r - 3\tilde{r} - 1) & v_7 &= V_{\mathcal{C}^3}, \\
\alpha_8 &= 2(r - 2\tilde{r}) & v_8 &= V_{\mathcal{C}^4}, \\
\alpha_9 &= (r + \tilde{r} - 2\hat{r} - 1) & v_9 &= V_{\eta^2 \mathcal{C}}.
\end{aligned} \tag{5.50}$$

The general strategy we shall follow is to consider specific classes of one-loop diagrams. With the strictures placed by these classes we shall then change some of the  $v_i$  to ensure that all  $v_i$  are non-negative. This is done in such a manner that (5.48) is unchanged so we must also adapt the corresponding  $\alpha_i$ s. To ensure that  $\mathcal{D}_\Gamma$  is then negative, we require that all the  $\alpha_i < 0$ . This gives us a number of sufficient conditions, some of which can be shown not to be necessary by appealing to Proposition 1. It then remains to show that the final list of conditions are also necessary.

The cases we consider are:

(i)  $E_{\mathcal{A}} \geq D + 1$ ; any number of  $E_{\mathcal{C}}$ ,  $E_{\bar{\eta}}^{\mathcal{A}, \mathcal{C}}$ ,  $E_{\bar{\eta}}^{\mathcal{A}, \mathcal{C}}$

The combination  $(E_{\mathcal{A}} - D - 1)$  is always non-negative, so we make the following replacements in (5.50) which leave (5.48) unchanged

$$\begin{aligned}
\alpha_1 \rightarrow \alpha_1 &= -1, & v_1 \rightarrow v_1 &= E_{\mathcal{A}} - D - 1, \\
\alpha_2 \rightarrow \alpha_2 &= -1, & v_2 \rightarrow v_2 &= 1.
\end{aligned} \tag{5.51}$$

All other  $\alpha_i$  and  $v_i$  remain unaltered. Requiring all the coefficients  $\alpha_i$  to be negative results, after the assumption of (5.29) and (5.39), in the following restraints being

placed on the parameters

$$r < 2\tilde{r}, \quad (5.52)$$

$$2r > -3, \quad (5.53)$$

$$\hat{r} < r + \tilde{r} + 1. \quad (5.54)$$

(ii)  $E_{\bar{\eta}}^A \geq 1$ ; any number of  $E_A, E_C, E_{\bar{\eta}}^C$

The new variable will be  $(E_{\bar{\eta}}^A - 1)$  rather than  $E_{\bar{\eta}}^A$  so we need to change the following components in (5.50)

$$\begin{aligned} \alpha_1 \rightarrow \alpha_1 &= (D - 2r - 3), & v_1 \rightarrow v_1 &= 1, \\ \alpha_5 \rightarrow \alpha_5 &= -(2r + 3), & v_5 \rightarrow v_5 &= (E_{\bar{\eta}}^A - 1). \end{aligned} \quad (5.55)$$

If all  $\alpha_i$  coefficients are to be negative, (5.52)–(5.54) are regained along with the extra condition  $D - 2r - 3 < 0$ .

(iii)  $E_{\bar{\eta}}^C \geq 1$ ; any number of  $E_A, E_C, E_{\bar{\eta}}^A$

The only changes to (5.50) that must be made are

$$\begin{aligned} \alpha_1 \rightarrow \alpha_1 &= D - 2(r + \tilde{r} - \hat{r} + 1), & v_1 \rightarrow v_1 &= 1, \\ \alpha_4 \rightarrow \alpha_4 &= -2(r + \tilde{r} - \hat{r} + 1), & v_4 \rightarrow v_4 &= (E_{\bar{\eta}}^C - 1), \end{aligned} \quad (5.56)$$

and we obtain the new constraint  $D - 2(r + \tilde{r} - \hat{r} + 1) < 0$ , which has to replace the previous weaker bound (5.54) (for any  $D \geq 0$ ).

(iii)  $E_C \geq 2$ ; any number of  $E_A, E_{\bar{\eta}}^{A,C}, E_{\bar{\eta}}^{A,C}$

With the new variable  $(E_C - 2)$  introduced, we adapt

$$\begin{aligned} \alpha_1 \rightarrow \alpha_1 &= D - 2(r - \tilde{r} + 1), & v_1 \rightarrow v_1 &= 1, \\ \alpha_3 \rightarrow \alpha_3 &= -(r - \tilde{r}), & v_4 \rightarrow v_4 &= (E_C - 2), \end{aligned} \quad (5.57)$$

and an additional constraint is found:  $r - \tilde{r} > \frac{D}{2} - 1$ .

(iv)  $\mathbf{E}_C = \mathbf{1}$ ,  $\mathbf{E}_A = \mathbf{E}_{\eta}^{A,C} = \mathbf{E}_{\bar{\eta}}^{A,C} = \mathbf{0}$

This gives rise to three possibilities since the internal loop can be one of three flavours.

$$\text{Internal } \mathcal{A} \text{ loop: } \mathcal{D}_{\Gamma}^{1-loop} = D - 2r + 2\tilde{r} - 2$$

$$\text{Internal } \mathcal{C} \text{ loop: } \mathcal{D}_{\Gamma}^{1-loop} = D - 2\tilde{r} - 2$$

$$\text{Internal ghost loop: } \mathcal{D}_{\Gamma}^{1-loop} = D + 2\tilde{r} - 2\hat{r} - 2$$

We require  $r - \tilde{r} > \frac{D}{2} - 1$  if the first diagram is to be finite (which will also make the third diagram finite). The second diagram requires the bound  $\tilde{r} > \frac{D}{2} - 1$ . The more general case with any allowed number of external  $\mathcal{A}$  and (anti)ghost lines does not change these conditions as they both contribute negatively to (5.48).

### 5.2.3 Final list of constraints

By the use of Proposition 1 it is possible to remove the upper bounds in these constraints. The final list of constraints for both multi- and single loop graphs is therefore:

$$r > \max\left(D - 2, \frac{D - 3}{2}, -\frac{3}{2}\right), \quad (5.58)$$

$$\tilde{r} > \frac{1}{2} \max\left(D - 2, \frac{D - 3}{2}, -\frac{3}{2}\right), \quad (5.59)$$

$$r - \tilde{r} > \frac{D}{2} - 1, \quad (5.60)$$

and, as ever, (5.29) and (5.39). With  $D \geq 1$ , these mean

$$r > D - 2, \quad (5.61)$$

$$\tilde{r} > \frac{D}{2} - 1, \quad (5.62)$$

$$r - \tilde{r} > \frac{D}{2} - 1, \quad (5.63)$$

$$\hat{r} \geq r > \tilde{r} - 1 > 0. \quad (5.64)$$

Suitable ranks for polynomials can be found by selecting integers which satisfy these bounds.

We now address the question of the necessity of these conditions. We noted that the diagrams of figure 5.1 seemed to demonstrate necessity. However, we have ignored supergroup factors and, when these are allowed for, we find that the unbroken parts of these diagrams will actually disappear at large loop momenta through the supertrace mechanism which will be discussed in the next section (the broken parts are finite by power counting). Necessity will actually arise from the broken sector of the  $SU(N|N)$  gauge theory. To see this we need to borrow a result from the next section, namely (5.72), which shows that unbroken one-loop corrections take the form of a product of two supertraces over the external fields. This carries over to the broken theory as well except that  $\langle \mathcal{C} \rangle = \sigma_3 \Lambda^{D/2-1}$  factors may also arise in these supertraces. Now, the condition  $r - \tilde{r} > \frac{D}{2} - 1$  arose from power counting the one-loop graph made by attaching an  $\mathcal{A}$  propagator to the  $\mathcal{CA}^2$  vertex [*i.e.* by inspection the vertex from  $-ig\Lambda[\mathcal{A}_\mu, \sigma_3]\{\tilde{c}^{-1}\}\nabla_\mu \mathcal{C}$  of (5.28)]. Thus  $r - \tilde{r} > \frac{D}{2} - 1$  is necessary for the contributions with group theory factor  $\text{str } \mathcal{C} \text{ str } \sigma_3$ . The condition  $\tilde{r} > D/2 - 1$  is necessary for finiteness of  $(\text{str } \mathcal{C})^2$  contributions arising from attaching a  $\mathcal{C}$  propagator to the  $\text{str } \mathcal{C}^4$  vertex. The final condition for any  $D \geq 1$ , namely  $r > D - 2$ , already follows from combining these two.

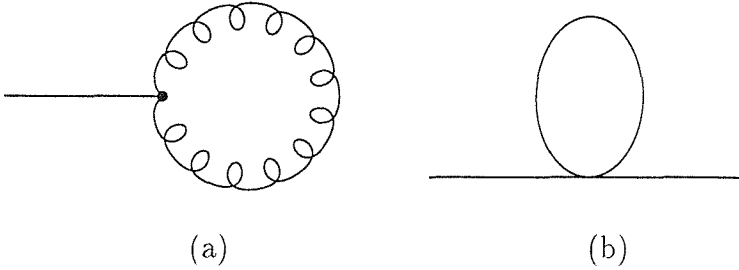


Figure 5.2: 1PI diagrams from which the necessity of conditions (5.61)–(5.64) are demonstrated.

By inspection of (5.48) and use of subsection 5.2.1 we can deduce that the only

diagrams that remain unregularised after the imposition of the constraints listed above, have the following properties:

- (i) One loop
- (ii) Up to  $D$  external  $\mathcal{A}$  legs
- (iii) No external  $\mathcal{C}$  or ghost legs
- (iv) Do not have  $\mathcal{A}^j \mathcal{C}$ ,  $\mathcal{C}^3$ ,  $\mathcal{C}^4$  or  $\mathcal{C} \eta \bar{\eta}$  interactions

Diagrams with these properties will be known as ‘One-loop Remainder Diagrams’.

### 5.3 Supertrace mechanism

The power counting arguments of the previous section are a demonstration of the well established problem that the introduction of higher covariant derivatives is not sufficient to regularise all one-loop diagrams in gauge theories [27]. The improvement in the high momentum behaviour of the propagators is not enough to compensate for the number of new interactions we have been forced to introduce. We obviously need further regularisation and this is the reason the  $SU(N|N)$  gauge group has been used. The aim is to demonstrate that the extra fields introduced by the supergroup provide a mechanism for cancellation to occur between component fields and hence regularise some of the remaining troublesome diagrams. Actually, gauge invariance arguments mean that the one-loop diagrams with  $3 < E_{\mathcal{A}} \leq D$  do not diverge in the manner one would expect from the naïve power counting, as will be demonstrated in section 5.4, and so we concentrate on the cases with  $E_{\mathcal{A}} \leq 3$  in this section.

There are three varieties of One-loop Remainder Diagrams: those with just  $\mathcal{C}$ ,  $\mathcal{A}$  or ghost internal propagators. We will calculate the group theory factors for the unbro-

ken parts of these diagrams and see that at large loop momentum they disappear, while we demonstrate that the broken parts are finite by power counting arguments.

### 5.3.1 One-loop Remainder Diagrams with $\mathcal{A}$ propagators

The large momentum behaviour of the  $\mathcal{A}$  propagator can be obtained from (D.3) and is found to be

$$\langle \mathcal{A}^\alpha(p) \mathcal{A}^\beta(-p) \rangle = \frac{c_p}{p^2} h^{\alpha\beta} \left[ \delta_{\mu\nu} + \frac{p_\mu p_\nu}{p^2} \left( \frac{\hat{c}_p}{\xi c_p} - 1 \right) \right] + \mathcal{O}(p^{2\tilde{r}-4r-4}) \quad (5.65)$$

The second term on the RHS arises from the symmetry breaking; the constraints introduced earlier mean that the parts of diagrams using these symmetry breaking terms are finite. We need to use pure  $\mathcal{A}^i$  vertices which either come from the unbroken interactions of (5.4) with index of divergence  $2r + 4 - i$ , or from the regularised mass term in (5.19) with index  $2\tilde{r} + 2 - i$ : using the symmetry breaking part of the propagator and/or the symmetry breaking vertices will result in the degree of divergence of the ensuing integral being bounded by  $\mathcal{D}_\Gamma \leq D - E_{\mathcal{A}} - 2(r - \tilde{r} + 1) < 0$ , *i.e.* these contributions are finite.

Feynman diagrams are constructed by creating propagators using Wick contraction between different supertraces originating from interactions. Concentrating on the group theory dependence only, we find tree diagrams take the following form:

$$\text{str}(X \mathcal{A}) \underbrace{\text{str}(\mathcal{A} Y)}_{\dots} = \text{str}(X Y) + \dots, \quad (5.66)$$

where the ellipsis denotes group theory factors arising from broken symmetry parts,  $X$  and  $Y$  are products of supermatrices, and we have used the completeness relation in the form of (4.50). In general, a term of the following structure should also be

included

$$-\frac{1}{4N}(\text{tr}X \text{str}Y + \text{str}X \text{tr}Y). \quad (5.67)$$

If this term was required, it would imply that the propagation of only  $\mathcal{A}^A$  would be inconsistent (*i.e.*  $\mathcal{A}^0$  would also be needed) since such terms, although they arise in the unbroken theory, actually break  $SU(N|N)$ . However we are saved by the fact that all  $\mathcal{A}$  interactions occur via commutators,<sup>4</sup> so by rearrangement  $X$  and  $Y$  can also be expressed as commutators. Since the supertrace of a commutator vanishes, so does (5.67).

One-loop diagrams are formed by Wick contracting within a supertrace. From the previous arguments, (5.66) and (4.50), we know this must be of the form

$$\text{str}(\underbrace{[\mathcal{A}, Z_1] Z_2 [\mathcal{A}, Z_3] Z_4}_{}) = \frac{1}{2} \left[ \text{str}(Z_1 Z_2) \text{str}(Z_3 Z_4) + \text{str}(Z_1 Z_4) \text{str}(Z_2 Z_3) \right. \\ \left. - \text{str}(Z_1 Z_2 Z_3) \text{str}(Z_4) - \text{str}(Z_1 Z_3 Z_4) \text{str}(Z_2) \right] + \dots, \quad (5.68)$$

or

$$\text{str}(\underbrace{\mathcal{A} [\mathcal{A}, Z_1]}_{}) = 0, \quad (5.69)$$

where  $Z_i$  are products of superfields and again the ellipsis correspond to suppressed (finite) terms from the broken sector. The possible  $\mathcal{O}\left(\frac{1}{N}\right)$  corrections from (4.50) cancel out for the same reasons as above. In the cases we are interested in  $E_{\mathcal{A}} \leq 3$ , so the terms in (5.68) yield either  $\text{str}\mathcal{A} = 0$  or  $\text{str}\mathcal{A} = 0$ . Thus we can conclude that One-loop Remainder diagrams with  $\mathcal{A}$  internal propagators are finite, because their contributions from the spontaneous symmetry breaking sector are finite by power counting, while the unbroken part has group theory factors which disappear.

---

<sup>4</sup>This is true in the  $\mathcal{A}^0$ -free representation; in the \*bracket version, extra interactions play the same rôle.

### 5.3.2 One-loop Remainder Diagrams with $\mathcal{C}$ propagators

From (D.5) we see that the large momentum behaviour of the  $\mathcal{C}$  propagator is

$$\langle \mathcal{C}_j^i(p) \mathcal{C}_l^k(-p) \rangle = \frac{\tilde{c}_p}{p^2} \delta_l^i (\sigma_3)^k_j + O(p^{-4-2m}), \quad (5.70)$$

where  $m = \min(2\tilde{r}, \hat{r})$ . Again we note that contributions arising from the broken part of the theory are finite by power counting as the degree of divergence of a one-loop diagram using the broken part of (5.70) is bounded by  $\mathcal{D}_\Gamma \leq D - E_{\mathcal{A}} - 2 - 2 \min(\tilde{r}, \hat{r} - \tilde{r}) < 0$ , and we have already shown that we need not consider  $\mathcal{CA}^j$  interactions.

Tree diagrams have the form

$$\text{str}(X_1 \mathcal{C}) \text{str}(\mathcal{C} X_2) = \text{str}(X_1 X_2) + \dots, \quad (5.71)$$

where the ellipsis signifies contributions from the broken sector. Note that we do not have to address the issue of  $O\left(\frac{1}{N}\right)$  corrections here. The one-loop diagram then takes the general form

$$\text{str}(\mathcal{C} Y_1 \mathcal{C} Y_2) = \text{str}Y_1 \text{str}Y_2 + \dots, \quad (5.72)$$

with broken sector contributions represented by the ellipsis. Similarly to the previous situation,  $Y_1$  and  $Y_2$  are the products of the remaining superfields, and with  $E_{\mathcal{A}} \leq 3$ , this leaves us with either  $\text{str}Y_1 = 0$  or  $\text{str}Y_2 = 0$ , and so One-loop Remainder Diagrams with  $E_{\mathcal{A}} \leq 3$  and  $\mathcal{C}$  internal propagators are also finite.

### 5.3.3 One-loop Remainder Diagrams with $\eta$ propagators

The analysis for these diagrams is the same as that for the  $\mathcal{A}$  propagators in subsection 5.3.1, which is unsurprising as  $\eta$  is linked to gauge transformations by BRST (see subsection 5.4.1). With the symmetry breaking terms once more finite by power

counting since their degree of divergence is bounded from above by the already negative  $D - E_{\mathcal{A}} - 2(\hat{r} - \tilde{r} + 1)$ , the unbroken sector yields one-loop diagrams of the same form as the RHS of (5.68) and/or (5.69), and so we can draw the same conclusions with regard to finiteness.

### 5.3.4 Example of explicit calculation of supergroup factors

In this subsection we present the explicit results of a calculation of the supergroup factors of diagrams using the Feynman rules of Appendix D. This hides much of the simplicity and elegance of the previous section since individual diagrams do not allow for the fact that vertices appear only as commutators.

Since the Feynman rules have been derived for a strict cycle of fields, diagrams are calculated by considering all possible topological variants. For example, figure 5.3 shows the two possibilities that arise for the one-loop correction to the  $\mathcal{A}$  propagator that uses just  $\mathcal{A}^3$  vertices.

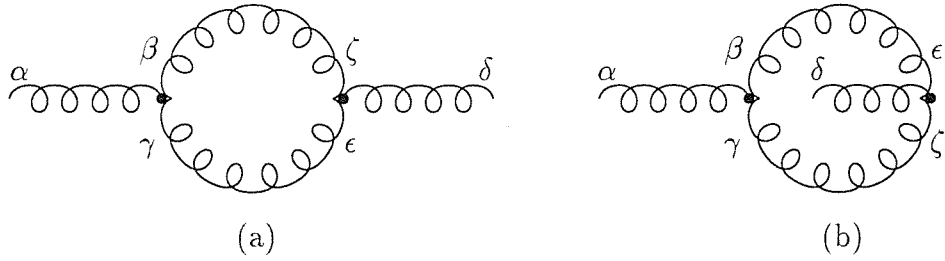


Figure 5.3: One-loop contributions to the  $\mathcal{A}$  propagator

We are only interested in the high momentum behaviour of such graphs; specifically we aim to demonstrate that the leading contribution vanishes in this regime, with subleading terms arising from broken terms already shown to be finite, and hence the diagram is UV regulated. We will use only the single index (*i.e.* adjoint index) notation here as the example uses only  $\mathcal{A}$  fields. Of course the same results are

obtained using the double index (*i.e.* fundamental and complex conjugate indices), which is the notation that appears more natural if  $\mathcal{C}$  fields are involved. Inspection of the momentum part of (D.9) reveals that we need not consider  $\sigma_3$  insertions; such contributions to these diagrams are already finite by power counting. If we take figure 5.3 (b) as an example, the group theory part of the calculation comes from (suppressing Lorentz indices and spacetime dependence):

$$\begin{aligned}
& \mathcal{A}^\alpha \mathcal{A}^\beta \mathcal{A}^\gamma \mathcal{A}^\zeta \mathcal{A}^\delta \mathcal{A}^\varepsilon \text{str}(S_\alpha S_\beta S_\gamma) \text{str}(S_\zeta S_\delta S_\varepsilon) \\
& \quad \boxed{\quad \quad \quad} \\
& \sim \mathcal{A}^\alpha \mathcal{A}^\beta \mathcal{A}^\delta \mathcal{A}^\varepsilon \text{str}(S_\alpha S_\beta S_\gamma) \text{str}(S_\zeta S_\delta S_\varepsilon) \\
& \sim \mathcal{A}^\alpha \mathcal{A}^\delta \mathcal{A}^\beta \mathcal{A}^\varepsilon \boxed{(-1)^{f(\beta)f(\delta)} h^{\gamma\zeta}} \text{str}(S_\alpha S_\beta S_\gamma) \text{str}(S_\zeta S_\delta S_\varepsilon) \\
& \sim \mathcal{A}^\alpha \mathcal{A}^\delta (-1)^{f(\beta)f(\delta)} h^{\beta\varepsilon} h^{\gamma\zeta} \text{str}(S_\alpha S_\beta S_\gamma) \text{str}(S_\zeta S_\delta S_\varepsilon) \\
& \sim \mathcal{A}^\alpha \mathcal{A}^{\delta(b)} h^{\beta\varepsilon} h^{\gamma\zeta} \text{str}(S_\alpha S_\beta S_\gamma) \text{str}(S_\zeta S_{\delta(b)} S_\varepsilon) \\
& \quad + \mathcal{A}^\alpha \mathcal{A}^{\delta(f)} h^{\varepsilon\beta} h^{\gamma\zeta} \text{str}(S_\alpha S_\beta S_\gamma) \text{str}(S_\zeta S_{\delta(f)} S_\varepsilon), \tag{5.73}
\end{aligned}$$

where we have used the property of cyclicity under the supertrace and taken the opportunity of Wick contracting two fields (to form an internal propagator) on the second line using the high momentum behaviour exhibited in (5.65). The notation  $\delta(b)$  ( $\delta(f)$ ) introduced in the final line means we only consider the bosonic (fermionic) parts of the  $\mathcal{A}^\delta$  field. Similarly for figure 5.3 (a) the group theory part is calculated to be

$$\mathcal{A}^\alpha \mathcal{A}^\delta h^{\beta\zeta} h^{\gamma\varepsilon} \text{str}(S_\alpha S_\beta S_\gamma) \text{str}(S_\zeta S_\delta S_\varepsilon) \tag{5.74}$$

Now we utilise the completeness relations in the forms (4.50) and (4.51). We then find that (5.73) and (5.74) both equate to

$$-\frac{1}{4N} \mathcal{A}^\alpha \mathcal{A}^\delta [\text{str}(S_\alpha \sigma_3 S_\delta) + \text{str}(\sigma_3 S_\alpha S_\delta)] = -\frac{1}{2N} \text{str}(\sigma_3 \mathcal{A}^2) \tag{5.75}$$

However, (D.8) shows us that the  $\mathcal{A}^3$  Feynman rule is antisymmetric in the exchange

of any two momenta. Consequently there is a relative minus sign between the two contributions of figure 5.3, but since they have the same momentum and group theory parts at large loop momentum, these two topologies cancel in this regime. The same argument applies to the diagrams with two internal  $\mathcal{C}$ 's or ghosts. Similar calculations have been performed (using the FORM algebra manipulation package) for all One-loop Remainder Diagrams with just two or three external  $\mathcal{A}$  lines and these diagram were again shown shown to be finite.

## 5.4 Ward identities

The only diagrams that now remain to be tested whether or not they are finite are the one-loop diagrams with  $3 < E_{\mathcal{A}} \leq D$  and  $E_{\mathcal{C}} = E_{\eta} = E_{\bar{\eta}} = 0$ , originating from the unbroken theory. In this section, we shall use gauge invariant arguments to demonstrate that the regularisation works up to  $D = 8$ . The key to doing this is the BRST construction [40]. We use only the unbroken action (5.30) as we have seen that all contributions from the broken sector are finite by power counting.

### 5.4.1 BRST

We introduce the BRST parameter  $\epsilon$  which is even under the group grading but odd under ghost grading. The BRST algebra is given as

$$\delta\mathcal{A} = \epsilon\Lambda^{D/2-2} [\nabla_{\mu}, \eta], \quad (5.76)$$

$$\delta\mathcal{C} = -i\epsilon[\mathcal{C}, \eta], \quad (5.77)$$

$$\delta\eta = ig^2\epsilon\eta^2, \quad (5.78)$$

$$\delta\bar{\eta} = \epsilon\Lambda^{D/2-2} \xi \tilde{c}^{-1} \partial_{\mu} \mathcal{A}_{\mu}. \quad (5.79)$$

The unbroken action (5.30) is invariant under these transformations, as is the naïve functional measure.

The next stage is to construct the Lee-Zinn-Justin identities [14]. We need to add source terms for the fields and non-linear BRST transformations:

$$S_{sources} = -\text{str} \int d^D x \left( \mathcal{J}_\mu \mathcal{A}_\mu + \mathcal{J}\mathcal{C} + \bar{\zeta}\eta + \bar{\eta}\zeta + \Lambda^{\frac{D}{2}-2} \mathcal{K}_\mu [\nabla_\mu, \eta] - ig\mathcal{H}[\mathcal{C}, \eta] + ig\mathcal{L}\eta^2 \right). \quad (5.80)$$

Here  $\mathcal{J}$  is an unconstrained superfield

$$\mathcal{J} = \begin{pmatrix} J^1 & K \\ \bar{K} & J^2 \end{pmatrix}, \quad (5.81)$$

but  $\mathcal{J}_\mu$  (distinguished from  $\mathcal{J}$  by the Lorentz index) expands only over<sup>5</sup>  $S_\alpha$  and  $\sigma_3$ :

$$\mathcal{J}_\mu = 2\mathcal{J}_\mu^\alpha S_\alpha + \frac{1}{2N} \mathcal{J}_\mu^\sigma \sigma_3, \quad (5.82)$$

so that

$$\text{str} \mathcal{J}_\mu \mathcal{A}_\mu = \mathcal{J}_\mu^\alpha \mathcal{A}_{\mu\alpha} + \mathcal{J}_\mu^\sigma \mathcal{A}_\mu^0, \quad (5.83)$$

and these same constraints apply to  $\zeta$ ,  $\bar{\zeta}$ ,  $\mathcal{H}$ ,  $\mathcal{K}$  and  $\mathcal{L}$ . We define the functional differential so as to extract the conjugate from under the supertrace [5], *i.e.* we require

$$\frac{\delta}{\delta J} \text{str} \int d^D x \mathcal{J}\mathcal{C} = \mathcal{C}, \quad (5.84)$$

so we have

$$\frac{\delta}{\delta \mathcal{J}} := \begin{pmatrix} \frac{\delta}{\delta J^1} & -\frac{\delta}{\delta K} \\ \frac{\delta}{\delta \bar{K}} & -\frac{\delta}{\delta J^2} \end{pmatrix}, \quad (5.85)$$

---

<sup>5</sup>If the \*bracket formalism is used, the expansion is just over  $S_\alpha$ .

with a similar definition for  $\delta/\delta\mathcal{C}$ . Analogously, we choose

$$\frac{\delta}{\delta\mathcal{J}_\mu} := 2S_\alpha\frac{\delta}{\delta\mathcal{J}_{\mu\alpha}} + \mathbb{1}\frac{\delta}{\delta\mathcal{J}_\mu^\sigma}, \quad (5.86)$$

$$\frac{\delta}{\delta\mathcal{A}_\mu} := 2S_\alpha\frac{\delta}{\delta\mathcal{A}_{\alpha\mu}} + \frac{\sigma_3}{2N}\frac{\delta}{\delta\mathcal{A}_\mu^0}, \quad (5.87)$$

and likewise for the other field and source differentials.

Viewing the BRST transformations (5.76)–(5.79) as changes in integration variables, we find the generator of connected Green's functions  $W = \ln Z$  satisfies the following relation

$$\xi\zeta\Lambda^{D/2-2}\cdot\hat{c}^{-1}\cdot\partial_\mu\frac{\delta W}{\delta\mathcal{J}_\mu} + \text{str}\int d^Dx\left(\mathcal{J}_\mu\frac{\delta W}{\delta\mathcal{K}_\mu} + \mathcal{J}\frac{\delta W}{\delta\mathcal{H}} - \bar{\zeta}\frac{\delta W}{\delta\mathcal{L}}\right) = 0. \quad (5.88)$$

We then perform the Legendre transformation to obtain the equivalent equation for the generator of 1PI diagrams

$$\Gamma + \xi\partial_\mu\mathcal{A}_\mu\cdot\hat{c}^{-1}\cdot\partial_\nu\mathcal{A}_\nu = -W + \text{str}\int d^Dx\left(\mathcal{J}_\mu\mathcal{A}_\mu + \mathcal{J}\mathcal{C} + \bar{\zeta}\eta + \bar{\eta}\zeta\right), \quad (5.89)$$

where  $\mathcal{A}_\mu$ ,  $\mathcal{C}$  and  $\eta$  must now be viewed as classical fields. The gauge fixing term has been extracted so that upon using the antighost Dyson-Schwinger equation

$$\text{str } T_A \left( \frac{\delta\Gamma}{\delta\bar{\eta}} - 2\Lambda^{2-D/2}\hat{c}^{-1}\tilde{c}\partial_\mu\frac{\delta\Gamma}{\delta\mathcal{K}_\mu} \right) = 0, \quad (5.90)$$

the simplified Lee-Zinn-Justin identities are obtained

$$\text{str}\int d^Dx\left(\frac{\delta\Gamma}{\delta\mathcal{A}_\mu}\frac{\delta\Gamma}{\delta\mathcal{K}_\mu} + \frac{\delta\Gamma}{\delta\mathcal{C}}\frac{\delta\Gamma}{\delta\mathcal{H}} + \frac{\delta\Gamma}{\delta\eta}\frac{\delta\Gamma}{\delta\mathcal{L}}\right) = 0. \quad (5.91)$$

### 5.4.2 Finiteness of diagrams with BRST source insertions

An issue which must now be addressed is the finiteness (or otherwise) of the new diagrams introduced by the BRST sources  $\mathcal{K}_\mu$ ,  $\mathcal{H}$  and  $\mathcal{L}$  in (5.80). Fortunately, since these interactions do not involve higher derivatives it is straightforward to adapt the arguments of section 5.2 to show such diagrams are superficially finite by power counting.

We first note that (5.32) remains the same, but (5.33)–(5.35) now become

$$L = I_{\mathcal{A}} + I_{\mathcal{C}} + I_\eta + 1 - \sum_i V_{\mathcal{A}^i} - \sum_j V_{\mathcal{A}^j \mathcal{C}} - \sum_k V_{\mathcal{A}^k \mathcal{C}^2} - V_{\eta^2 \mathcal{A}} - V_{\eta^2 \mathcal{C}} - V_{\mathcal{C}^3} - V_{\mathcal{C}^4} - V_{\mathcal{K}_\eta} - V_{\mathcal{K} \mathcal{A} \eta} - V_{\mathcal{H} \mathcal{C} \eta} - V_{\mathcal{L} \eta^2}, \quad (5.92)$$

$$E_{\mathcal{A}} = -2I_{\mathcal{A}} + \sum_i i V_{\mathcal{A}^i \mathcal{C}} + \sum_j j V_{\mathcal{A}^j \mathcal{C}} + \sum_k k V_{\mathcal{A}^k \mathcal{C}^2} + V_{\eta^2 \mathcal{A}} + V_{\mathcal{K} \mathcal{A} \eta}, \quad (5.93)$$

$$E_{\mathcal{C}} = -2I_{\mathcal{C}} + \sum_j V_{\mathcal{A}^j \mathcal{C}} + 2 \sum_k V_{\mathcal{A}^k \mathcal{C}^2} + V_{\eta^2 \mathcal{C}} + 3V_{\mathcal{C}^3} + 4V_{\mathcal{C}^4} + V_{\mathcal{H} \mathcal{C} \eta}. \quad (5.94)$$

The ghost equation (5.36) in the desired form

$$E_{\bar{\eta}}^{\mathcal{A}} + E_{\bar{\eta}}^{\mathcal{C}} = -I_\eta + V_{\eta^2 \mathcal{A}} + V_{\eta^2 \mathcal{C}} \quad (5.95)$$

is unchanged, while we also have the new (trivial) relations

$$E_{\mathcal{K}} = V_{\mathcal{K}_\eta} - V_{\mathcal{K} \mathcal{A} \eta} \quad (5.96)$$

$$E_{\mathcal{H}} = V_{\mathcal{H} \mathcal{C} \eta} \quad (5.97)$$

$$E_{\mathcal{L}} = V_{\mathcal{L} \eta^2} \quad (5.98)$$

The net result of this is that  $\mathcal{D}_\Gamma$  in the form (5.38) picks up the new terms

$$-(2r+3)E_{\mathcal{K}} - (r+\tilde{r}+3)E_{\mathcal{H}} - (2r+4)E_{\mathcal{L}}. \quad (5.99)$$

Proposition 1 still holds as do the sufficient conditions (5.45)–(5.47) since these ensure that (5.99) provides a negative contribution to  $\mathcal{D}_\Gamma$ . The only set of diagrams that remain unregularised by the covariant derivatives are exactly those defined before as One-loop Remainder Diagrams. Thus all diagrams involving BRST source terms are finite in any dimension  $D$ .

### 5.4.3 Finiteness of one-loop diagrams using Ward Identities

We write  $\Gamma$  in terms of its classical and one-loop parts,  $\Gamma = \Gamma^0 + \hbar \Gamma^1$ . In the unbroken theory we expand the one-loop pure  $\mathcal{A}$  vertices as (similar to (C.3) and the double supertrace result of the previous section)

$$\frac{1}{2!} \sum_{n,m=2} \frac{1}{nm} \int d^D x_1 \cdots d^D x_n d^D y_1 \cdots d^D y_m \Gamma_{\mu_1 \cdots \mu_n, \nu_1 \cdots \nu_m}^1(x_1, \dots, x_n; y_1, \dots, y_m) \text{str}[\mathcal{A}_{\mu_1}(x_1) \cdots \mathcal{A}_{\mu_n}(x_n)] \text{str}[\mathcal{A}_{\nu_1}(y_1) \cdots \mathcal{A}_{\nu_m}(y_m)] \quad (5.100)$$

The only  $\mathcal{O}(\hbar)$  terms in (5.91) with one  $\eta$  and otherwise only  $\mathcal{A}$ s come from

$$\text{str} \int d^D x \left( \frac{\delta \Gamma^1}{\delta \mathcal{A}_\mu} \frac{\delta \Gamma^0}{\delta \mathcal{K}_\mu} + \frac{\delta \Gamma^0}{\delta \mathcal{A}_\mu} \frac{\delta \Gamma^1}{\delta \mathcal{K}_\mu} \right), \quad (5.101)$$

and so we can deduce that

$$p_1^{\mu_1} \Gamma_{\mu_1 \cdots \mu_n, \nu_1 \cdots \nu_m}^1(p_1, \dots, p_n; q_1, \dots, q_m) = \Gamma_{\mu_2 \cdots \mu_n, \nu_1 \cdots \nu_m}^1(p_1 + p_2, p_3, \dots, p_n; q_1, \dots, q_m) - \Gamma_{\mu_2 \cdots \mu_n, \nu_1 \cdots \nu_m}^1(p_2, \dots, p_{n-1}, p_n + p_1; q_1, \dots, q_m) + \text{finite}, \quad (5.102)$$

where ‘finite’ denotes parts arising from the second term of (5.101) (finiteness following from the results of subsection 5.4.2). Similar Ward identities can be obtained using the cyclicity and invariance under the exchange of the two sets of arguments implied by (5.100) [similar to (C.6) and (C.7)]. If we set  $n = m = 2$ , (5.102) and its counterparts will relate the longitudinal parts of the four-point vertex to the unbroken

three-point vertices, which we know from the preceding section vanish. Hence, we know that the longitudinal part of the four-point vertex is finite in any dimension.

Thus a divergence, if it is to exist, has to arise in the totally transverse part. However, this part of the four-point vertex must have a tensor structure involving at least four external momenta. This means that the superficial degree of divergence has been over estimated by four as these powers of momentum are not available for use as loop momentum, *i.e.* instead of  $\mathcal{D}_\Gamma = D - 4$  we have  $\mathcal{D}_\Gamma = D - 8$ . Thus we can infer that the one-loop four-point pure  $\mathcal{A}$  vertex is finite in all dimensions  $D < 8$ .

This argument can be extended to show the finiteness of all the remaining diagrams. The longitudinal part of the five-point pure  $\mathcal{A}$  vertex is related to the difference of finite<sup>6</sup> four-point vertices plus finite corrections, while the transverse part actually has  $\mathcal{D}_\Gamma = D - 5 - 5$  and so is finite for all  $D < 10$ . Proceeding in this manner we see that for  $D < 8$ , the remaining  $3 < E_{\mathcal{A}} < D$  One-loop Remainder diagrams are finite. Thus all 1PI diagrams are finite in  $D < 8$  as a consequence of a combination of power counting, the supertrace mechanism and gauge invariance.

## 5.5 Unitarity

It was noted earlier that the supertrace gives rise to the wrong sign action for certain fields such as  $A_\mu^2$ . The functional integrals over these fields that appear in the partition function need to be analytically continued in a manner consistent with the  $SU(N|N)$  symmetry in order for them to make sense. Equivalently, the system could be defined through exact RG methods [4, 5] which do not suffer from such problems of definition. Rather than being a sign of instability, *i.e.* the choice of Fock vacuum leading to an unbounded Hamiltonian, covariant quantisation with these wrong signs results in the

---

<sup>6</sup>For  $D < 8$ .

appearance of negative norm states. These states are unphysical and lead to a non-unitary S-matrix. A simple quantum mechanics example which demonstrates this point is given below. The situation here is similar in many ways to the Gupta-Bleuler quantisation procedure [23], which also has to handle the wrong sign action for time-like photons in quantum electrodynamics. Again, choices of vacua exist, but Lorentz covariant quantisation picks out the ones with negative norm states. Unfortunately, we have no Gupta-Bleuler condition to exclude unphysical states. Instead we will find that in the continuum limit  $\Lambda \rightarrow \infty$ ,  $A_\mu^1$  and  $A_\mu^2$  fields decouple enabling a unitary  $SU(N)$  Yang-Mills theory to be recovered in the  $A_1$  sector.

### 5.5.1 $U(1|1)$ quantum mechanics

We define the Hermitian superposition  $\mathcal{X}$  to be

$$\mathcal{X} = \begin{pmatrix} x^1 & \vartheta \\ \bar{\vartheta} & x^2 \end{pmatrix}, \quad (5.103)$$

and consider the Lagrangian (in Minkowski space) of a simple harmonic oscillator:

$$L = \frac{1}{2} \text{str} \dot{\mathcal{X}}^2 - \frac{1}{2} \text{str} \mathcal{X}^2. \quad (5.104)$$

Classically this Lagrangian is invariant under  $SU(1|1)$  transformations  $\delta \mathcal{X} = i[\omega, \mathcal{X}]$ , however we also get for free invariance under  $U(1|1)$ . By Noether's theorem, these transformations are generated by the charges

$$\mathcal{Q} = i[\mathcal{X}, \dot{\mathcal{X}}], \quad (5.105)$$

through the Poisson bracket with  $\text{str} \omega \mathcal{Q}$ . Note that the charge for  $\omega \sim \mathbb{1}$  vanishes which is a reflection of its trivial action on  $\mathcal{X}$ . With a supercovariant derivative

defined as in (5.85), the supermomentum is given by

$$\mathcal{P} := \frac{\partial}{\partial \dot{\mathcal{X}}} L = \dot{\mathcal{X}}. \quad (5.106)$$

This differs by some convenient signs from the usual set of definitions. We can then write the Hamiltonian as

$$H = \text{str } \mathcal{P} \dot{\mathcal{X}} - L, \quad (5.107)$$

while quantisation is via the graded commutator:

$$[(\mathcal{X})^a{}_b, (\mathcal{P})^c{}_d]_{\pm} = i (\sigma_3)^a{}_d \delta^c{}_b. \quad (5.108)$$

By including arbitrary constant supermatrices  $U$  and  $V$ , we can easily see that this respects  $U(1|1)$ :

$$[\text{str } U \mathcal{X}, \text{str } V \mathcal{P}] = i \text{str } UV, \quad (5.109)$$

and this actually corresponds to the usual relations using the usual definitions for momenta:

$$p^i = \frac{\partial L}{\partial \dot{x}^i}, \quad (5.110)$$

$$p_{\vartheta} = \frac{\partial L}{\partial \dot{\vartheta}}, \quad (5.111)$$

$$p_{\bar{\vartheta}} = \frac{\partial L}{\partial \dot{\bar{\vartheta}}}. \quad (5.112)$$

Care needs to be taken since the naïve ordering suggested by (5.105) will not leave  $\mathcal{Q}$  supertraceless after quantisation. This problem can be cured by subtracting the supertrace which corresponds, as we will see, to normal ordering:

$$\mathcal{Q} = i [\mathcal{X}, \mathcal{P}] - \frac{i}{2} \sigma_3 \text{str} [\mathcal{X}, \mathcal{P}] = i [\mathcal{X}, \mathcal{P}] + 2\sigma_3. \quad (5.113)$$

The annihilation and creation operators are chosen to be

$$A = \frac{(\mathcal{X} + i\mathcal{P})}{\sqrt{2}}, \quad (5.114)$$

$$A^\dagger = \frac{(\mathcal{X} - i\mathcal{P})}{\sqrt{2}}, \quad (5.115)$$

with the normalised vacuum defined to be  $A|0\rangle = 0$ . These operators have the expected graded commutation relations:

$$[(A)_b^a, (A^\dagger)_d^c]_\pm = (\sigma_3)_d^a \delta_d^c. \quad (5.116)$$

The vacuum respects  $U(1|1)$  since  $\mathcal{Q}|0\rangle = 0$  and we also note that the supercharges (5.113) may be written as  $\mathcal{Q} =: [A^\dagger, A] : i.e.$  we introduce normal ordering.

We can rewrite (5.114) and (5.115) in terms of components using the usual definitions of momenta contained in (5.110)–(5.112). We then find that  $x^1$  has the usual form of annihilation operator, namely  $a^1 = (x^1 + ip^1)/\sqrt{2}$ , but the one for  $x^2$  actually contains a wrong sign:  $a^2 = (x^2 - ip^2)/\sqrt{2}$ . This gives rise to a wrong sign commutation relation  $[a^2, a^{2\dagger}] = -1$  as can be easily seen from (5.116). This sign is precisely what is needed to compensate for the wrong sign of  $a^{2\dagger}a^2$  in the Hamiltonian,  $H = \text{str } A^\dagger A + 2$ , and ensuring that it is bounded from below. However, it also results in negative norms appearing in the ‘2’ sector. With the normalised ket vectors in this sector given by

$$|n\rangle = \frac{1}{\sqrt{n!}}(a^{2\dagger})^n|0\rangle, \quad (5.117)$$

we find that

$$\langle n|n\rangle = (-1)^n. \quad (5.118)$$

Any attempt to rectify this by altering the sign in  $a^2$  results in an unbounded Hamiltonian and a  $U(1|1)$  and  $SU(1|1)$  violating vacuum.

### 5.5.2 Recovery of unitarity in $A^1$ sector

We established in sections 5.2, 5.3 and 5.4 that covariant derivative spontaneously broken  $SU(N|N)$  theory is finite in all dimensions  $D < 8$ . However, more is required if this is to be a suitable regulating method for  $SU(N)$  Yang-Mills theory. We also need to establish that in the limit  $\Lambda \rightarrow \infty$ ,  $SU(N)$  Yang-Mills theory can be recovered from the  $SU(N|N)$  scheme.

Except for  $A_\mu^i$ , all fields become infinitely heavy<sup>7</sup> in the  $\Lambda \rightarrow \infty$  limit and consequently drop out of the spectrum, so at low energies the gauge group is just  $SU(N) \times SU(N)$ . We need to ascertain that there is no interaction between the two  $SU(N)$  gauge fields, thus enabling us to ignore the  $A^2$  sector in this limit.

Such a problem is addressed by the Appelquist-Carazzone decoupling theorem [42]. This theorem states that for a renormalisable theory, as the mass scale of the heavy sector tends to infinity, the effective Lagrangian is given by a renormalisable one for the light fields with corrections which vanish by inverse powers of the heavy scale which is identified with the overall cutoff of the effective theory.<sup>8</sup> Our case is actually even simpler than this as the heavy mass and cutoff scales have always been identified so we need not concern ourselves with subtleties arising from exchanges of limits of these scales. It must be stressed that the Appelquist-Carazzone decoupling theorem is only applicable to initially renormalisable theories. The standard analysis for Yang-Mills theory carries over to the supergroup case, so we know that spontaneously broken  $SU(N|N)$  is renormalisable in  $D \leq 4$ .

We therefore conclude that in  $D \leq 4$  dimensions, the effective  $SU(N) \times SU(N)$  theory can be described by an effective Lagrangian containing just these fields with

---

<sup>7</sup>The fermionic  $\eta^i$  fields also remain massless. Strictly speaking, we should take into account the effects of the ghosts and BRST in the following analysis. However these do not alter the conclusions of the Appelquist-Carazzone decoupling theorem [43].

<sup>8</sup>For example, this theorem is used to justify the assumption that a spontaneously broken Grand Unified Theory is equivalent to the Standard Model  $SU(3) \times SU(2) \times U(1)$  at low scales.

couplings  $g_i \neq g$ , and with other interactions weighted by appropriate powers of  $\Lambda$  as determined by dimensions. If such an interaction between the  $A^1$  and  $A^2$  fields was to exist, it would have to contain at least two traces, one for each sector. The lowest dimension interaction comes from a group theory structure  $\text{tr}A_\mu^1 A_\nu^1 \text{tr}A_\rho^2 A_\sigma^2$  with the Lorentz indices somehow contracted. To be gauge invariant under  $SU(N) \times SU(N)$  it must take the form (up to  $\ln \Lambda$  corrections)

$$\Lambda^{-D} \text{tr}F_{\mu\nu}^1 F_{\rho\sigma}^1 \text{tr}F_{\alpha\beta}^2 F_{\gamma\delta}^2, \quad (5.119)$$

where  $F_{\epsilon\eta}^i$  is the field strength of  $A^i$  and the Lorentz indices are again contracted in some fashion. This is irrelevant in any dimension and since it is the minimal dimension interaction, we know that all other interactions are irrelevant and disappear as  $\Lambda \rightarrow \infty$ .<sup>9</sup>

The fact that we have decoupled sectors as  $\Lambda \rightarrow \infty$  is actually a statement that unitarity has been restored in the  $A^1$  sector. A non-unitary amplitude can only arise from contributions with internal  $A^2$  propagators. Cutkosky cutting such an amplitude will then result in a non-vanishing amplitude connecting the  $A^1$  and  $A^2$  sector [23] which we have shown cannot exist in the continuum limit.

## 5.6 Summary and conclusions

A method of regularising  $SU(N)$  Yang-Mills theory in a gauge invariant manner in fixed dimensions  $D \leq 4$  has been established. By the use of a higher covariant derivatives all but a small number of one-loop 1PI diagrams of spontaneously broken  $SU(N|N)$  gauge theory were shown to be finite. In turn, these troublesome diagrams were themselves shown to be finite in  $D < 8$  either by cancellations caused by the

---

<sup>9</sup>This is true in  $D \leq 4$  dimensions. In  $D > 4$  the couplings  $g_i$  are non-renormalisable and higher order interactions are unsuppressed. Thus not only is  $D \leq 4$  sufficient, it is also necessary.

supersymmetry through the supertrace mechanism, or by appealing to gauge invariance arguments via Ward Identities. For the scheme to provide regularisation for  $SU(N)$  Yang-Mills theory it is necessary to be able to recover it when the regularisation scheme is tuned to a certain limit. The first stage in this was to introduce spontaneous symmetry breaking so that all fields except the field we wish to regulate and a wrong sign copy, gain mass. When these masses are taken to infinity they decouple from the massless fields. The last issue to address is whether the remaining massless fields interact in the continuum limit; if so, the embedded  $SU(N)$  theory would violate unitarity. Fortunately, the Appelquist-Carazzone theorem, applicable in  $D \leq 4$ , guarantees no such interactions can exist.

There are a number of obvious applications and extensions to this work. Since these ideas first arose within the context of the exact RG, it would be very appealing to construct a fully  $SU(N|N)$  invariant flow equation. Another attractive aspect of this work would be to investigate large  $N$  Yang-Mills theory. The interest here lies with the fact that at large  $N$ , the supertrace mechanism ensures that there are no quantum corrections in the symmetric phase. Of course these ideas would also benefit from the introduction of quarks (and their bosonic superpartners) so direct comparison with physically important theories such as quantum chromodynamics would be possible.

# Appendix A

## Proof of eq. (4.29)

This proof of (4.29) is based upon that of [24]. Suppose we have a supermatrix of the special form

$$\mathbf{N} = \begin{pmatrix} \mathbf{A} & \mathbf{B} \\ \mathbf{0} & \mathbf{D} \end{pmatrix}. \quad (\text{A.1})$$

Then it is evident that

$$\exp \mathbf{N} = \begin{pmatrix} \exp \mathbf{A} & \mathbf{B}' \\ \mathbf{0} & \exp \mathbf{D} \end{pmatrix}, \quad (\text{A.2})$$

for some complicated  $\mathbf{B}'$  whose exact form is not required. Then by using the definition of the superdeterminant (4.20) we find

$$\text{sdet} \mathbf{N} = \frac{\det(\exp \mathbf{A})}{\det(\exp \mathbf{D})}. \quad (\text{A.3})$$

Since  $\mathbf{A}$  and  $\mathbf{D}$  are ordinary matrices, we can further conclude that

$$\text{sdet} \mathbf{N} = \frac{\exp \text{tr} \mathbf{A}}{\exp \text{tr} \mathbf{D}}. \quad (\text{A.4})$$

i.e. the result (4.29) holds if  $\mathbf{N}$  is of the form (A.2). Similarly, it holds if  $\mathbf{N}$  is of the form

$$\mathbf{N} = \begin{pmatrix} \mathbf{A} & \mathbf{0} \\ \mathbf{C} & \mathbf{D} \end{pmatrix}. \quad (\text{A.5})$$

Next we use the relation (which we shall not prove here)  $\text{sdet}(\mathbf{R} \mathbf{S}) = \text{sdet}\mathbf{R} \text{sdet}\mathbf{S}$  (for any supermatrices  $\mathbf{R}$  and  $\mathbf{S}$ ), to deduce that

$$\text{sdet} \left[ \exp \begin{pmatrix} \mathbf{A} & \mathbf{B} \\ \mathbf{C} & \mathbf{D} \end{pmatrix} \exp \begin{pmatrix} -\mathbf{A} & -\mathbf{B} \\ \mathbf{0} & -\mathbf{D} \end{pmatrix} \right] \quad (\text{A.6})$$

$$= \text{sdet} \left[ \exp \begin{pmatrix} \mathbf{A} & \mathbf{B} \\ \mathbf{C} & \mathbf{D} \end{pmatrix} \right] \text{sdet} \left[ \exp \begin{pmatrix} -\mathbf{A} & -\mathbf{B} \\ \mathbf{0} & -\mathbf{D} \end{pmatrix} \right] \quad (\text{A.7})$$

$$= \text{sdet} \left[ \exp \begin{pmatrix} \mathbf{A} & \mathbf{B} \\ \mathbf{C} & \mathbf{D} \end{pmatrix} \right] \exp \left[ -\text{str} \begin{pmatrix} \mathbf{A} & \mathbf{B} \\ \mathbf{0} & \mathbf{D} \end{pmatrix} \right] \quad (\text{A.8})$$

$$= \text{sdet} \left[ \exp \begin{pmatrix} \mathbf{A} & \mathbf{B} \\ \mathbf{C} & \mathbf{D} \end{pmatrix} \right] \exp \left[ -\text{str} \begin{pmatrix} \mathbf{A} & \mathbf{B} \\ \mathbf{C} & \mathbf{D} \end{pmatrix} \right] \quad (\text{A.9})$$

However we could use the Campbell-Baker-Hausdorff formula to rewrite (A.6) as

$$\text{sdet} \left[ \exp \left\{ \begin{pmatrix} \mathbf{0} & \mathbf{0} \\ \mathbf{C} & \mathbf{0} \end{pmatrix} + \mathbf{M}' \right\} \right], \quad (\text{A.10})$$

where  $\mathbf{M}'$  is a set of commutators partitioned as

$$\mathbf{M}' = \begin{pmatrix} \mathbf{A}' & \mathbf{0} \\ \mathbf{C}' & \mathbf{D}' \end{pmatrix}. \quad (\text{A.11})$$

Since the matrix to be exponentiated in (A.10) is of the form (A.5) (*i.e.* of a form for which we know (4.29) holds), (A.10) becomes

$$\exp \left[ \text{str} \left\{ \begin{pmatrix} 0 & 0 \\ C & 0 \end{pmatrix} + M' \right\} \right] = 1, \quad (\text{A.12})$$

since the supertrace of commutators vanishes. Thus we know

$$\text{sdet} \left[ \exp \begin{pmatrix} A & B \\ C & D \end{pmatrix} \right] \exp \left[ -\text{str} \begin{pmatrix} A & B \\ C & D \end{pmatrix} \right] = 1, \quad (\text{A.13})$$

and that (4.29) holds for general supermatrices.

## Appendix B

### Completeness relations

#### B.1 $SU(N|M)$

The generators of  $SU(N|M)$  provide a complete set of supertraceless matrices (as can be demonstrated by a simple counting argument). Hence a general (non-super) matrix denoted  $\mathbf{X}$  can be extended in these generators supplemented by any matrix with an non-vanishing supertrace. For the purposes of this derivation we employ the identity  $\mathbb{1}_{N+M} = \begin{pmatrix} \mathbb{1}_N & 0 \\ 0 & \mathbb{1}_M \end{pmatrix}$  to perform the latter rôle. Thus we have

$$\mathbf{X} = X^A T_A + \tilde{X} \mathbb{1}_{N+M}, \quad (\text{B.1})$$

where  $X^A$  and  $\tilde{X}$  are coefficients and there is an implied sum over  $A$ . Furthermore,

$$\begin{aligned} X^A &= 2 \text{str}(T^A \mathbf{X}), \\ \tilde{X} &= \frac{1}{N-M} \text{str}(\mathbf{X}). \end{aligned} \quad (\text{B.2})$$

Thus we can re-express (B.1) as

$$(X)^i_j = 2(\sigma_3)^k_l (T^A)^l_m (X)^m_k (T_A)^i_j + \frac{1}{N-M} (\sigma_3)^k_l (X)^l_k \delta^i_j. \quad (\text{B.3})$$

Since  $\mathbf{X}$  is an arbitrary matrix, this implies that

$$\delta^i_m \delta^k_j = 2(\sigma_3)^k_l (T^A)^l_m (T_A)^i_j + \frac{1}{N-M} (\sigma_3)^k_m \delta^i_j, \quad (\text{B.4})$$

which, after re-arrangement and relabelling, returns the form of (4.45):

$$(T^A)^i_j (T_A)^k_l = \frac{1}{2} (\sigma_3)^i_l \delta^k_j - \frac{1}{2(N-M)} \delta^i_j \delta^k_l. \quad (\text{B.5})$$

## B.2 $SU(N|N)$

The  $S_\alpha$  generators of  $SU(N|N)$  as defined above (4.46) form a complete set of traceless and supertraceless matrices. As a consequence, a general (non-super) matrix  $\mathbf{Y}$  can be expanded in terms of  $S_\alpha$ ,  $\mathbb{1}_{2N}$  and  $\sigma_3$ , *i.e.*

$$\mathbf{Y} = Y^\alpha S_\alpha + \tilde{Y} \mathbb{1}_{2N} + \hat{Y} \sigma_3, \quad (\text{B.6})$$

where there is a sum over  $\alpha$  and the coefficients  $Y^\alpha$ ,  $\tilde{Y}$  and  $\hat{Y}$  are determined by

$$\begin{aligned} Y^\alpha &= 2 \text{str}(S^\alpha \mathbf{Y}), \\ \tilde{Y} &= \frac{1}{2N} \text{tr}(\mathbf{Y}), \\ \hat{Y} &= \frac{1}{2N} \text{str}(\mathbf{Y}), \end{aligned} \quad (\text{B.7})$$

which means that

$$(Y)^i_j = 2(\sigma_3)^k_l (S^\alpha)^l_m (Y)^m_k (S^\alpha)^i_j + \frac{1}{2N} (Y)^k_k \delta^i_j + \frac{1}{2N} (\sigma_3)^k_l (Y)^l_k (\sigma_3)^i_j. \quad (\text{B.8})$$

Using the fact that  $\mathbf{Y}$  is an arbitrary matrix, we deduce that

$$\delta^i_m \delta^k_j = 2(\sigma_3)^k_l (S^\alpha)^l_m (S_\alpha)^i_j + \frac{1}{2N} \delta^k_m \delta^i_j + \frac{1}{2N} (\sigma_3)^k_m (\sigma_3)^i_j, \quad (\text{B.9})$$

leading to the completeness relation for the  $S_\alpha$  generators of  $SU(N|N)$  (4.49)

$$(S^\alpha)^i_j (S_\alpha)^k_l = \frac{1}{2} (\sigma_3)^i_l \delta^k_j - \frac{1}{4N} \left[ (\sigma_3)^i_j \delta^k_l + \delta^i_j (\sigma_3)^k_l \right]. \quad (\text{B.10})$$

# Appendix C

## Wine notation

We introduce the ‘wine’ notation of refs [3, 4, 5]. Given a generic kernel  $W(p^2/\Lambda^2)$ , we can construct the wine  ${}_{\mathbf{x}l}^i\{W\}_{j\mathbf{y}}^k$ . This functional is a gauge covariantization of the original kernel, and incorporates parallel transport of the tensor representation. If  $u_i^l(x)$  and  $v_k^j(y)$  are  $N \otimes \bar{N}$  representations of the gauge group, we have

$$\mathbf{u}\{W\}\mathbf{v} := \int d^D x d^D y u_i^l(x) {}_{\mathbf{x}l}^i\{W\}_{j\mathbf{y}}^k v_k^j(y) \quad (\text{C.1})$$

A wide choice exists for the exact form of the wine; we shall only use the following representation

$$\mathbf{u}\{W\}\mathbf{v} = \text{str} \int d^D x u(x) W(-\nabla^2/\Lambda^2) \cdot v(x), \quad (\text{C.2})$$

where  $\nabla_\mu$  is defined as in (5.2). The wine can be expanded in momentum space in terms of the gauge field [see (5.1)] as

$$\begin{aligned} \mathbf{u}\{W\}\mathbf{v} &\equiv \mathbf{v}\{W\}\mathbf{u} = \\ &\sum_{m,n=0}^{\infty} \int d^D r d^D s d^D p_1 \dots d^D p_n d^D q_1 \dots d^D q_n W_{\mu_1 \dots \mu_n, \nu_1 \dots \nu_m}(p_1, \dots, p_n; q_1, \dots, q_n; r, s) \\ &\text{str} [\mathbf{u}(r) \mathcal{A}_{\mu_1}(p_1) \dots \mathcal{A}_{\mu_n}(p_n) \mathbf{v}(s) \mathcal{A}_{\nu_1}(q_1) \dots \mathcal{A}_{\nu_m}(q_m)]. \end{aligned} \quad (\text{C.3})$$

Such an expansion is represented graphically in figure C.1, with the labelling scheme shown in figure C.2.

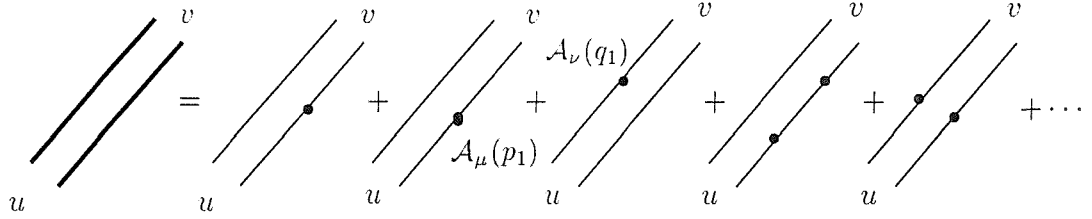


Figure C.1: Wine expansion, where the thick lines represent the full series.

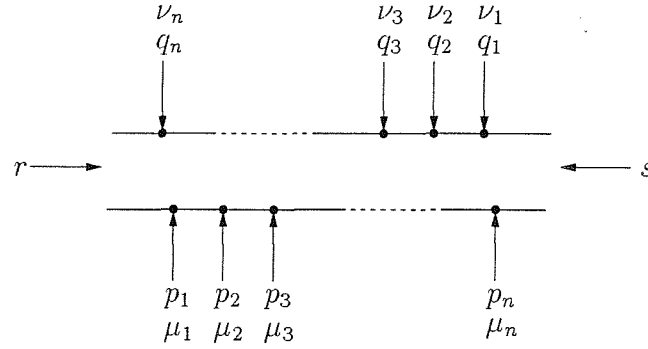


Figure C.2: Convention for wine labelling

We use the following shorthand to reduce the plethora of arguments indices, commas and semi-colons. For the  $n = 0$  case of (C.3), we replace the second string of  $\mathcal{A}$  fields by the identity and define

$$W_{\mu_1 \dots \mu_n}(p_1, \dots, p_n; r, s) \equiv W_{\mu_1 \dots \mu_n}(p_1, \dots, p_n; ; r, s), \quad (\text{C.4})$$

while for the  $m = n = 0$  case we regain the original kernel

$$W_p \equiv W( ; ; p, -p) = W(p^2/\Lambda^2). \quad (\text{C.5})$$

Evidently from the definition of a wine we have the exchange identity

$$W_{\mu_1 \dots \mu_n, \nu_1 \dots \nu_m}(p_1, \dots, p_n; q_1, \dots, q_n; r, s) = W_{\nu_1 \dots \nu_m, \mu_1 \dots \mu_n}(q_1, \dots, q_n; p_1, \dots, p_n; s, r). \quad (\text{C.6})$$

Furthermore, charge conjugation invariance (arising from the symmetry  $\mathcal{A}_\mu \leftrightarrow -\mathcal{A}_\mu^T$ ) implies

$$\begin{aligned} W_{\mu_1 \dots \mu_n, \nu_1 \dots \nu_m}(p_1, \dots, p_n; q_1, \dots, q_n; r, s) \\ = (-1)^{n+m} W_{\mu_n \dots \mu_1, \nu_m \dots \nu_1}(p_n, \dots, p_1; q_m, \dots, q_1; s, r). \end{aligned} \quad (\text{C.7})$$

## Appendix D

# Some Feynman rules for $SU(N|N)$ gauge theory

Some of the Feynman rules for the broken action contained in (5.28) are given here. The Feynman rules were derived as follows: each rule is the sum of all possible ways of assigning the relevant fields to points but maintaining the order within supertraces. This means that when it comes to calculating diagrams, care has to be taken to ensure that all possible combinatorics and topologies are taken into account. The following short hand is employed:

$$b^{\alpha\beta} \equiv \frac{1}{2} (h^{\alpha\beta} + h^{\beta\alpha}), \quad (D.1)$$

$$f^{\alpha\beta} \equiv \frac{1}{2} (h^{\alpha\beta} - h^{\beta\alpha}), \quad (D.2)$$

as well as the wine notation described in Appendix C.

The  $\mathcal{A}$  propagator is

$$\begin{aligned}
& \mathcal{A}_\mu^\alpha \xrightarrow[p]{\text{---}} \mathcal{A}_\nu^\beta \\
&= b^{\alpha\beta} \left\{ \frac{g_{\mu\nu}}{c_p^{-1} p^2} + \frac{p_\mu p_\nu}{p^4} \frac{(c_p^{-1} - \xi \hat{c}_p^{-1})}{\xi c_p^{-1} \hat{c}_p^{-1}} \right\} \\
&+ f^{\alpha\beta} \left\{ \frac{g_{\mu\nu}}{c_p^{-1} p^2 + 4\Lambda^2 \tilde{c}_p^{-1}} + \frac{p_\mu p_\nu}{(c_p^{-1} p^2 + 4\Lambda^2 \tilde{c}_p^{-1})} \frac{(c_p^{-1} - \xi \hat{c}_p^{-1})}{(\xi \hat{c}_p^{-1} p^2 + 4\Lambda^2 \tilde{c}_p^{-1})} \right\}. \quad (\text{D.3})
\end{aligned}$$

In double index notation we find

$$\begin{aligned}
& \langle (\mathcal{A}_\mu)^i{}_j(p) (\mathcal{A}_\nu)^k{}_l(-p) \rangle \\
&= \frac{1}{4} \left[ \left\{ \delta^i{}_l (\sigma_3)^k{}_j + (\sigma_3)^i{}_l \delta^k{}_j - \frac{1}{N} [\delta^i{}_j (\sigma_3)^k{}_l + (\sigma_3)^i{}_j \delta^k{}_l] \right\} \right. \\
&\quad \times \left. \left\{ \frac{g_{\mu\nu}}{c_p^{-1} p^2} + \frac{p_\mu p_\nu}{p^4} \frac{(c_p^{-1} - \xi \hat{c}_p^{-1})}{\xi c_p^{-1} \hat{c}_p^{-1}} \right\} \right] \\
&+ \frac{1}{4} \left[ \left\{ \delta^i{}_l (\sigma_3)^k{}_j - (\sigma_3)^i{}_l \delta^k{}_j \right\} \right. \\
&\quad \times \left. \left\{ \frac{g_{\mu\nu}}{c_p^{-1} p^2 + 4\Lambda^2 \tilde{c}_p^{-1}} + \frac{p_\mu p_\nu}{(c_p^{-1} p^2 + 4\Lambda^2 \tilde{c}_p^{-1})} \frac{(c_p^{-1} - \xi \hat{c}_p^{-1})}{(\xi \hat{c}_p^{-1} p^2 + 4\Lambda^2 \tilde{c}_p^{-1})} \right\} \right]. \quad (\text{D.4})
\end{aligned}$$

The  $\mathcal{C}$  propagator is given by

$$\langle \mathcal{C}^i{}_j(p) \mathcal{C}^k{}_l(-p) \rangle = \frac{\tilde{c}_p}{p^2} \delta^i{}_l (\sigma_3)^k{}_j + \frac{2\xi \tilde{c}_p^2}{\Lambda^2 \hat{c}_p} (\delta^i{}_l (\sigma_3)^k{}_j - (\sigma_3)^i{}_l \delta^k{}_j). \quad (\text{D.5})$$

The superghost propagator is found to be

$$\eta^\alpha \xrightarrow[p]{\text{---}} \bar{\eta}^\beta = 2 \left[ \frac{b^{\alpha\beta}}{\hat{c}_p^{-1} \tilde{c}_p p^2} + \frac{f^{\alpha\beta}}{\hat{c}_p^{-1} \tilde{c}_p p^2 + 4\Lambda^2 \xi^{-1}} \right]. \quad (\text{D.6})$$

Or equivalently

$$\begin{aligned} \left\langle \eta^i{}_j(p) \bar{\eta}^k{}_l(-p) \right\rangle &= \frac{1}{2} \left[ \left\{ \delta^i{}_l (\sigma_3)^k{}_j + (\sigma_3)^i{}_l \delta^k{}_j - \frac{1}{N} \left[ \delta^i{}_j (\sigma_3)^k{}_l + (\sigma_3)^i{}_j \delta^k{}_l \right] \right\} \frac{1}{\hat{c}_p^{-1} \tilde{c}_p p^2} \right. \\ &\quad \left. + \left\{ \delta^i{}_l (\sigma_3)^k{}_j - (\sigma_3)^i{}_l \delta^k{}_j \right\} \frac{1}{\hat{c}_p^{-1} \tilde{c}_p p^2 + 4\Lambda^2 \xi^{-1}} \right]. \quad (\text{D.7}) \end{aligned}$$

The pure  $\mathcal{A}^3$  interaction was found to have the Feynman rule

$$\begin{aligned}
 & \mathcal{A}_\mu^\alpha \mathcal{A}_\nu^\beta \mathcal{A}_\lambda^\gamma = 2g \left[ c_p^{-1}(p_\nu \delta_{\lambda\mu} - p_\lambda \delta_{\mu\nu}) + c_\nu^{-1}(q; r, p)(p_\lambda r_\mu - p_\nu r_\lambda) \right. \\
 & \quad \left. + \Lambda^2 \tilde{c}_\nu^{-1}(q; r, p) \delta_{\mu\lambda} + 2 \text{ cycles of } (p_\mu, q_\nu, r_\lambda) \right] \\
 & \quad \times \text{str}(S^\alpha S^\beta S^\gamma). \tag{D.8}
 \end{aligned}$$

Three point interactions with inserted  $\sigma_3$ s (arising from the symmetry breaking) also occur. The positioning of a  $\sigma_3$  is indicated by a wedge.

$$\begin{aligned}
 & \text{Diagram:} \\
 & \text{Left: } A_\mu^\alpha \text{ (wavy line), } p \text{ (arrow), } A_\nu^\beta \text{ (wavy line), } q \text{ (arrow), } A_\lambda^\gamma \text{ (wavy line), } r \text{ (arrow).} \\
 & \text{Right:} \\
 & = 2g\Lambda^2 \left[ \tilde{c}_\nu^{-1}(q; p, r) \delta_{\mu\lambda} + \tilde{c}_\mu^{-1}(p; r, q) \delta_{\nu\lambda} + \tilde{c}_\lambda^{-1}(r; q, p) \delta_{\mu\nu} \right] \\
 & \quad \times \text{str}(\sigma_3 S^\alpha \sigma_3 S^\beta S^\gamma). \tag{D.9}
 \end{aligned}$$

(We refrain from including the double index versions of these vertices.)

Some more three point Feynman rules are given below.

$$\begin{aligned}
& \left\langle (\mathcal{A}_\mu)^i{}_j(p) \mathcal{C}_l^k(q) \mathcal{C}_n^m(r) \right\rangle \\
&= \frac{g}{4} \left[ \tilde{c}_r^{-1} r_\mu - \tilde{c}_q^{-1} q_\mu + \tilde{c}_\mu^{-1}(p; r, q) q \cdot r \right] \\
&\quad \times (\sigma_3)^k{}_n \left[ \delta^i{}_l (\sigma_3)^m{}_j - \frac{1}{2N} \left\{ (\sigma_3)^i{}_j \delta^m{}_l + \delta^i{}_j (\sigma_3)^m{}_l \right\} \right]. \quad (\text{D.10})
\end{aligned}$$

$$\mathcal{A}_\mu^A \circ \overbrace{\circlearrowleft \circlearrowleft \circlearrowleft}^p = -g \hat{c}_r^{-1} \tilde{c}_r r_\mu \text{str}(S^\alpha S^\beta S^\gamma) \quad (D.11)$$

$$\begin{array}{c}
 \text{Diagram:} \\
 \text{Left: } \mathcal{A}_\mu^A \text{ (curly line)} \text{ and } \text{O} \text{ (dashed line)} \text{ with label } p. \\
 \text{Right: } = g \hat{c}_q^{-1} \tilde{c}_q q_\mu \text{ str}(S^\alpha S^\beta S^\gamma) \\
 \text{with labels: } \eta^C \text{ (dashed line), } q \text{ (dashed line), } \bar{\eta}^B \text{ (dashed line).}
 \end{array}
 \quad (D.12)$$

# Bibliography

- [1] K. Wilson and J. Kogut, Phys. Rep. **12C** (1974), 75.
- [2] see *e.g.* C. Becchi, [hep-th/9607188](#); M. Bonini *et al.*, Nucl. Phys. **B409** (1993) 441, **B418** (1994) 81, **B421** (1994) 81, **B437** (1995) 163; U. Ellwanger, Phys. Lett. **B335** (1994) 364; U. Ellwanger *et al.*, Z. Phys. **C69** (1996) 687; M. Reuter and C. Wetterich, Nucl. Phys. **B417** (1994) 181, **B427** (1994) 291; M. D'Attanasio and T.R. Morris, Phys. Lett. **B378** (1996) 213.
- [3] T.R. Morris in *The Exact Renormalization Group*, eds. Kraznitz *et al.* (World Sci., Singapore, 1999) 1.
- [4] T.R. Morris, Nucl. Phys. **B573** (2000) 97.
- [5] T.R. Morris, JHEP **12** (2000) 012 .
- [6] L.P. Kadanoff, Physics **2** (1966) 263.
- [7] T.R. Morris, Int. J. Mod. Phys. **A9** (1994), 2411.
- [8] T.R. Morris, Prog. Theor. Phys. Suppl. **131** (1998), 395.
- [9] C. Bagnuls and C. Bervillier, [hep-th/0002034](#).
- [10] T.R. Morris, Phys. Lett. **B334** (1994) 355.
- [11] T.R. Morris, Int. J. Mod. Phys. **B12** (1998) 1343.

- [12] T.R. Morris, Nucl. Phys. **B458[FS]** (1996), 477.
- [13] J. Polchinski, Nucl. Phys. **B231** (1984) 269.
- [14] see *e.g.* J. Zinn-Justin, *Quantum Field Theory and Critical Phenomena* (Clarendon Press, Oxford, 1993).
- [15] J.F. Nicholl, T.S. Chang and H.E. Stanley, Phys. Rev. Lett. **33** (1974) 540; A. Hasenfratz and P. Hasenfratz, Nucl. Phys. **B270** (1986) 687.
- [16] T.R. Morris and J.F. Tighe, JHEP **08** (1999) 007.
- [17] T.R. Morris and J.F. Tighe, Int. J. Mod. Phys. **A16** (2001) 2905.
- [18] M. Bonini *et al.*, Nucl. Phys. **B483** (1997) 475.
- [19] see *e.g.* M. Reuter, N. Tetradis and C. Wetterich, Nucl. Phys. **B401** (1993) 567; N. Tetradis and C. Wetterich, Nucl. Phys. **B398** (1993) 659, **B422** (1994) 541; C. Wetterich, Phys. Lett. **B301** (1993) 90; J. Berges, N. Tetradis and C. Wetterich, Phys. Rev. Lett. **77** (1996) 873; Phys. Lett. **B393**; T. Papenbrock and C. Wetterich, Z. Physik **C65** (1995) 519; D. Litim, Mod. Phys. Lett. **A12** (1997) 2287; N. Tetradis, Phys. Lett. **B409**.
- [20] M. Lüscher and P. Weisz, Nucl. Phys. **B290** (1987) 25, **B318** (1989) 705.
- [21] T.R. Morris, Phys. Lett. **B329** (1994), 241; T.R. Morris, Int. J. Mod. Phys. **B12** (1998), 1343.
- [22] B. DeWitt, *Supermanifolds* (Cambridge University Press, Cambridge, 1992).
- [23] see *e.g.* C. Itzykson and J.B. Zuber, *Quantum Field Theory* (McGraw-Hill, New York, 1980).
- [24] J. F. Cornwell, *Group Theory in Physics Volume 3 – Supersymmetries and Infinite-Dimensional Algebras* (Academic Press, London, 1989).

[25] I. Bars, in *Introduction to Supersymmetry in Particle and Nuclear Physics*, eds. Castaños *et al.* (Plenum, New York, 1984) 107.

[26] W. Pauli and F. Villars, Rev. Mod. Phys. **21** (1949) 434.

[27] A.A. Slavnov, Theor. Math. Phys. **13** (1972) 1064; B.W. Lee and J. Zinn-Justin, Phys. Rev. **D5** (1972) 3121.

[28] M. Asorey and F. Falceto, Nucl. Phys. **B327** (1989) 427; B.J. Warr, Ann. Phys. **183** (1988) 1.

[29] T.D. Bkeyev and A.A. Slavnov, Mod. Phys. Lett. **A11** (1996) 1539; M. Asorey and F. Falceto, Phys. Rev. **D54** (1996) 5290; K. Nittoh, [hep-th/0012043](#).

[30] J.I. Latorre and T.R. Morris, JHEP **11** (2000) 004.

[31] Y.A. Golfand and E.P. Likhtman, JETP Lett. **13** (1971) 323; D.V. Volkov and V.P. Akulov, JETP Lett. **16** (1972) 438; J. Wess and B. Zumino, Nucl. Phys. **B70** (1974), 149.

[32] H. Miyazawa, Phys. Rev. **170** (1968) 1586; Prog. Theor. Phys. **36** (1966) 1266.

[33] Y. Ne'eman, Phys. Lett. **81B** (1979) 190.

[34] S. Arnone, Yu.A. Kubyshin, T.R. Morris and J.F. Tighe, [hep-th/0102011](#).

[35] S. Arnone, Yu.A. Kubyshin, T.R. Morris and J.F. Tighe, Int. J. Mod. Phys. **A16** (2001) 1989.

[36] S. Arnone, Yu.A. Kubyshin, T.R. Morris and J.F. Tighe, [hep-th/0106258](#).

[37] J.G. Taylor, Phys. Lett. **84B** (1979) 79.

[38] G. 't Hooft, Nucl. Phys. **B35** (1971) 167.

[39] L.D. Faddeev and V.N. Popov, Phys. Lett. **25B** (1967) 29.

[40] C. Becchi, A. Rouet and R. Stora, Commun. Math. Phys. **52** (1975) 55; M.Z. Iofa and I.V. Tyutin, Theor. Math. Phys. **27** (1976) 316.

[41] see *e.g.* S. Weinberg, *The Quantum Theory of Fields Volume 1* (Cambridge University Press, Cambridge, 1995).

[42] T. Appelquist and J. Carazzone, Phys. Rev. **D11** (1975) 2856; K. Symanzik Comm. Math. Phys. **34** (1973) 7.

[43] Y. Kazama and Y.-P. Yao, Phys. Rev. **D25** (1982) 1605.